JANAIR
JOINT ARMY-NAVY AIRCRAFT INSTRUMENTATION RESEARCH

JANAIR Report 680709
March 27, 1970

Holographic Head-Up Display -- Phase II Final Report

by

T. J. Harris, R. S. Schools, G. T. Sincerbox,
D. W. Hanna, D. G. Delay

International Business Machines Corporation
Systems Development Division, Poughkeepsie, New York

Jointly sponsored by
Office of Naval Research
Naval Air Systems Command
Army Electronics Command
under
Contract N00014-68-C-0300

IBM

JANAIR Report 680709 March 27, 1970

Holographic Head-Up Display -- Phase II
Final Report

by

T. J. Harris, R. S. Schools, G. T. Sincerbox,
D. W. Hanna, D. G. Delay

Jointly sponsored by
Office of Naval Research
Naval Air Systems Command
Army Electronics Command
under
Contract N00014-68-C-0300

IBM

International Business Machines Corporation
Systems Development Division, Poughkeepsie, New York

NOTICE

Change of Address

Organizations receiving JANAIR Reports on the initial distribution list should confirm correct address. This list is located at the end of the report just prior to the DD Form 1473. Any change in address or distribution list should be conveyed to the Office of Naval Research, Code 461, Washington, D.C. 20360 ATTN: JANAIR Chairman.

Disposition

When this report is no longer needed it may be transmitted to other organizations. Do not return it to the originator or the monitoring office.

Disclaimer

The findings in this report are not to be construed as an official Department of Defense or Military Department position unless so designated by other official documents.

FOREWORD

This report presents work which was performed under the Joint Army Navy Aircraft Instrumentation Research (JANAIR) Program, a research and exploratory development program directed by the United States Navy, Office of Naval Research. Special guidance is provided to the program for the Army Electronics Command, the Naval Air Systems Command, and the Office of Naval Research through an organization known as the JANAIR Working Group. The Working Group is currently composed of representatives from the following offices:

- U.S. Navy, Office of Naval Research, Aeronautics, Code 461, Washington, D.C.
  - Aircraft Instrumentation & Control Program Area
- U.S. Navy, Naval Air Systems Command, Washington, D.C.
  - Avionics Division; Navigation Instrumentation and Display Branch (NAVAIR 5337)
  - Crew Systems Division; Cockpit/Cabin Requirements and Standards Branch (NAVAIR 5313)
- U.S. Army, Army Electronics Command, Avionics Laboratory, Fort Monmouth, New Jersey
  - Instrumentation Technical Area (AMSEL-VL-I)

The Joint Army Navy Aircraft Instrumentation Research Program objective is: To conduct applied research using analytical and experimental investigations for identifying, defining and validating advanced concepts which may be applied to future, improved Naval and Army aircraft instrumentation systems. This includes sensing elements, data processors, displays, controls and man/machine interfaces for fixed and rotary wing aircraft for all flight regimes.

ABSTRACT

Numerous applications of display systems require the presentation of visual information that can be continuously altered with time. In particular, a head-up display system as used by an aircraft commander must provide a simulation of the real-world exterior to his vehicle, and, at the same time, represent any change in his attitude with respect to a predetermined segment of this real world.

In the particular case of an aircraft landing approach, one can characterize the pilot's view of the aircraft carrier and its subsequent variations into six degrees of freedom. The display must provide the view corresponding to the instantaneous values of these parameters and change as any one or more of the parameters change.

This report describes the results of a continuation of the development work initiated in Phase I of the contract on displays of this type using sideband or carrier-frequency Fresnel holographic recorded images.

The goals of Phase II were to study the various modes and techniques derived in Phase I and other possibilities, to select the approach that offered the best potential for use in Navy carrier-based aircraft and to build a laboratory model of this selected system.

The selected approach uses a GaAs injection laser diode light source to interrogate a hologram of an aircraft carrier model. The real image from the hologram is optically relayed to a special IR vidicon, and the image is then transmitted electrically to a CRT monitor. This approach was selected for several reasons, but chiefly because it is compatible with some of the existing aircraft equipment. A laboratory model of this system was constructed.

This work was performed by the IBM Systems Development Division, Product Development Laboratory, at Poughkeepsie, N.Y. with assistance from IBM's Federal Systems Division, Electronics Systems Center, at Owego, N.Y.

CONTENTS

ILLUSTRATIONS

SYMBOLS

U_s	complex amplitude of signal wavefront	6
$A(x, y)$	amplitude of signal wavefront	6
i	imaginary unit satisfying the equation $i^2 = -1$	6
$\varphi(x, y)$	spatial phase of signal wavefront	6
z_o	location of object	6
x_r, y_r, z_r	point of origin of reference beam	6
U_r	complex amplitude of reference wave	8
A^*	complex conjugate of signal wavefront	8
B	amplitude of reference wave	8
B^*	complex conjugate of reference wave amplitudes	8
$\vec{k}$	propagation vector of reference wave $\lvert\vec{k}\rvert = \frac{2\pi}{\lambda}$	8
λ	wavelength of radiation	8
U	complex amplitude distribution of interference pattern	8
U^*	complex conjugate of amplitude distribution of interference pattern	8
T_a	amplitude transmittance of hologram	8
t	exposure time	8
U_r'	illuminating wavefront (complex amplitude of)	8
$U'(xy)$	reconstructed wavefront (complex amplitude of)	8
z	location of center of curvature of read-out illumination	10
f	focal length of a lens	10
$T_{\ell+}$	transform operator of a positive lens	10
$T_{\ell-}$	transform operator of a negative lens	12
θ	angular shift introduced by a prism	13
T_p	transform operator of a prism	13
f_H	focal length of hologram "lens"	13
z'	reconstructed image location	14
M	lateral magnification of reconstructed image	14
$\vec{r}$	vector position of a point in three-dimensional space	97
$\hat{i}, \hat{j}, \hat{k}$	unit vectors along the x, y, and z coordinate axes	97

1. INTRODUCTION

Developments in holographic displays during Phase I[1] of this contract indicated the possibility of advancements in the evolution of head-up display systems. Holographic images are true three-dimensional images, exhibiting all the depth and parallax of their real-world counterparts with a realism and detail that are not limited by a computer's storage capacity. Being truly three-dimensional, holographic images may be manipulated in six degrees of freedom, to simulate the relative motion of the scenes that they represent. This manipulation may be done directly, without going through a coordinate transform computation for each point in the image, as is required with contact analog imagery.

The object of an ideal head-up display is to present an image to a pilot that is identical to the view he would see if the landing area were not obscured by foul weather or darkness. The efforts in Phase I of this contract involved analysis of exactly what happens to the real image of a carrier perceived by a pilot on a carrier landing approach when the plane yaws, pitches, rolls, changes glide path, and changes range. According to this analysis, a change in glide path is perceived as a different view of the carrier. The relative distance from the carrier (range) is perceived as a variation in the image size of the carrier. Yaws and pitches of the plane are perceived as translations of the carrier image right or left and up or down in the windscreen. As the plane rolls, the image appears to rotate about an axis, which is the line of sight. A holographically generated image system to simulate the real view of the carrier must, therefore, use image manipulation techniques that reproduce the effects of yaw, pitch, roll, glide path changes, and range changes of the real carrier image. One outstanding problem in such a system is to achieve manipulation of each degree of freedom entirely independent of manipulations of all other degrees of freedom.

The experimental investigations of Phase I indicated that there appears to be little difficulty in producing quality holograms of an extended, three-dimensional object. The only restrictions encountered were those imposed by geometry and space, which tend to limit the minimum angle between signal and reference beams,

the physical separation of the reference point from the recording plate, and model illumination techniques. These limitations are not serious. Phase I efforts were restricted to conventional holography of the sideband Fresnel class and did not include Fourier, Fraunhoffer, or Lippmann type configurations.

The type of hologram considered is capable of creating either a real or virtual image, according to the manner in which it is illuminated. This fact coupled with the understanding of the general problem derived from the analysis indicated that it would be possible to structure the display system using either a holographically generated real or virtual image. Each approach provides convenient solutions to a different subset of problems associated with the required degrees of freedom; that is, the real image allows ease in manipulating the change in glide path (perspective) and pitch and yaw motions, while in a virtual image mode it is more convenient to simulate range change in addition to providing better image quality. Both systems were considered during Phase I, but at the end of that period there was not sufficient information to select a best approach.

Some mechanisms to simulate various independent degrees of freedom were constructed during Phase I. It had been anticipated that range change would be the most difficult to simulate with purely holographic techniques. Range change was successfully simulated without the use of multiple holograms. The single hologram approach eliminates flicker problems. In particular, it was shown that it is impossible to achieve a holographic angular magnification greater than unity and that this may limit the total range of range simulation using holography.

Designs of head-up display systems using holographic real and virtual images were suggested at the end of Phase I. Systems that use a model rather than a holographic image have also been suggested.[2-7] The Phase I experiments and investigations provided convincing results that holography offered the best approach to the simulation of an aircraft landing. In fact, it is the only approach, besides actual models, that permits real-time continuous selection of views of the landing area.

The systems using either a real or virtual image structured during Phase I were studied during Phase II. Although the virtual image is more pleasing and realistic to view, it must be removed to infinity in order to satisfy the requirements on eye accommodation. Once this is done it no longer matters whether the original image were two- or three-dimensional so long as the image can be changed in perspective. In fact, a three-dimensional image would be of no use and even dangerous if it were located so that the pilot could change perspective views by just moving his head. The perspective view should change only with changes in the relative position of the aircraft and aircraft carrier.

The results of the above considerations, the complexity of implementing the approaches suggested at the end of Phase I, and the attractiveness of using the CRT head-up display facilities available for low-light-level TV systems for night use[9] led us to design a new system. This system is the result of Phase II and is the concept upon which a laboratory model was fabricated. The laboratory model uses a gimballed hologram with a closed-circuit TV system. The hologram is illuminated by an IR GaAs laser diode.

The results of Phase II indicate that future work should include the following:

1. Improvement in holographic image quality.
2. Simplification of the mechanical manipulator and making it more rugged.
3. Increased magnification range.
4. Improved packaging.
5. Human factors implications.
6. Refined scale models and closed-circuit TV systems.
7. Application of improved injection laser light sources.

2. THEORY OF HOLOGRAPHY

2.1 INTRODUCTION

The ability of a hologram to record and re-create information regarding a three-dimensional object space has stimulated serious investigations to determine its display potential. At present, there is a wide spectrum of applications under consideration. These extend from static or storage-type displays at one extreme to real world tracking or simulation at the other. The implementation of a dynamic display requires its information content to be modified in conjunction with a real time event. The extent to which an accurate duplication can be obtained is determined by the degree to which the holographic image can be manipulated. These manipulations are subject to certain constraints that, for the most part, can be determined from the theory of the holographic process.

It is the purpose of this section to review the basic concepts of holography. In addition, the analogy between the hologram and a variable focal length lens will be developed.

2.2 CONCEPTS OF HOLOGRAPHY

The optical wavefront emanating from a three-dimensional object space can be completely† characterized if an amplitude and phase is assigned to each object point. Conversely, if the amplitude and phase at each point within a cross-section of the wavefront is known then the original object can be uniquely determined. This is the essence of holography. That is, a hologram records the phase and amplitude information contained in the wavefront as it passes through the sampling (recording) plane. This information is stored in such a manner that, at any later time, a new wavefront may be generated that contains the same phase and amplitude variations. To an observer, this reconstructed wavefront is indistinguishable from the original wavefront created by the three-dimensional object. Consequently, the observer will see a reconstructed image of this object which has long since been removed from the system. All of the three-

†It is assumed that the radiation is monochromatic and that scalar theory applies (i.e., polarization effects are not considered).

dimensional effects associated with the original object will also be present. This includes parallax, perspective, and depth. The physical dimensions of the hologram, however, will introduce some restrictions on the location of the observer. That is, the hologram samples only a finite area of the wavefront. This produces the illusion of looking at an object through a window.

It is only through a process termed interference that the information on a wavefront can be recorded. This is necessitated by the fact that a photosensitive medium is a square-law type of detector. That is, it responds only to the intensity of the incident radiation. Since the intensity is the square of the amplitude, it does not contain any phase data. This limitation can be circumvented by causing the signal wavefront to overlap with a second wavefront in the region of space where the recording (sample) is to be taken. If both wavefronts are monochromatic and coherent with each other, there is an interaction between them. At any given point, the amplitudes of each wave will combine producing a new amplitude. The relative phase between them determines the new amplitude. Depending on the phase difference, all values between the sum or the difference of the components may result. If the second wavefront is properly selected so that it may be re-established at any later time, it becomes a reference against which the phase variations in the signal wavefront are measured and recorded. The resulting intensity variation is indicative of the amplitude and phase information in the signal wavefront. This can be directly recorded. It is sometimes convenient to think of the resulting intensity distribution as a complicated fringe pattern. The weight or strength of the fringes at any given point is proportional to the signal amplitude at that point and their spacing is a measure of the phase variations. If, for example, the object were a point source and the reference beam a plane wave, the resulting intensity pattern would be a set of concentric rings. The spacing of the rings would decrease with distance from the central point. The resulting hologram would look (and act) very much like a zone plate.

Exposure of a suitable photosensitive medium to the interference pattern will result in a density variation on the processed photograph, which is now a hologram. By proper selection of both the parameters and processing, this variation can be controlled. In particular, the amplitude transmittance of the resulting hologram can be made to be proportional to the intensity of the exposing interference pattern. The hologram can now be illuminated with a wavefront identical to the original reference beam. In passing through the hologram, this wavefront will acquire an amplitude and phase variation identical to the original signal wavefront (to within a constant multiplier). Consequently, the wavefront leaving the hologram plane will be indistinguishable from the wavefront that would have come from the object itself.

The intent of this section is to present the concepts of the holographic process. An extensive list of references on the holographic process and applications, as well as a complete development and discussion of parameter interrelationships and techniques is contained in our report on Phase I of this investigation.[1]

2.3 MAGNIFICATION THEORY

A convenient way of treating magnification effects in the holographic reconstruction process is to consider the hologram as being a combination of image generator and variable focal length lens. One may then apply conventional optical formulas to determine both image size and position. That this is indeed an accurate representation (to within the paraxial approximation) can be seen from the mathematical description of the reconstruction process that follows. As shown in Figure 1, an arbitrary object centered on the z-axis at position $(0, 0, -z_o)$ and illuminated with coherent radiation can be considered to produce a complex wavefront, U_s, in the recording plane $(x, y, 0)$.

$$U_s = A(x,y)\, e^{i\varphi(x,y)} \qquad (1)$$

This wavefront can be caused to interfere with a coherent spherical wavefront emanating from a point located at $(x_r, y_r, -z_r)$. This wavefront, called a reference wave U_r, can be described† as a constant amplitude with a quadratically varying

† See the Appendix

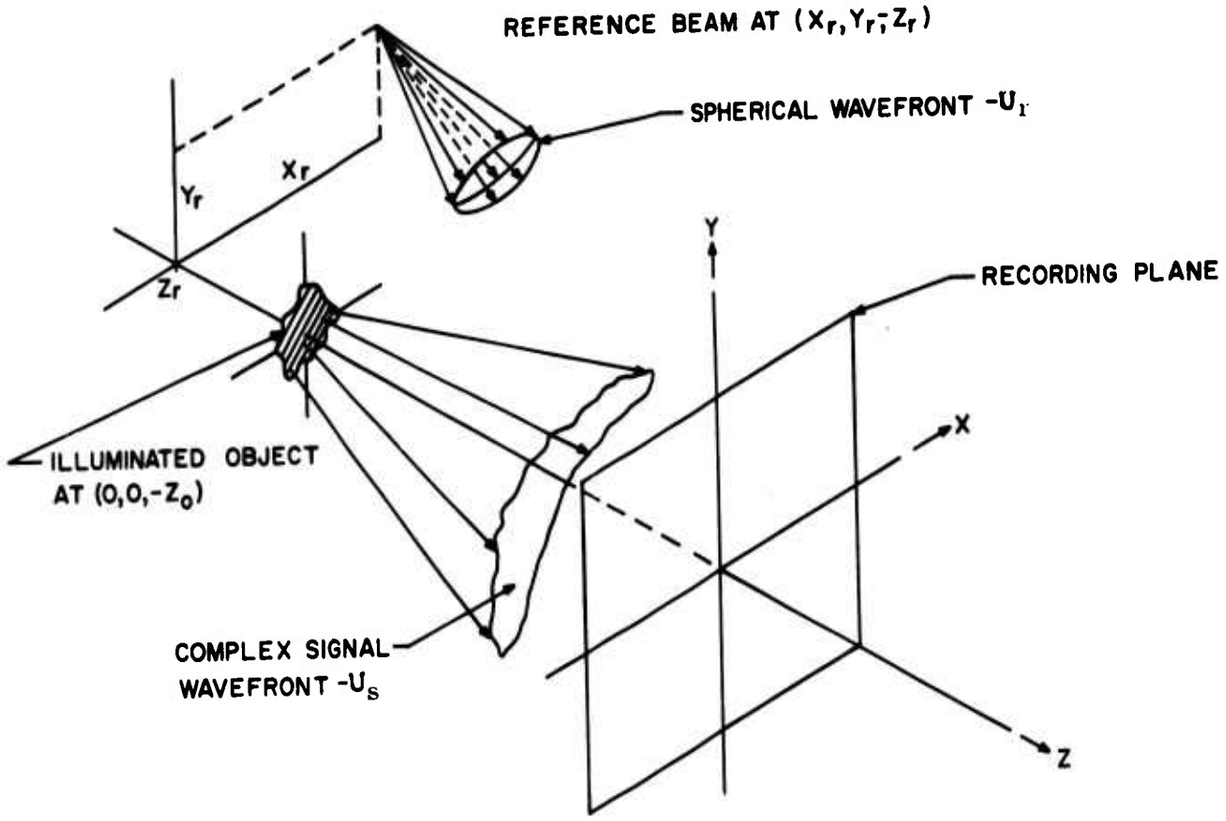

Figure 1. General Recording Configuration.

phase in the x-y plane. An additional linear phase term is included to account for the offset of the reference point from the z-axis. Thus the reference wave can be expressed as

$$U_r = B\, e^{\frac{ikr^2}{2z_r}}\, e^{-i\vec{k}\cdot\vec{r}} \tag{2}$$

The interference of this reference beam with the signal radiation produces an intensity distribution that is given by

$$UU^* = (U_s + U_r)(U_s^* + U_r^*)$$

$$= \left[A(x,y)\, e^{i\varphi(x,y)} + B\, e^{\frac{ikr^2}{2z_r}}\, e^{-i\vec{k}\cdot\vec{r}}\right]\left[A^*(xy)\, e^{-i\varphi(xy)} + B^* e^{\frac{-ikr^2}{2z_r}}\, e^{+i\vec{k}\cdot\vec{r}}\right]$$

$$= |A(x,y)|^2 + |B|^2 + A(xy)\, e^{i\varphi(xy)}\, B^* e^{\frac{-ikr^2}{2z_r}}\, e^{+i\vec{k}\cdot\vec{r}}$$

$$+ A^*(xy)\, e^{-i\varphi(xy)}\, B\, e^{\frac{ikr^2}{2z_r}}\, e^{-i\vec{k}\cdot\vec{r}} \tag{3}$$

If we assume that the amplitude transmittance of the exposed and processed photograph (now a hologram) is a linear function of the exposing intensity distribution, then

$$T_a = kt\, UU^* \tag{4}$$

Subsequent illumination of the hologram with another spherical wave U'_r will generate a wavefront that is the product of this amplitude transmittance and the readout wavefront. The amplitude of this new wavefront is

$$U'(xy) = U'_r(xy)\, T_a(xy) \tag{5}$$

In the special case where the readout wavefront is identical to the original reference wavefront the result is

$$U'(xy) = U_r T_a(xy) = Be^{\frac{ikr^2}{2z_r}} e^{-i\vec{k}\cdot\vec{r}} T_a = \left[kt\, Be^{\frac{ikr^2}{2z_r}} e^{-i\vec{k}\cdot\vec{r}} \right] \cdot$$

$$\left[|A|^2 + |B|^2 + A(xy)\, e^{i\varphi(xy)}\, B^* e^{\frac{-ikr^2}{2z_r}} e^{+i\vec{k}\cdot\vec{r}} \right.$$

$$\left. + A^*(xy)\, e^{-i\varphi(xy)}\, Be^{\frac{+ikr^2}{2z_r}} e^{-i\vec{k}\cdot\vec{r}} \right] \qquad (6)$$

The first two terms represented by

$$kt\, Be^{\frac{ikr^2}{2z_r}} e^{-i\vec{k}\cdot\vec{r}} \left(|A|^2 + |B|^2 \right) \qquad (7)$$

are a modulation of the readout illumination and contain no usable information. This is the zero-order or undiffracted wavefront. The third term, however, becomes simply

$$kt\, |B|^2\, A(xy)\, e^{i\varphi(xy)} \qquad (8)$$

which is identical to the original wavefront except for some constants affecting brightness. Hence, an observer would see an accurate reconstruction of the original object. This is a virtual image since the light appears to come only from behind the hologram.

The fourth term is the reconstructed real image of the original object (i.e., it can be focused on a screen). This is modified by two exponentials that introduce a combination lens and prism action on the image. This will be considered in greater detail later.

If the conjugate of the reference beam had been used for readout (i.e., a converging spherical wave rather than a diverging wave), then the fourth term would have produced an accurate real image. This image is pseudoscopic. The third term, the virtual image, would now be modified by a lens-prism combination.

In the more general case, readout can be accomplished with a spherical wavefront of different curvature and direction. Since we are dealing with a thick emulsion and hence must consider the Bragg effect, it is best to keep the direction of the spherical wave constant and vary only the curvature. We may express this readout wavefront as

$$U'_r(xy) = B\, e^{\frac{-ikr^2}{2z}}\, e^{-i\vec{k}\cdot\vec{r}} \tag{9}$$

where z is the location of the plane from which the light is diverging (i.e., negative z) or towards which it is converging (positive z). The reconstructed wavefront is now given by

$$U'(xy) = ktB\Big[(|A|^2 + |B|^2)\, e^{\frac{-ikr^2}{2z}}\, e^{-\vec{k}\cdot\vec{r}} + B^*A(xy)e^{i\varphi(xy)}\, e^{\frac{-ikr^2}{2}(\frac{1}{z}+\frac{1}{z_r})} + B\,A^*(xy)\, e^{-i\varphi(xy)}\, e^{\frac{-ikr^2}{z}(\frac{1}{z}-\frac{1}{z_r})}\, e^{2i\vec{k}\cdot\vec{r}} \Big] \tag{10}$$

The resulting images, real and virtual, are both modulated by exponential terms. It will now be shown that the quadratic exponential behaves as a thin spherical lens and the linear exponential as a deflecting prism.

It is well known that the effect of a lens is to introduce a phase shift onto an incident wavefront and thereby modify its curvature and direction. An expression for this phase shift can be obtained by considering what happens when a spherical wavefront is incident on a lens. As shown in Figure 2, a spherical wave originating at the axial focal point of a positive lens (z = -f) will be converted into a plane wave also traveling along the axis (neglecting diffraction). That is, this lens causes the transformation

$$A\, e^{\frac{ikr^2}{2f}} \rightarrow A \tag{11}$$

If we denote this transformation as an operator $T_{\ell+}$, we are saying that

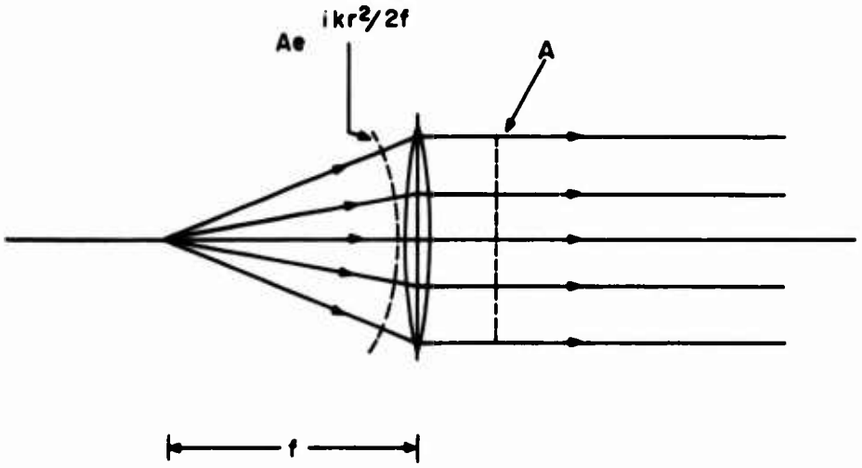

Figure 2. Transform Properties of a Lens

$$T_{\ell+}\left[A\, e^{\frac{ikr^2}{2f}}\right] = A \tag{12}$$

To satisfy this equation

$$T_{\ell+} = e^{-ikr^2/2f} \tag{13}$$

where f is the focal length of the lens. As a test, let us calculate what happens to a spherical wave emanating from an arbitrary point, z, in the object space of a lens of focal length +f (i.e., negative z). The resulting wavefront is given by

$$\begin{aligned} U &= T_{\ell+}\left[A\, e^{\frac{ikr^2}{2z}}\right] \\ &= e^{\frac{-ikr^2}{2f}}\, A\, e^{\frac{ikr^2}{2z}} \\ &= A\, e^{\frac{-ikr^2}{z}\left(\frac{1}{f}-\frac{1}{z}\right)} \end{aligned} \tag{14}$$

This is the equation of a converging spherical wave directed at the point z' where

$$\frac{1}{z'} = \frac{1}{f} - \frac{1}{z}$$

or

$$\frac{1}{z'} + \frac{1}{z} = \frac{1}{f} \tag{15}$$

This is identical to the classical lens equation relating image and object distances to focal length.

In the same manner, it can be shown that a negative lens has the transformation operator

$$T_{\ell -} = e^{+ikr^2/2f} \tag{16}$$

where f is understood to be the magnitude of the negative focal length.

If we wish to use the standard convention that the focal length of a positive lens is written as a positive number and that of a negative lens as a negative number, then in general

$$T_{\ell} = e^{-ikr^2/2f} \tag{17}$$

We may use the same analysis to determine that the effect of the linear exponential is to introduce an angular shift in the wavefront direction; i.e., it acts like a prism. In Figure 3 we see that a prism operates on an axial plane

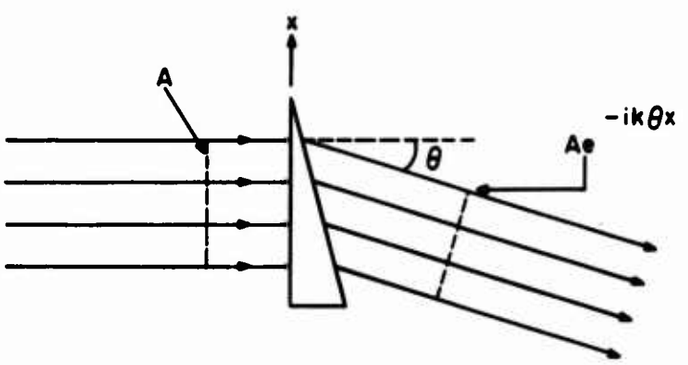

Figure 3. Transform Properties of a Prism.

wave, A, to produce a plane wave traveling at a direction θ to the axis. Such a plane wave may be written as $A\, e^{-ik\theta x}$.

$$T_p A = A\, e^{-ik\theta x}$$

or

$$T_p = e^{-ik\theta x} \tag{18}$$

In two dimensions, this becomes

$$T_p = e^{-i\vec{k} \cdot \vec{r}} \tag{19}$$

A negative exponential indicates a downward deflecting prism and a positive exponential an upward deflecting prism.

In view of these analogies we may now analyze the reconstruction expression of equation (10). The image terms are repeated below.

$$A(xy)\, e^{i\varphi(xy)}\, e^{\frac{-ikr^2}{2}\left(\frac{1}{z} + \frac{1}{z_r}\right)} \tag{20}$$

$$A^*(xy)\, e^{-i\varphi(xy)}\, e^{\frac{-ikr^2}{2}\left(\frac{1}{z} - \frac{1}{z_r}\right)}\, e^{-2i\vec{k} \cdot \vec{r}} \tag{21}$$

The virtual image term (20) can now be interpreted as the image resulting from an "object" $A(xy)\, e^{i\varphi(xy)}$ located at $(0, 0, -z_o)$ and being operated on by a lens of focal length, f_H, given by

$$\frac{1}{f_H} = \left(\frac{1}{z} + \frac{1}{z_r}\right) \tag{22}$$

This relationship is shown in Figure 4. The resulting image position and magnification can be determined by applying the conventional lens equations, using z_o as the "object" distance and f_H as the lens focal length. It should be noted that the focal length is either positive or negative depending on the

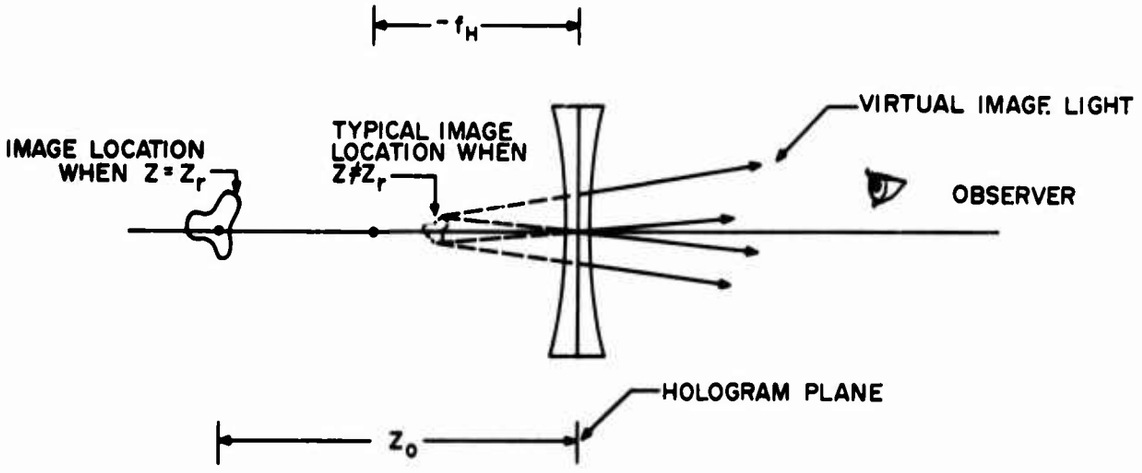

Figure 4. Lens Action During Virtual Image Reconstruction.

relative values (and signs) of z and z_r. As can be seen in Figure 5, the effective focal length of the hologram lens can be continuously varied from $+\infty$ to $-\infty$. In order to obtain focal lengths in the range $0 < f_H < z_r$, the readout illumination must be converging as it passes through the plate, i.e., $z > 0$.

According to the lens equation, the image position z', object position z_o, and focal length f_H are related by

$$\frac{1}{z_o} + \frac{1}{z'} = \frac{1}{f_H} \tag{23}$$

Solving this equation for z' and inserting the expression for f_H from (22), the position of the final holographic image is given by

$$\frac{1}{z'} = \left(\frac{1}{z_r} - \frac{1}{z_o} + \frac{1}{z}\right) \tag{24}$$

In the same manner, the lateral magnification is given by†

$$M = \frac{-z'}{z_o} = \left(1 - \frac{z_o}{z} - \frac{z_o}{z_r}\right)^{-1} \tag{25}$$

†Compare with equation (45) of the Phase I report, p. 41.

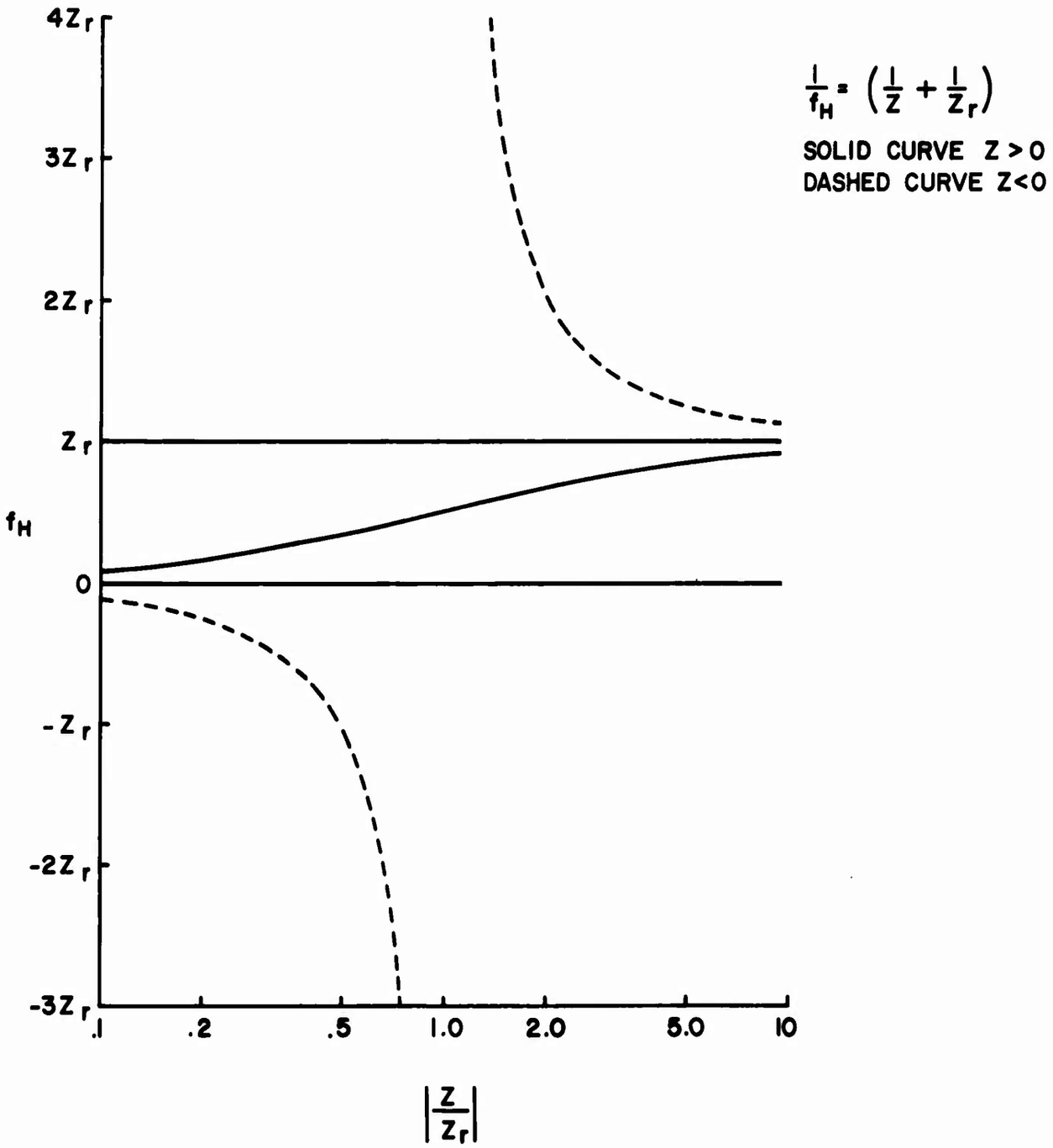

Figure 5. Variation of Focal Length with Reconstruction Radius of Curvature (Virtual Image Mode).

Because of the lens action, the image resulting from (20) is not necessarily a virtual image. This can be seen if we solve (23) for the image position.

$$z' = \frac{z_o f_H}{z_o - f_H} \tag{26}$$

While z_o is always positive (by lens convention), f_H may assume both positive and negative values (see Figure 5). For all negative values of f_H, z' is also negative and the image is virtual. When f_H is positive and greater than z_o, the image is likewise virtual. However, when $f_H < z_o$, the image becomes real. This switchover may or may not be advantageous in some systems applications.

The real image term (21) in the reconstruction is only slightly more difficult to interpret. As was shown in the previous report,† the complex conjugate of a wavefront produces a real image of the object generating that wavefront. The real image is located in a position that is symmetric to the original object with respect to the plane where the conjugate operation is performed. This is shown in Figure 6. In our case, the plane of symmetry is the hologram itself and the resulting image is formed at $z' = +z_o$. The first exponential in (21) indicates that before the image is formed at $+z_o$ it passes through a "lens" of focal length

$$\frac{1}{f_H} = \left(\frac{1}{z} - \frac{1}{z_r}\right) \tag{27}$$

This lens is located in the hologram plane. That is, the object that this lens operates on is located to the right of the lens as shown in Figure 7. Such an object is commonly termed a virtual object. This situation is similar to an optical system in which two lenses are in close proximity; i.e., the image from the first lens is directed towards the object space of the second lens. The variation in focal length with z is shown in Figure 8 and can be seen to be the negative of the curve in Figure 5.

†Phase I report, p. 119.

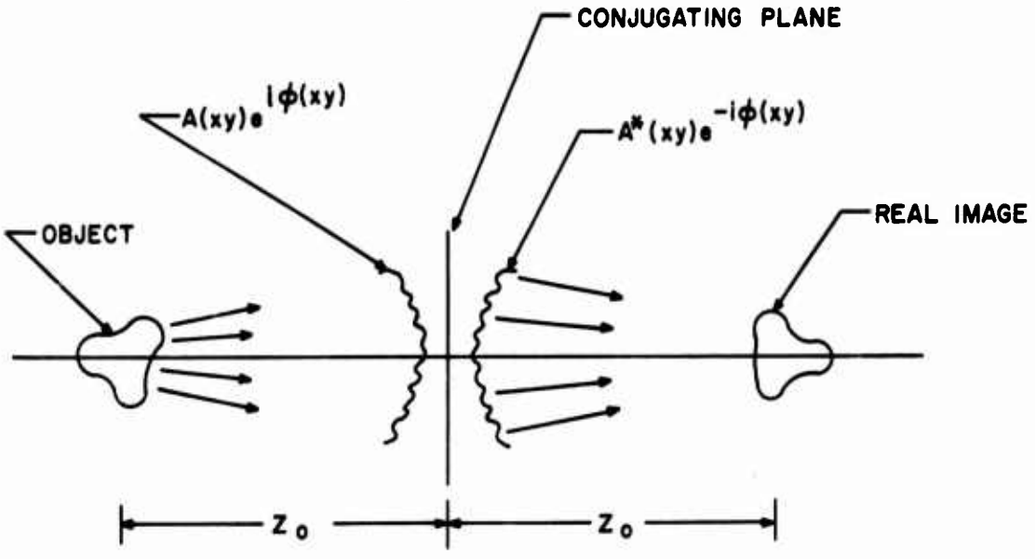

Figure 6. Conjugate Images.

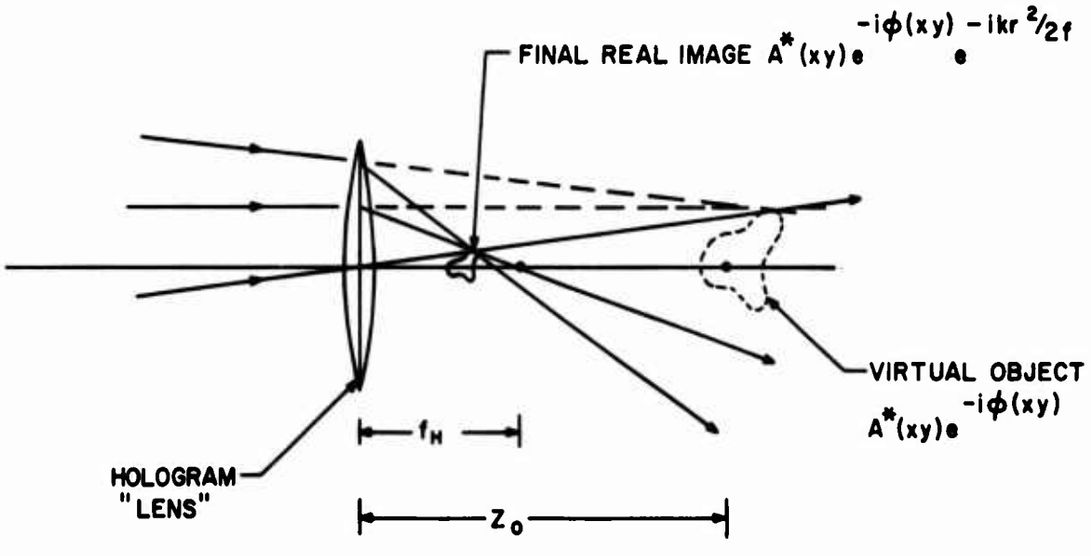

Figure 7. Lens Action During Real Image Reconstruction.

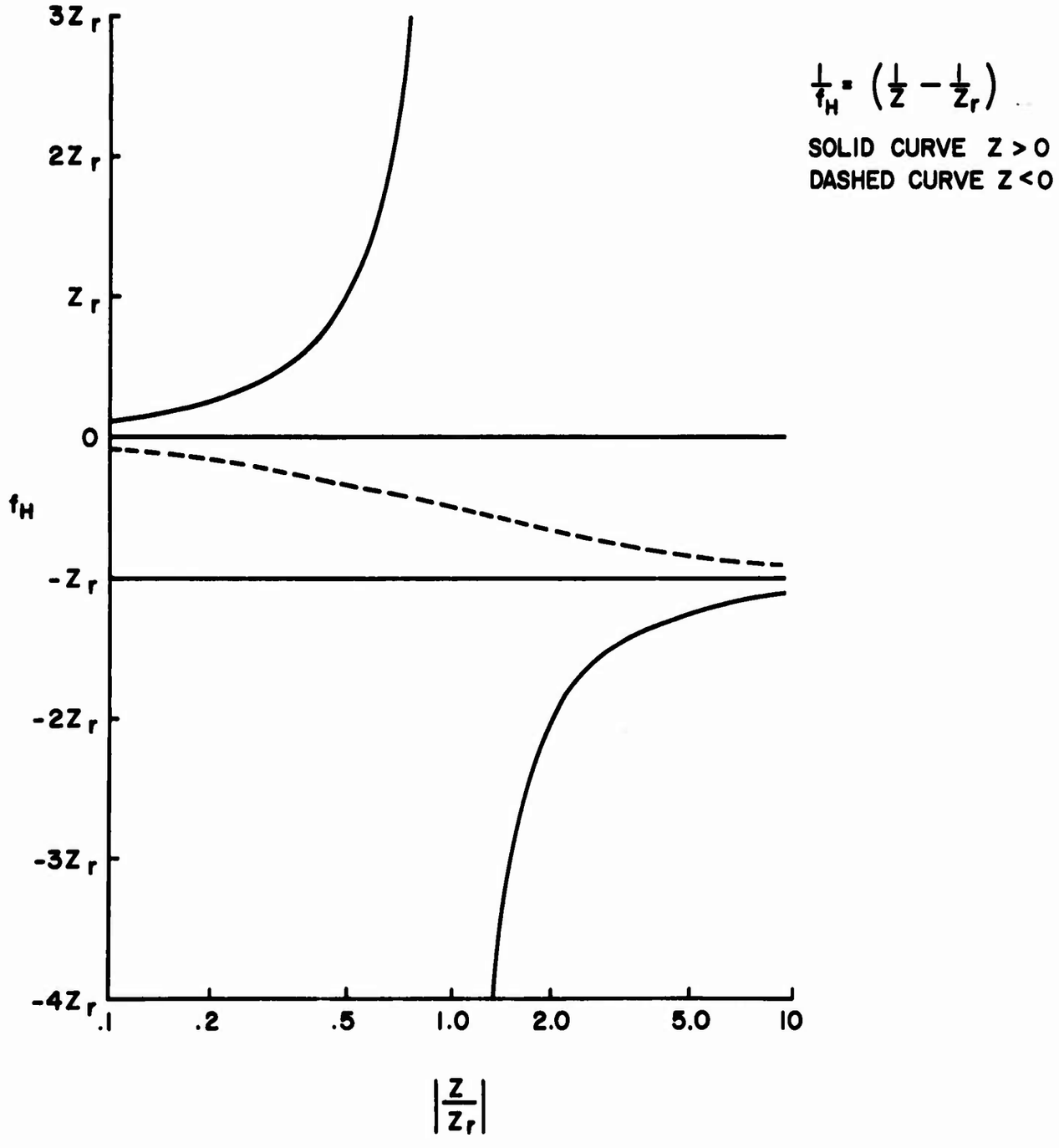

Figure 8. Variation of Focal Length with Reconstruction Radius of Curvature (Real Image Mode).

Using the lens equation as before, the final image position and magnification are given by

$$\frac{1}{z'} = \left(\frac{-1}{z_r} + \frac{1}{z_o} + \frac{1}{z}\right) \tag{28}$$

$$M = \left(1 + \frac{z_o}{z} - \frac{z_o}{z_r}\right)^{-1} \tag{29}$$

Again, due to the sign of f_H, the image may be either real or virtual.

The other exponential in (21) introduces a prism effect on the image wavefront, which causes an angular shift in its direction. This angle is twice the original reference beam angle for the case where the object is located on the z-axis. In general, the images from (20) and (21) are formed at equal and opposite angles to the readout beam direction.

This prism effect can be removed from the real image by illuminating the hologram from the opposite direction of the original reference beam (i.e., by rotating the plate 180°). At the same time, the Bragg effect due to the finite thickness of the emulsion can be minimized by inverting the curvature of the readout wavefront. In other words, if a diverging beam with the central ray at an angle θ to the axis is used as a reference, then a converging beam with its central ray at an angle $180 + \theta$ will produce a better real image. The image terms (20) and (21) now become

$$A(xy)\, e^{i\varphi(xy)}\, e^{\frac{-ikr^2}{2}\left(\frac{1}{z} + \frac{1}{z_r}\right)}\, e^{+2i\vec{k}\cdot\vec{r}} \tag{30}$$

$$A^*(xy)\, e^{-i\varphi(xy)}\, e^{\frac{-ikr^2}{2}\left(\frac{1}{z} - \frac{1}{z_r}\right)} \tag{31}$$

The prism effect now appears in the virtual image term but not in the real, as desired. The lens operating on the real image now has a focal length given by

$$\frac{1}{f_H} = \left(\frac{1}{z} - \frac{1}{z_r}\right) \tag{32}$$

The image position and magnification become

$$\frac{1}{z'} = \left(\frac{1}{z} - \frac{1}{z_r} + \frac{1}{z_o}\right) \tag{33}$$

$$M = \left(1 + \frac{z_o}{z} - \frac{z_o}{z_r}\right)^{-1} \tag{34}$$

Again, either a real or virtual image may be generated depending on the relative values of z, z_r, and z_o. The properties of the undeviated real or virtual images are summarized in Table I. The first two columns show the type and location of the images if they are reconstructed at unit magnification. The virtual image is obtained by using an illuminating wavefront equal to the original reference wavefront. The real image is obtained by using an illuminating wavefront that is the conjugate of the original reference wavefront and that passes through the hologram in the opposite direction (i.e., to remove the "prism" effect as previously discussed). These images become the virtual objects for the hologram lens that occurs when the illuminating and reference wavefronts have different curvatures. By the lens convention of signs these images are located at $+z_o$ and $-z_o$ respectively. The third column is the effective focal length of the hologram lens, f_H. The variable z can assume all values -- positive and negative. A positive z indicates converging light, and a negative z indicates diverging light. The final image position is determined from the lens equation using f_H and the virtual object position. The resulting image magnification is the negative of the final image position divided by the virtual object position.

Since the magnification can be either positive or negative depending on the relative values of the parameters, the resulting image can become either real or virtual. The last two columns show the conditions on the effective focal length (f_H) and hence the center of curvature of the wavefront (z) necessary to produce either a real or virtual final image. As an illustration, Figure 9 is a plot of the magnification as a function of center of curvature position (z) when the initial image is a real image (lower half of Table I). This curve shows that when the

Table I. Summary of reconstruction parameters and image types.

Reconstruction at unit magnification $z = \pm z_r$		Reconstruction with magnification $-\infty < z < +\infty$					
Image type	Image position	Focal length $1/f_H$	Image position $1/z'$	Image magnification $1/M$	Final image type	Conditions for image type	
						f_H	z
virtual	$-z_o$	$\frac{1}{z}+\frac{1}{z_r}$	$\frac{1}{z}+\frac{1}{z_r}-\frac{1}{z_o}$	$1-\frac{z_o}{z}-\frac{z_o}{z_r}$	real	$0<f_H<z_o$	$0<z<\frac{z_o z_r}{z_r-z_o}$
					virtual	$z_o<f_H<\infty$	$\frac{z_o z_r}{z_r-z_o}<z<\infty$
							$-\infty<z<-z_r$
						$-\infty<f_H<0$	$-z_r<z<0$
real	$+z_o$	$\frac{1}{z}-\frac{1}{z_r}$	$\frac{1}{z}-\frac{1}{z_r}+\frac{1}{z_o}$	$1+\frac{z_o}{z}-\frac{z_o}{z_r}$	real	$0<f_H<+\infty$	$0<z<z_r$
						$-\infty<f_H<-z_o$	$z_r<z<\infty$
							$-\infty<z<-\frac{z_o z_r}{z_r-z_o}$
					virtual	$-z_o<f_H<0$	$-\frac{z_o z_r}{z_r-z_o}<z<0$

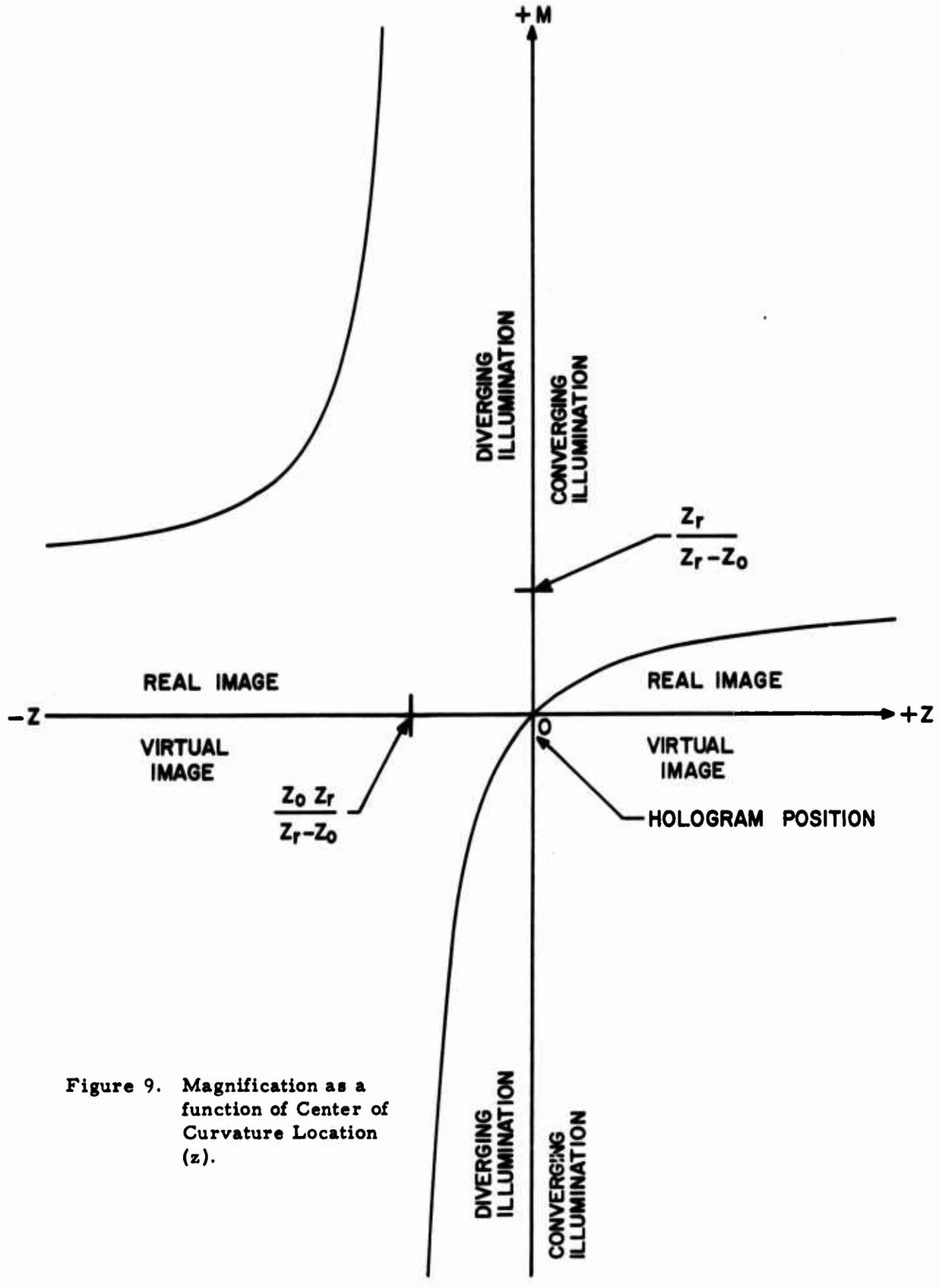

Figure 9. Magnification as a function of Center of Curvature Location (z).

center of curvature of the readout illumination is at $z = -\infty$ the resulting image is real with a magnification of $z_r/(z_r - z_o)$. As the center of curvature moves towards the hologram (diverging light), the image remains real and its magnification increases. At the same time the image moves away from the hologram plane towards $z' = +\infty$. When $z = z_o z_r/(z_r - z_o)$, the image becomes virtual with large magnification The virtual image size decreases as the point approaches the hologram and goes to zero when the center of curvature is on the hologram plane. As the center of curvature passes through the hologram plane (now converging light), the image becomes real. The image remains real and increases in size as the point moves away from the hologram. As the center of curvature approaches $z = +\infty$, the magnification approaches $M = z_r/(z_r - z_o)$ -- the same value at which the process started. The readout illumination is now a plane wave and the entire cycle can be started over again with no discontinuities.

From this we see that the image magnification, and simultaneously the image position, can be varied continuously between $\pm\infty$ by changing the curvature of the readout illumination. This effect will be used in the simulation system to provide range change information. A later section will discuss the design of a lens system to vary the curvature of the readout illumination so as to utilize part of this effect.

3. GOALS

The general goals of Phase II of this contract were to study the various modes and techniques derived from Phase I and other suitable techniques, and to select one of these techniques as the basis for designing and building a holographic head-up display feasibility model. The important factors that were considered are image quality, brightness of final image, maximizing the changes possible in the degrees of freedom of the image, and minimizing overall package size. The selection of the most feasible system was influenced by our desire, if possible, to have a system that would be compatible with existing equipment in the aircraft. Graphical and/or numerical data within the holographic display and interfacing questions were not studied.

The major effort was devoted to building a laboratory model encompassing the best features of the Phase I concepts. These include holographic range and perspective changes. New means to change pitch, yaw, and roll of the image were investigated. Initially, the control of these parameters would be completely manual. Size was not to be a dominant factor, except that efforts were made to make the unit as compact as possible. Other problems, such as packaging, weight, suitability in an aircraft environment, cost, and psychological factors, were considered but not studied during the contract.

The design goals of the display for the various parameters and the ranges of parameters to be included in the model are listed below. Differences that occur will be explained in a later section. All manipulations are to be done under manual control, and no provision was made to project the image to infinity.

View Parameter	System Goals	Model Design Goals
Range	32X size change	15X
Perspective view	$\pm 14^{\circ}$ horizontal	$\pm 14^{\circ}$
	$\pm 3^{\circ}$ vertical	$\pm 12^{\circ}$
Pitch	$\pm 10^{\circ}$	$\pm 5^{\circ}$
Yaw	$\pm 10^{\circ}$	$\pm 5^{\circ}$
Roll	$\pm 15^{\circ}$	$\pm 15^{\circ}$

In summary, the goal was to investigate holographic techniques in conjunction with optical, mechanical, and electronic techniques to display and manipulate an image of an aircraft carrier in the six degrees of freedom to simulate a real-world situation.

4. DESCRIPTION OF POSSIBLE APPROACHES AND TRADE-OFFS

4.1 INTRODUCTION

The availability of either a real or virtual image from a hologram made it possible during Phase I to structure a display system along two parallel routes. Although the virtual image is more pleasing and realistic to view, it must be removed to or near infinity in order to satisfy the requirements of eye accommodation. Once this is done, it no longer matters whether the original image were two- or three-dimensional so long as the image can be changed in perspective. In fact, a three-dimensional image would be of no use, and even dangerous, if it were located so that the pilot could change perspective view by just moving his head. The perspective view should change only with changes in the relative position of the aircraft and aircraft carrier. In developing a system along these two routes, it was soon determined that each image favors a different subset of the required degrees of freedom. For example, range change is easier to accomplish with the virtual image, and glide path select is easier with the real image. Consequently, neither approach appeared to have a clear-cut advantage over the other. In view of this, both systems will be described here and their trade-offs indicated. In addition, two nonholographic systems will be proposed. A new system will then be discussed that combines the better features of all these systems. This is the result of Phase II and is the concept upon which a feasibility model was fabricated.

4.2 VIRTUAL IMAGE MODE

In structuring a display system around a holographically created image, the question arises as to how much manipulation can be performed with the hologram itself. In this way our reliance on conventional optics can be minimized as long as it is not done at the price of undue complications.

In utilizing the virtual image, therefore, attention was immediately directed toward what was considered the key problem: simulating range change. Since it had already been determined that this simulation can be accomplished through image magnification alone, a means to provide this via the hologram

must be found. It turns out that the virtual image becomes magnified if the radius of curvature of the readout illumination is different from the radius of curvature of the original reference beam.

Although this technique does indeed produce magnification, there is also associated with it a proportional change in image position. The net effect of this is that with respect to the hologram plane, there is no increase in the angular size of the virtual image; that is, if we double the size of the image, it moves twice as far away from the plate, but the angular size remains constant. An observer in the hologram plane would therefore see no change in the image size since it is angular magnification that is perceived by the eye. Fortunately, however, one cannot conveniently view the image from the hologram plane. Because of this, the image position with respect to the actual observation plane is no longer directly proportional to its size. Under these circumstances a change in angular size can then be seen. This change is restricted by the geometry to provide only image demagnification. In this case the largest image would be identical in size to the original object. In order to utilize this in a display system, the hologram must be generated from a location, which is scaled with respect to the object and which represents the closest approach to be simulated. One can then start with a highly demagnified image and continually increase its size by this technique so as to represent decreasing range.

A means for changing the curvature of the readout wavefront is shown in Figure 10, which is a schematic representation of a virtual image system. It involves the translation of a short focal length microscope objective between the lens plane and focal plane of a second longer focal length lens.

It is generally known that the virtual image from a hologram provides different perspective views of the image as the observer changes his viewing orientation. The total perspective change possible is limited by the hologram size and the hologram-object separation. The pilot however, cannot move his head to do this; in fact, he should not be allowed to do so as it could provide him with false information. Hence a means must be found to move the hologram so that he looks through the section corresponding to his glide path. While a simple translation of the hologram in two dimensions perpendicular to the line of sight

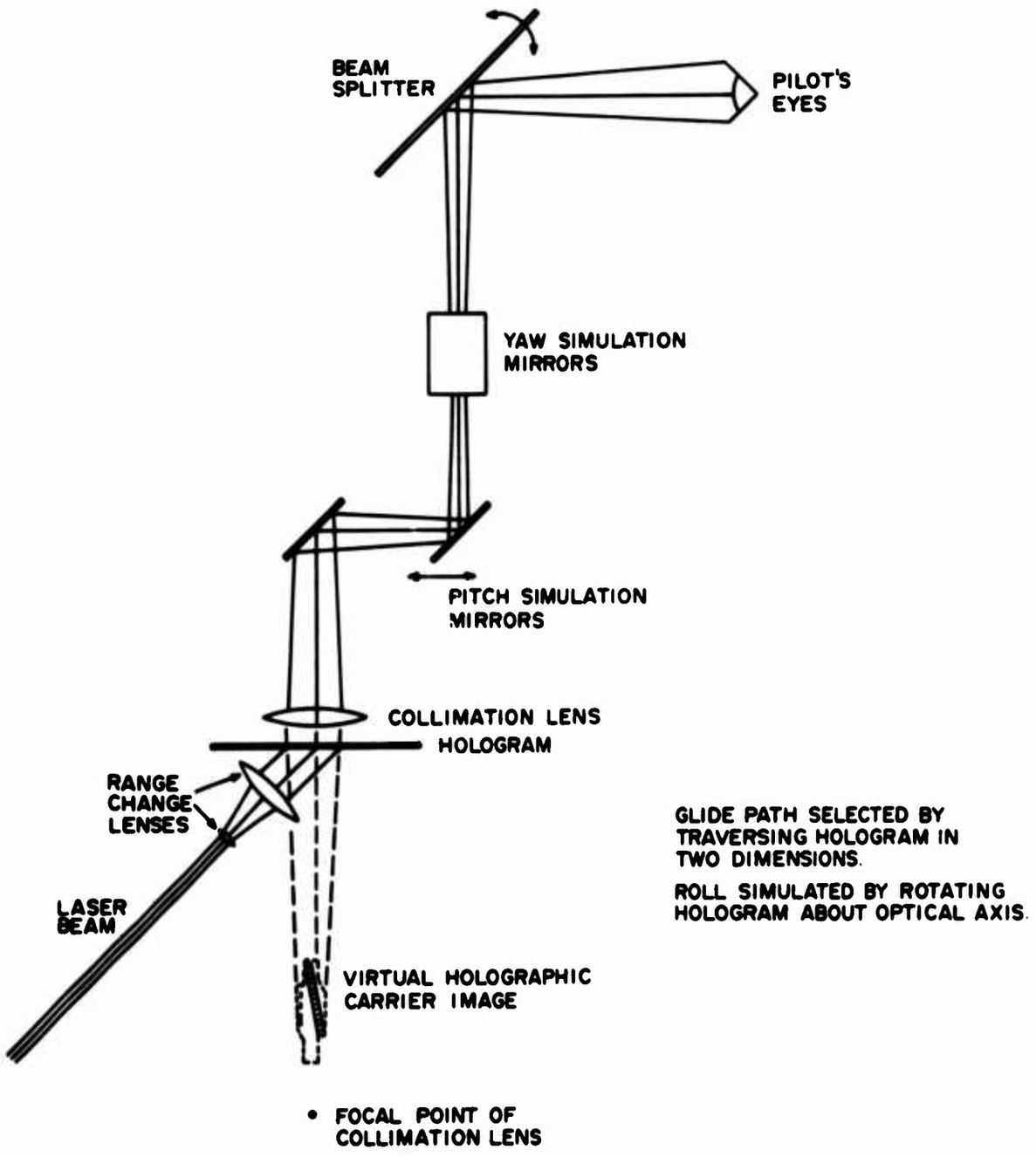

Figure 10. Complete Simulation System Using the Holographic Virtual Image.

causes the view to change (as seen through a small window) there is associated with this a corresponding image translation. This requires the observer to move his head in order to see the image through the fixed window. This problem can be reduced if the hologram is constrained to move on the surface of a sphere having its center located at the image position.

Figure 11 illustrates one configuration that was considered for directly manipulating the virtual holographic image to achieve perspective changes. Also included are the range change optics. For clarity the diagram is broken down into three composite diagrams (Figures 12a, b, c) which, when superimposed, make up Figure 11. Figure 12a is the basic optical system used to illuminate the hologram with the coherent reconstruction beam. The smaller of the two lenses is movable along its axis (as will be illustrated later); the larger remains fixed with respect to the hologram. The larger lens must be large enough to illuminate uniformly the entire area of the hologram. Together, the fixed and the movable lens comprise the range change optics by providing a variable curvature of the wavefront. To change the perspective angles in the image, the hologram and the variable divergence angle optics are mounted to a frame that is gimballed to rotate through limited angles about a point corresponding to the center of the virtual image. The frame is represented by the irregular outline; the frame gimballing will be illustrated later. The frame is shown displaced in the plane of the paper through an angle, θ. Since the virtual image is to be viewed directly, a large, high-power laser is required to illuminate the hologram. The laser is too large and hence must be external to the frame in a fixed location. To bring the laser beam into the moving assembly, an arrangement of two movable mirrors is required. Both mirrors are gimballed in two axes and are driven by parallelogram linkages as shown. The first mirror, whose vertex corresponds to the center of the image (and the frame gimbal center), is mounted to a carriage that moves normal to the hologram with respect to the movable frame; in actuality, it stands still while the frame translates with respect to it. Since the distance between the mirror vertices changes as the frame translates, the link that connects the two mirror gimbals and their associated parallelogram linkages must telescope while maintaining its four pivot points collinear.

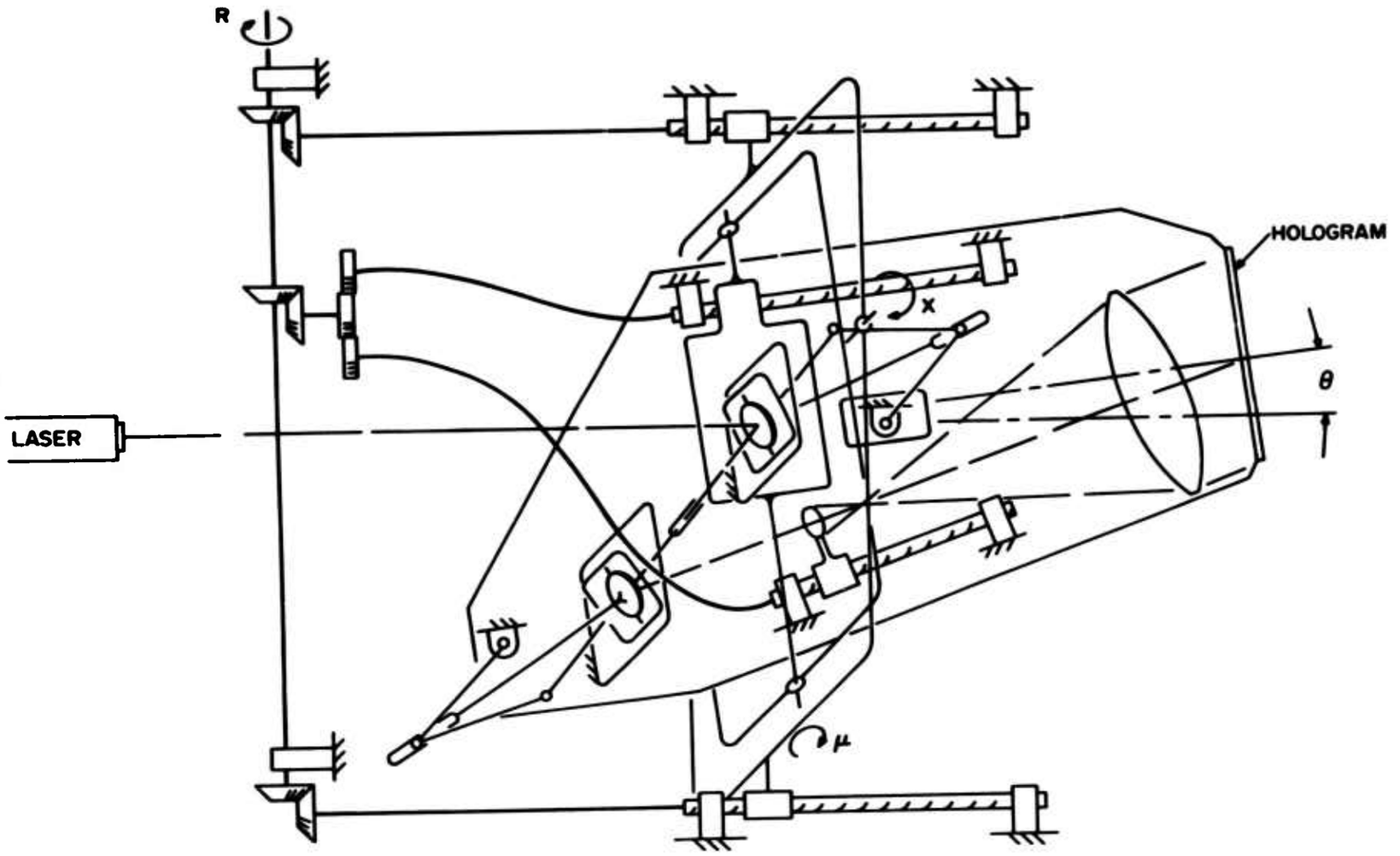

Figure 11. Virtual Image Holographic Display Mechanism.

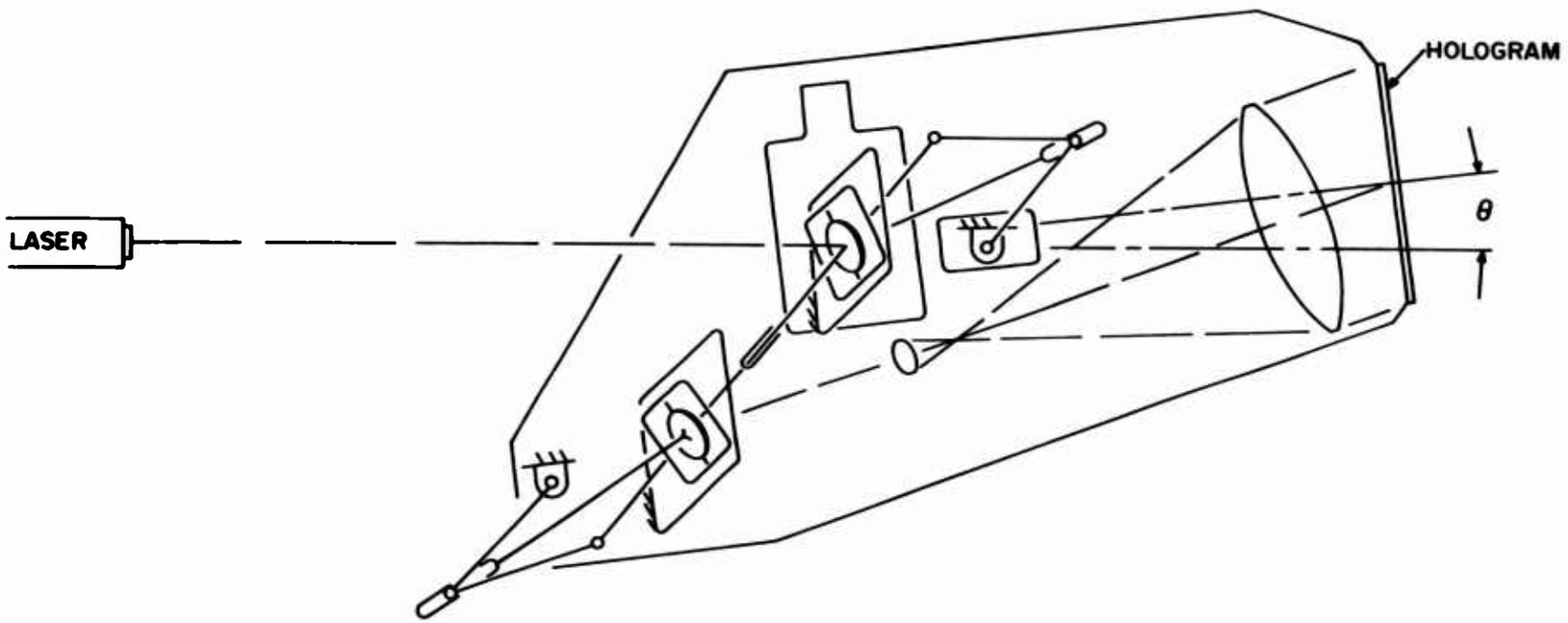

Figure 12a. Basic Optical System Used to Illuminate the Hologram.

Figure 12b shows the linear drive for the first mirror carriage and for the small traveling lens used to alter the radius of curvature of the reconstruction beam and thereby minify the image. The linear drive on the mirror corresponding to the center of the image is necessary because, as the image minifies, it moves closer to the hologram. These two linear drives are represented in the diagram as lead screws set in bearings attached to the frame. In actuality at least one of these drives would be a cylindrical cam rather than a constant-pitch screw, since in this system the image size and position is not a linear function of displacement of the traveling lens. These two linear drives are driven by flexible shafts (to permit rotational and translational motion of the frame), the driven ends of which are attached to spur gears that are in turn driven by a common pinion. Rotation of this pinion affects the variable magnification, or range change, and is independent of frame rotation.

Figure 12c shows the gimbal arrangement that permits the angular perspective changes. Note that the gimbal supports the carriage carring the first mirror, corresponding to the center of the holographic virtual image. This ensures that the image remains laterally fixed in space during perspective changes. Since the image will ultimately be collimated to infinity, it is permissible to allow the image to translate along the longitudinal axis and hold the eye-to-hologram distance constant. This reduces the volume that the gimballed frame sweeps out in its excursions. In order to hold the eye-to-hologram distance constant, the entire gimbal frame must translate longitudinally with respect to the frame during range change. Figure 12c shows the lead screws for doing this. These lead screws and the other range change functions are coupled to a common drive shaft by means of bevel gears.

The display mechanism, as described this far, serves only to provide for three of the six degrees of image freedom: the two angular perspective changes and range change. In order to provide changes in the depression angle and azimuth angle of the observer's line-of-sight (relating to pitch and yaw of the aircraft), the entire mechanism could be mounted on a carriage that would translate left and right or up and down in the observer's field of view. This would

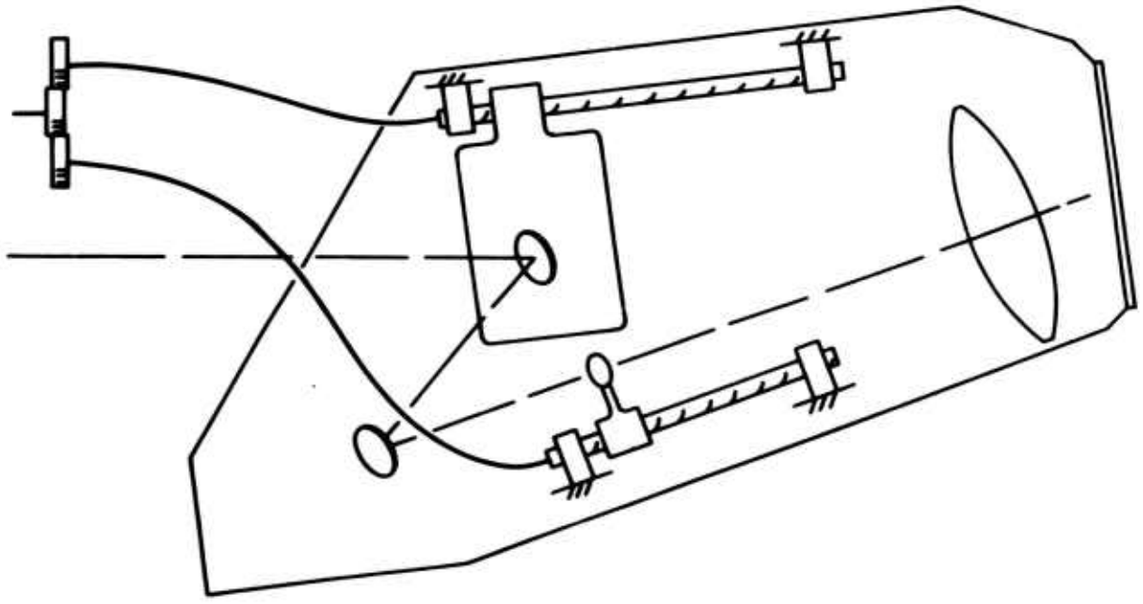

Figure 12b. Linear Drive for Traveling Lens for Range Change.

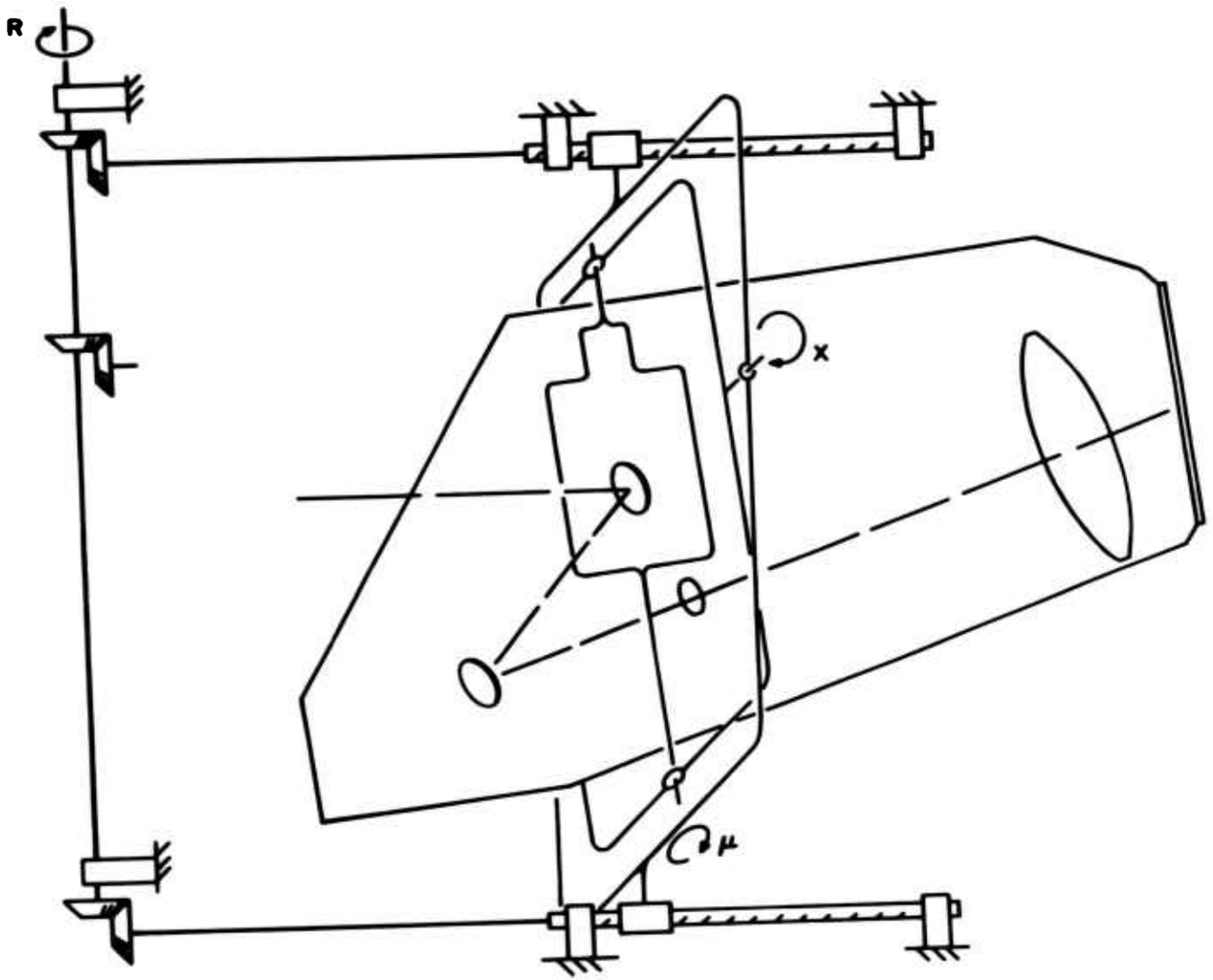

Figure 12c. Gimbal Arrangement for Angular Perspective Changes.

necessitate another set of mirrors to bring the laser beam into the mechanism from its fixed external source.

It is also possible to achieve pitch and yaw simulation by utilizing the fact that the hologram can be considered to be a grating. Since the grating equation must be satisfied at all times, the readout beam can be introduced at an angle different from that of the original reference beam. This causes the image to appear in a different angular position. For small angles these effects are almost equal. While this effect certainly occurs, we must also remember that the hologram is really a three-dimensional grating, and hence the Bragg condition must also be satisfied. This results in the image intensity's being related to the difference between the original reference angle and the readout angle (in addition to other factors). The relationship is such that the reconstructed amplitude follows a sin x/x curve as the angular difference is increased. The useful range over which the sin x/x curve can be used is determined by the initial carrier frequency of the hologram. Low frequencies allow a large angular change before the image is extinguished at the first minimum of the sin x/x curve. At 45°, for example, the image becomes extinguished at $\pm 5^{\circ}$ rotation, which of course is less than our estimated requirement of $\pm 10^{\circ}$. This technique introduces other problems: how to direct the light from this angularly repositioned image to the pilot's eyes, and, in addition, how to incorporate this with the range change technique. Consequently, the original design provided pitch and yaw simulation by the use of mirrors as shown in Figure 10.

In this configuration, the image is translated over the field of the windscreen by a set of mirrors that move in two dimensions. At the same time, the beam splitter is pivoted so that the image rays are always directed to the pilot's eyes.

The last degree of freedom, roll, represents a rotation of the image with respect to a frame of reference fixed in the windscreen. This is accomplished by rotating both the hologram and readout beam about the optic axis. This axis is directed from the image through the center of the window and remains fixed. The reason for rotating the readout beam is to allow the Bragg equation to be satisfied at all times.

Figure 10 also shows the inclusion of a collimating lens used to project the virtual image out to a distance that will minimize accommodation requirements. The only constraint on this lens is that its focal length must be quite large. This is to reduce magnification distortions that would be encountered when a three-dimensional object is located inside the focal plane of a lens.

In regard to the utilization of this technique in a head-up display system, the following conclusions should be considered.

1. The pilot will view an aerial image, the brightness of which will be directly proportional to the output power of the laser. High-power lasers operating in the visible spectrum are quite large and difficult to maintain.
2. Some "peep-hole" effect will result from the need to present a view of only one glide path at any given time.
3. Range change simulation can be accomplished by changing the curvature of the readout illumination. This is a continuous effect.
4. Glide path information (perspective view) requires a simultaneous translation and rotation of the hologram. The mechanical device to perform this function will have to be desiged to withstand airborne operations.
5. Pitch and yaw simulation requires a synchronized motion of mirrors and combining glass. A nonrigidly mounted combining glass may not be acceptable.
6. Roll simulation requires a mechanical rotation of the hologram mount and illuminating optics (and possibly the light source).
7. Projection of the virtual image to infinity is complicated by the fact that the image location changes as the image is magnified. Consequently, the collimating lens must also move.

4.3 REAL IMAGE MODE

The other holographic image, the real image, can also be used to simulate the required degrees of motion. Since this image is pseudoscopic, it must be displayed on a screen in order to be viewed. The resulting two-dimensionality of this image would be objectionable if it were not for the systems requirement that the image be projected to near infinity. When this is done, the image exhibits the desired realism and in many cases cannot be distinguished from a similarly projected virtual image.

The manner by which a real image is reconstructed from a hologram can be done in such a way that two of the degrees of motion are easily simulated. These are the angles that determine the perspective view corresponding to the aircraft's position with respect to the carrier (the glide path of the aircraft). The recording process is such that an arbitrarily located area element in the hologram receives and stores information about only one particular perspective view of the object. This is the view corresponding to the angular direction of the area element with respect to the object. Consequently, if only this area is illuminated in the reconstruction process, then the resulting image will appear as if it were being viewed from that direction. In a similar manner the interrogating beam can be moved over the entire surface of the hologram and hence create an image that can be continually varied in perspective.

A convenient way of doing this is shown in the systems drawing of Figure 13. In this method, the laser beam can be positioned to location on the hologram by means of a mirror that is pivoted about two orthogonal axes. The resulting image is displayed on screen A-A. It should be noted that in order to reconstruct a real image from every location in the hologram plane, the grating equation must be satisfied at all points. This is usually done by illuminating the hologram with a beam of light having a radius of curvature that is the opposite of the original reference beam. In addition the beam must be incident on the hologram from the opposite direction; that is, a diverging reference beam must become a converging beam for reconstruction. In order to provide this for the

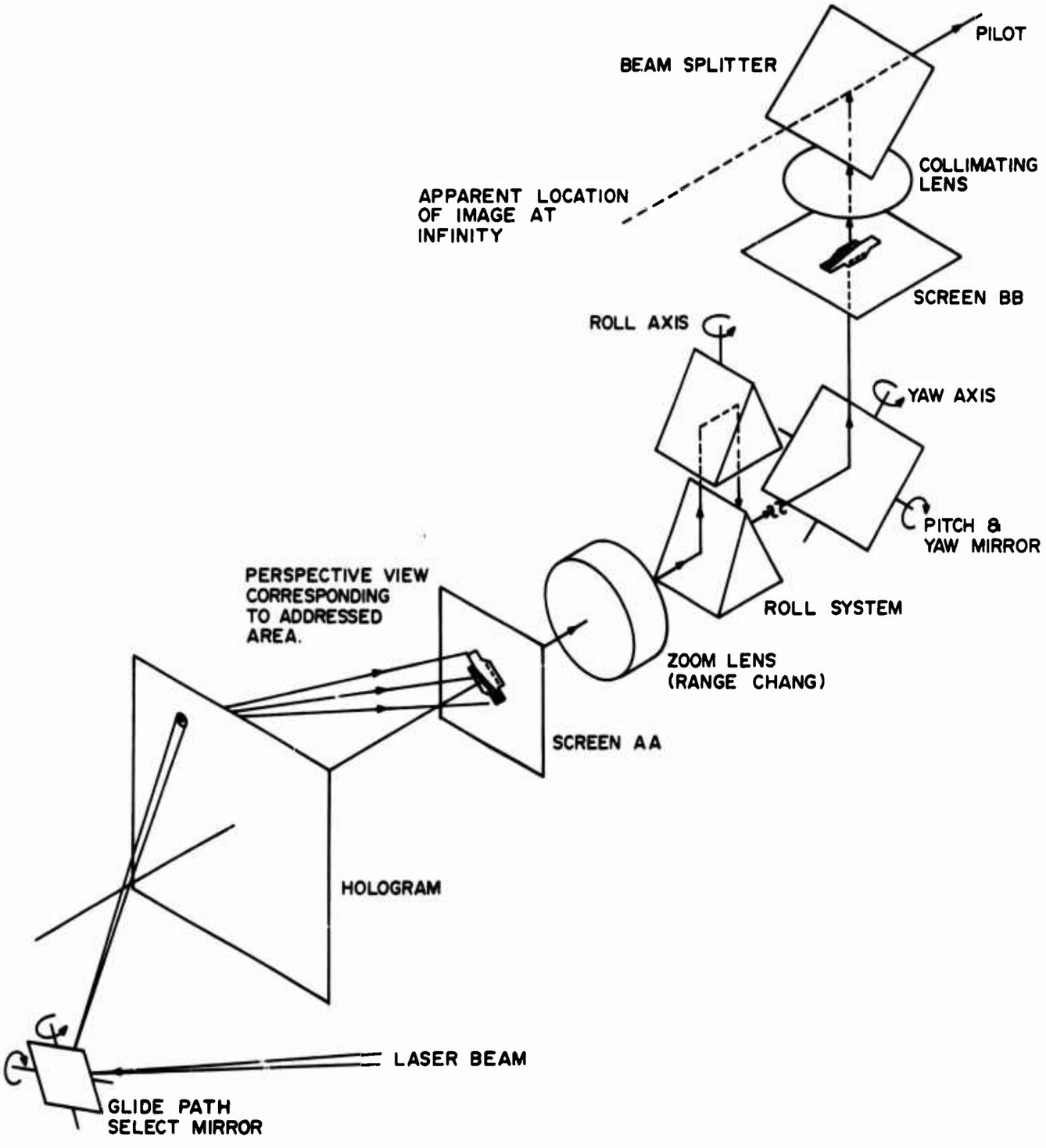

Figure 13. Real Image Display System.

system, the writing configuration must be modified. This modification amounts to using a converging reference beam with its points of convergency located at the point where the pivoted mirror will be placed. (A diverging reference beam is normally used in the recording process in conventional holography.)

Since we are dealing with a three-dimensional real image that must be displayed on some type of viewing screen, it is necessary to provide sufficient depth of focus. This can be done in a manner analogous to conventional optics by stopping down the lens. In this case the effective hologram "lens" is stopped down by reducing the diameter of the illuminating beam. While this produces the desired degree of focus, a secondary effect begins to appear. That is, the image begins to lose continuity and starts to break up into what is called a speckle pattern. As a result, good depth of focus is obtained only at the sacrifice of image continuity.

Because of the difficulty in controlling this effect, the simulation of range change by manipulating the curvature of the illuminating wavefront is not easily implemented. In addition, associated with the magnification resulting from this technique, there is a corresponding shift in the image location. This would require the viewing screen to translate as the image is magnified in order to maintain focus.

Although this technique was considered further in this phase, the preliminary design utilized more conventional optics. This is the incorporation of a zoom lens into the system. Such a lens will act on the displayed real image to magnify and relay it to a second viewing screen. Control of this lens will be derived from the carrier-to-aircraft telemetry.

Simulation of the pitch and yaw motion of the aircraft requires that the displayed image be translated over the surface of the viewing screen. While this may be possible by using the grating effect as discussed for the virtual image, the magnitude of this effect is, as yet, not large enough. A particularly simple means for simulating pitch and yaw is to introduce a mirror between the zoom lens and the

final viewing screen. Pivoting of this lens would allow the magnified image to be positioned to a location on the screen corresponding to the attitude of the aircraft.

The final degree of freedom, aircraft roll, can be simulated in the same manner as for the virtual image. This is a rotation of both the hologram and the readout beam about an axis passing through the reconstructed image and normal to the viewing screen. Another possibility is to use the device shown in Figure 13. This device is the mirror equivalent of a dove prism. As in the virtual system, a collimating lens is introduced to reduce the need for changes in eye accommodation when actual visual contact is established.

In regard to the utilization of this technique in a head-up display system the following conclusions should be considered.

1. As with the virtual system, image brightness is directly related to laser power. In addition, the presence of diffusing screens further reduces image brightness.
2. A trade-off between image quality and depth of focus is required.
3. Range change simulation by changing the curvature of the readout illumination will require the diffusing screen to translate in synchronization.
4. Range change simulation by conventional zoom optics may require an excessive separation between object and image screens.
5. Glide path select by addressing various locations on the hologram causes the image-forming light to strike the diffuser at many different angles. Image intensity will not be constant since the zoom lens sees only the light directed along the forward axis.
6. Pitch and yaw simulation require the pivoting of a single mirror element.
7. Roll simulation is accomplished by either a mechanical rotation of the hologram and illuminating optics or by rotating the image with mirrors.

8. Projection of the image to infinity is simplified since it is now two-dimensional and does not move.

4.4 NONHOLOGRAPHIC MODES

4.4.1 Television Link

A carrier model and a TV camera on board the aircraft carrier offer another method of performing the simulation without the use of holography. The TV camera is focused on the carrier model. The model and camera are manipulated so that the camera receives an image identical to the image that the pilot sees during his approach to the carrier. The appropriate image of the carrier is transmitted to the landing aircraft via a television link. The television picture in the aircraft is presented on the same head-up display the pilot already has for presenting symbolic information.

The roll, pitch, yaw, range, and glide path of the aircraft are known on the ship by means of radar and communication links between aircraft and ship. All this information is fed to a TV camera, which is focused on a model of the carrier as shown in Figure 14. The camera mount permits the camera to be moved to the right or left and up or down about a pivot point located in the center of the carrier model. This motion permits the selection of the glide path of the aircraft. To simulate the pitch and yaw of the aircraft, the camera is mounted in a gimbal arrangement that permits the camera to pitch and yaw exactly as the aircraft is doing. The pitching and yawing of the camera moves the image up or down and to the right or left on the pilot's CRT or beam splitter. Roll is simulated by rotating the camera about its optical axis. Range change or image size is controlled by a zoom lens mounted on the front of the camera.

To add additional realism to the simulation, the carrier model could also be mounted in a gimbal arrangement. The model could then be made to pitch, yaw, and roll with respect to the camera exactly as the real ship is doing with respect to some fixed frame of reference.

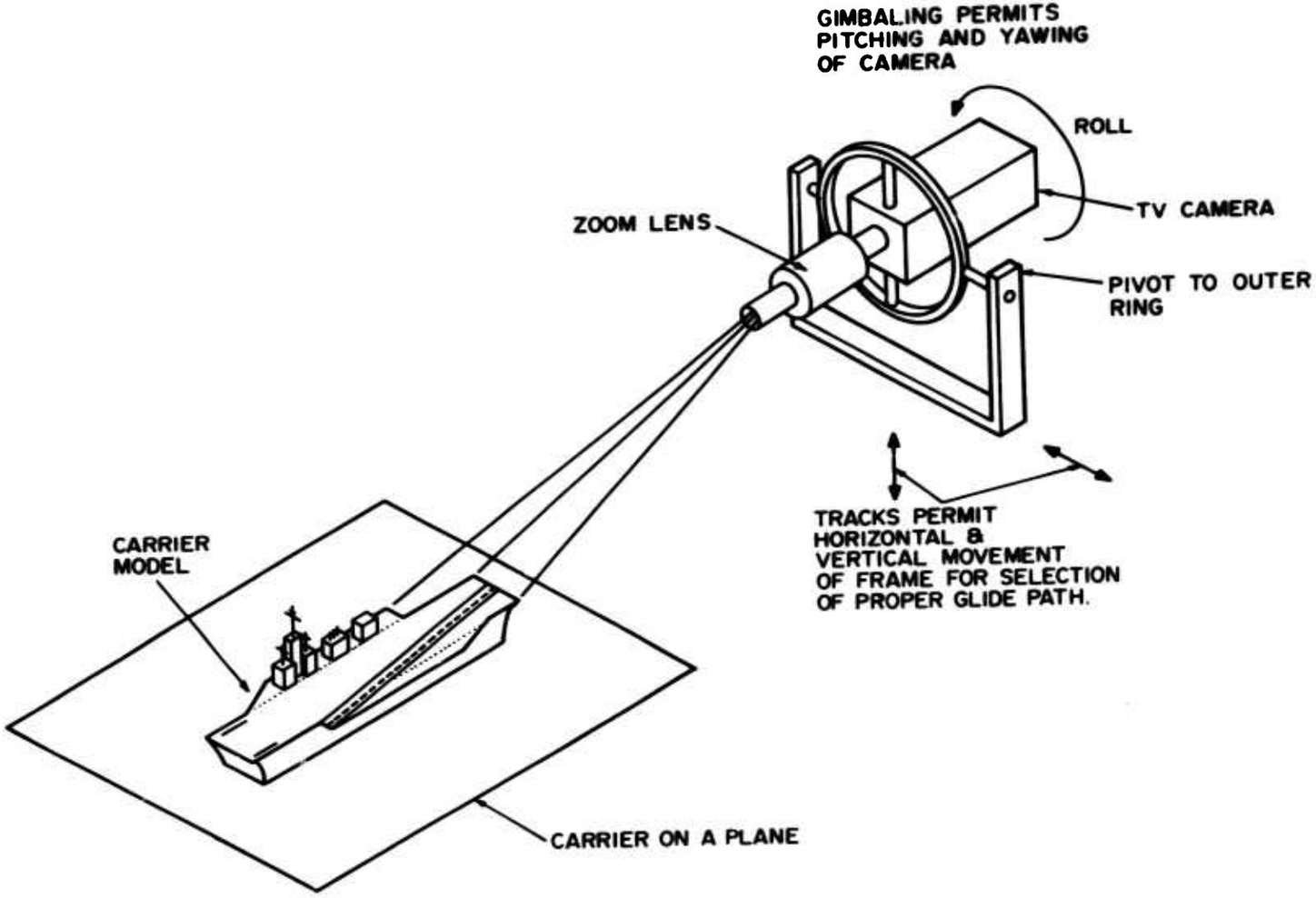

Figure 14. TV Link Head-Up Display System.

In the implementation of this type of system one must take into consideration the bandwidth of the data link necessary to transmit this information. In addition, a means must be devised to control more than one aircraft in the approach cone. This may require multiple telemetry channels as well as more than one simulator.

4.4.2 Model

The hologram used in the previously described holographic real-image display system has the primary function of generating a real image of an aircraft carrier. This image is then operated on, for the most part, by conventional optics so as to simulate the view that would be seen from an aircraft. The real image, however, may be replaced with an actual model; if it is properly manipulated, the same degrees of freedom may be satisfied and displayed. This can be accomplished by using the mechanisms shown in Figure 15. As before, the effect of range change is accomplished by imaging the model onto a viewing screen by means of a zoom lens and producing magnification.

The change in perspective view (glide path) is accomplished by mounting the model on a gimbal system that allows the model to be rotated about two axes. One axis is vertical and the other is horizontal. Both axes are through the flight deck, and both axes are perpendicular to the optic axis of the system. Rotation about these axes provides a different perspective view to the zoom lens. This view is relayed to the screen.

The effect of aircraft pitch and yaw appears, as discussed previously, as a translation of the image in the field of the windscreen. The zoom lens and carrier model with gimbal are an integral unit, such that, when this system is pivoted about the center of the lens, the carrier remains on the optic axis of the lens. The entire optic axis, however, moves and thereby changes the location of the projected image on the screen. The axes of rotation are shown in Figure 15. In general, as long as the carrier model is constrained to the optic axis of the lens, the entire system may be pivoted about any point to provide translation of the image. It is also possible to keep the above system fixed and translate the image by reflecting it from a pivoted mirror as described previously.

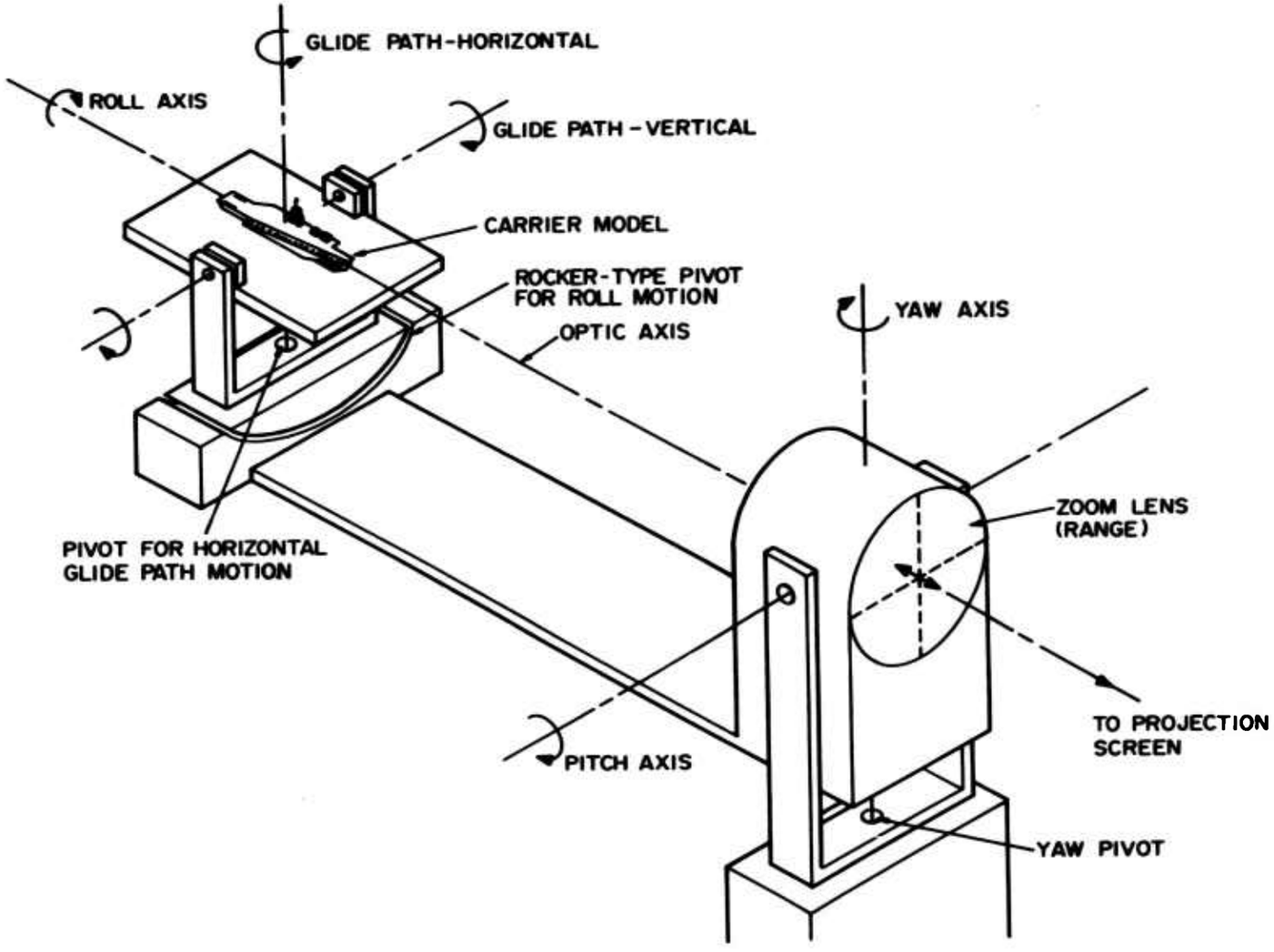

Figure 15. Head-Up Display System Using a Scale Model.

The last degree of freedom roll, is seen by the pilot as an angular tilt of the carrier and true horizon with respect to an arbitrary reference on his windscreen. This can be accomplished in this system by including an additional gimbal on the carrier model support. This gimbal is such as to allow the model to be rotated about the optic axis so that the perspective view is not altered. This is shown in Figure 15, where both the model and glide path gimbals are mounted on a rocker-type gimbal whose center of curvature is on the optic axis.

The remainder of the system consists of a viewing screen, a collimating lens, and a beam splitter, which are used in the same manner as for the real image display system. An additional feature of this system is that the display can be generated in full color by using the proper model and illumination. Laser illumination is no longer needed.

One could also combine these two techniques and have the TV system on board the aircraft. This would eliminate the need for a wide bandwidth data link and allow each aircraft to be independent. The problem, however, would now become that of systems size. The TV camera (or zoom lens) must have a very short working distance and still be capable of sufficient magnification change to simulate range change. Distortion at these working distances may be difficult to control. In addition, there is no simple way to distinguish between the landing areas of different aircraft carriers or even air fields. The hologram technique could include a cassette of plates, each one representing a different carrier or runway.

To explore this approach, a scale model carrier was in fact set up in the laboratory to serve as a basis of comparison for our holographic approach. A 10 to 1 Angénieux 12-120 mm focal length zoom lens was used with a close-up attachment with a 1-1/2" model set at 4 feet from the lens. The model remained in good focus with acceptable perspective distortion over the size change of 10 to 1. (The model was illuminated with an ordinary white light source.) Coupled with the TV system it provided an excellent image for comparison purposes. There

was no disturbing graininess in the image. Because the light source had no appreciable spatial coherence, the lens could be stopped down (to f/22 for example) so that good image quality could be maintained along with a large depth of field.

4.5 GIMBALLED HOLOGRAM SYSTEM

There are several disadvantages to the schemes previously described. Some of these are:

1. Large loss of light with off-axis imaging and/or a large number of diffusing screens.
2. Complex optical train
3. Relatively large package
4. Difficulty in using both holographic characteristics of interest: magnification and perspective changes
5. Unavailable compact high-power visible lasers, which makes a device for viewing images directly against a high light ambient impractical

The basic idea of the approach described in this section is to provide a fixed optical axis for the image space, regardless of the perspective view or image size at any given time. If the hologram is mounted such that it rotates about a fixed point located in the hologram plane and the illuminating beam is directed to the point of rotation, the reconstructed image will always fall along a fixed axis. Figure 16 shows the method of changing perspective view in one dimension. With the entire plate illuminated, the various perspective views, A, B, and C, can be seen by moving the observer's eye from a point on the left of the corresponding point on the right. In order that the perspective views come out along the system's optical axis, two steps are involved. First, the plate is translated to the point corresponding to the view desired, here view C. At this time the view rays come out as shown by arrow C'. The reconstructed image would be seen to the left of the original position. Second, the plate is rotated about the fixed axis by the angle that is the arctangent of the ratio of plate movement and object distance. The source rotates with the plate so that

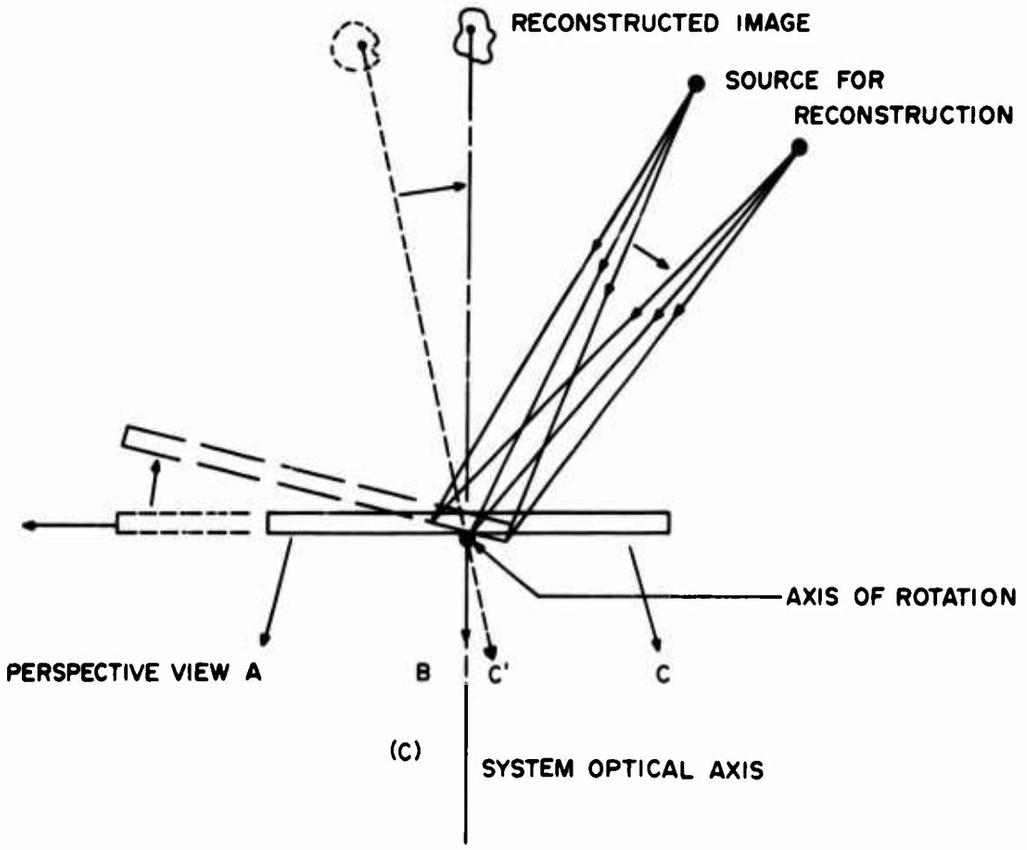

Figure 16. Method of Changing Perspective View.

the reconstructing beam illuminates a small region about the axis. The recording step must be done with collimated light so that Bragg "detuning" will not occur during the translation step. Actually, both of these steps must be done together in order that a smooth transition takes place. The result of these motions keeps the reconstructed image on axis while changing perspective.

Magnification of the image is accomplished by moving the source point toward or away from the hologram. This is most easily done by translating a lens that is converging a collimated laser beam. Although the virtual image is shown in the figure, the system will use the real image. In either case, the beam would be formed by a lens or set of lenses that would be translated to move the effective source point.

The reconstructed image now becomes the object for further optical transformation. For example, it can be viewed directly on a screen or relayed by lenses to a TV camera for further display. Since the image moves in and out along the axis as the size changes, the viewing screen or TV camera must move, or if further lenses are used, they must be refocused. For example, if a lens is placed such that the reconstructed image is maintained at its focal plane, the image would be projected at infinity. If a lens located at the TV camera is focused at infinity, the final image is on the camera photosensitive surface. The size of the final image can be controlled by the ratio of lens focal lengths. The displayed image is kept in focus by moving the first lens at the same rate as the holographic image. In fact, since movement of two lenses is involved (magnification change and focusing lens), these lenses can be mechanically linked and driven together.

TV systems and head-up viewers are items already in or planned to be included in naval aircraft. A TV system allows the resulting image to be displayed against a high light ambient background. This would be difficult to achieve with known compact visible lasers and viewing screens. One such grouping of possible equipment is shown in Figure 17. A carrier-aircraft telemetry link, a low-light-level TV viewing system, and the holographic carrier landing system are all linked to a CRT and presented to the pilot through a head-up display viewer.

In addition to this, many of the view parameters can be easily affected and changed within the TV system. For example, roll of the aircraft can be simulated by rotating the deflection yoke of the CRT, or by revolving of the camera unit about the optical axis. Pitch and yaw can be done entirely within the TV system. By applying a bias signal to the deflection coils, the image can be made to move up or down and left or right. Also, by using shrinking raster techniques in the camera, the size of the resulting image can be changed, thus augmenting the size changes made optically.

This approach involves mechanical movement of the light source, making small lasers desirable. The smallest available are solid-state laser diodes. The GaAs lasers operating in the near IR (9400 Å) range are typical, and at room temperature they provide 1-10 milliwatts average radiated light.

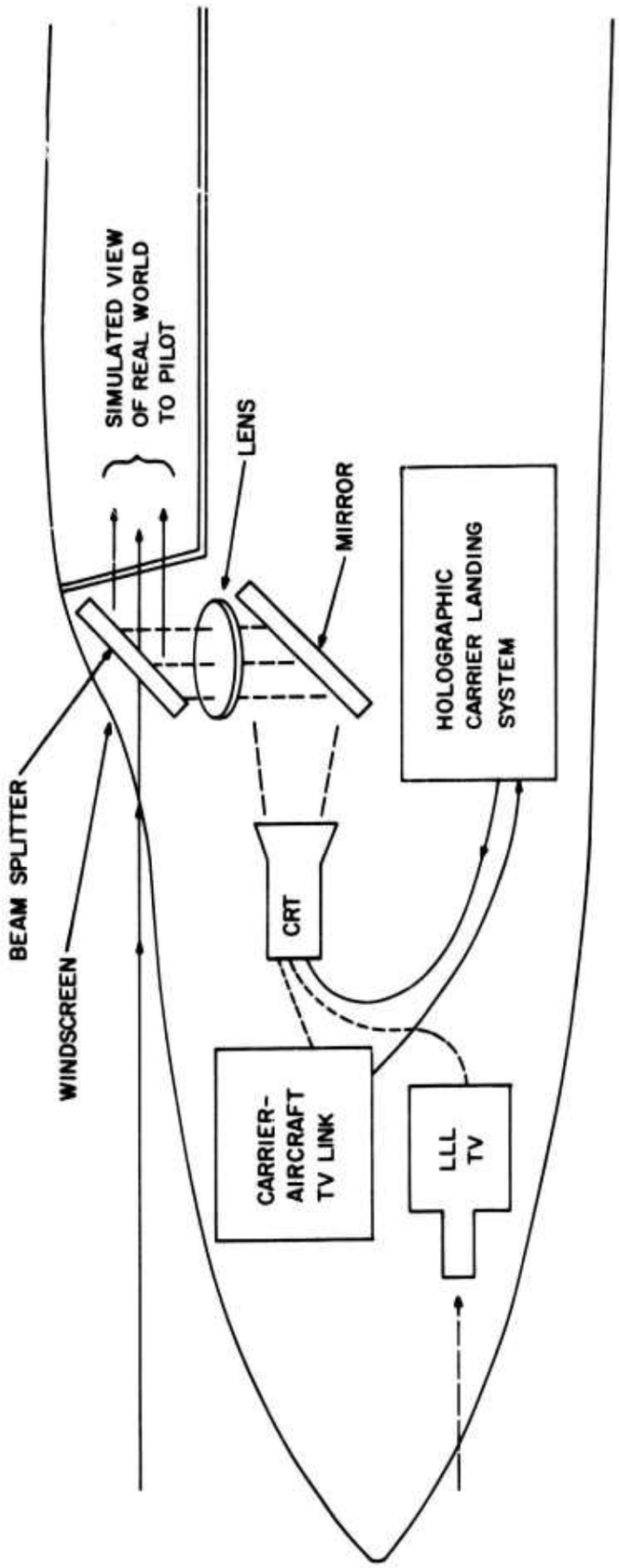

Figure 17. Aircraft Head-Up Display.

There are some disadvantages with this approach. First, a mechanism is required to move the hologram plate. Mechanical devices of this nature would have to be made rugged before installing them in aircraft. Second, the IR diode is a nonpoint source and has a relatively large spectral bandwidth. These two factors may reduce the overall image quality over that obtainable with a gas laser. Future development of smaller, more spatially and temporarily coherent sources will help in this area.

The general conclusions to be considered in regard to utilization of a hologram-TV approach are:

1. The gimballed hologram is a technique where use of both holographic magnification and perspective changes can be made with relative ease.
2. A fixed optical axis is maintained for the reconstructed image. This allows a more efficient use of light and/or a simpler optical train.
3. A mechanical device for positioning the hologram and light source is required.
4. Mechanical motions of lenses and relative tracking are required.
5. A TV system provides great flexibility in and control of the view parameter changes. High brightness images are possible, and such a TV system is compatible with existing aircraft equipment.
6. The holographic image quality has some defects. At present, it does not match that possible with a scale model illuminated with white light.
7. The system offers reasonable compactness.

5. DESCRIPTION OF LABORATORY MODEL

5.1 INTRODUCTION

The gimballed hologram-TV system was selected as the approach for the feasibility mode. An overall conceptual view is shown in Figure 18. The IR diode and range changing optics are mounted off the inner gimbal yoke and moving with it. As the plate is translated, it rotates as explained previously, so that the reconstructed image always falls along a fixed (optical) axis. A lens images the holographic real image to infinity and the TV camera lens, set at infinity, focuses the final image on the camera tube face. The real image, however, when projected on a screen and viewed from the back of the scene, will be the mirror image of the original scene. This same phenomenon will occur in this case, causing a reversed image on the CRT monitor. This can be corrected electronically by changing the direction of sweep in the CRT or by using a modified model. The range change optics and imaging lens move together by a mechanical link.

A schematic view of the system optics is shown in Figure 19. A beam expander consisting of two converging lenses and a pinhole shape the beam from the IR diode and collimate it. The range change optics consist of a positive and negative lens, which form a converging beam to a focus past the hologram. The positive lens moves so as to move the focused spot closer or farther from the hologram, thereby varying the image size and position. The real image is formed between 2 and 10 inches from the hologram due to the positioning of the illuminating beam. This means that the first imaging lens must move from a position where its focal plane is 2" from the hologram to one 10" from the focal plane, or a total travel of 8". These two motions are linked together mechanically and both are driven by lead screws on linear stages. The camera lens refocuses the image onto the camera tube face and the image appears on the monitor. Under manual control the TV camera unit can be rotated to simulate roll, and through electronic control, the bias on the deflection coils of the monitor is changed to simulate pitch and yaw. Shrinking raster is controlled by potentiometers connected to the linear stage holding the imaging lens. As it moves, the potentiometers are turned by a pulley arrangement, and the resulting control voltages are in step with the optical magnification change. Shrinking raster thus takes place simultaneously with optical magnification change.

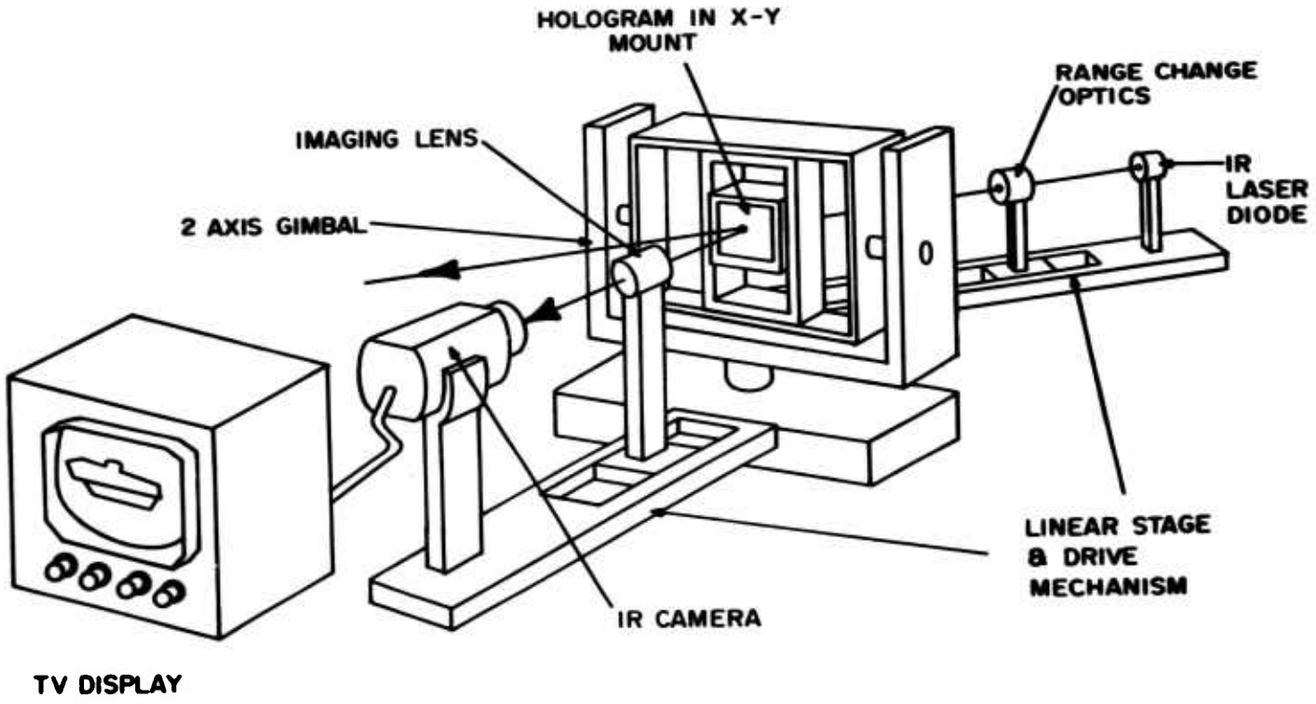

Figure 18. Feasibility Model.

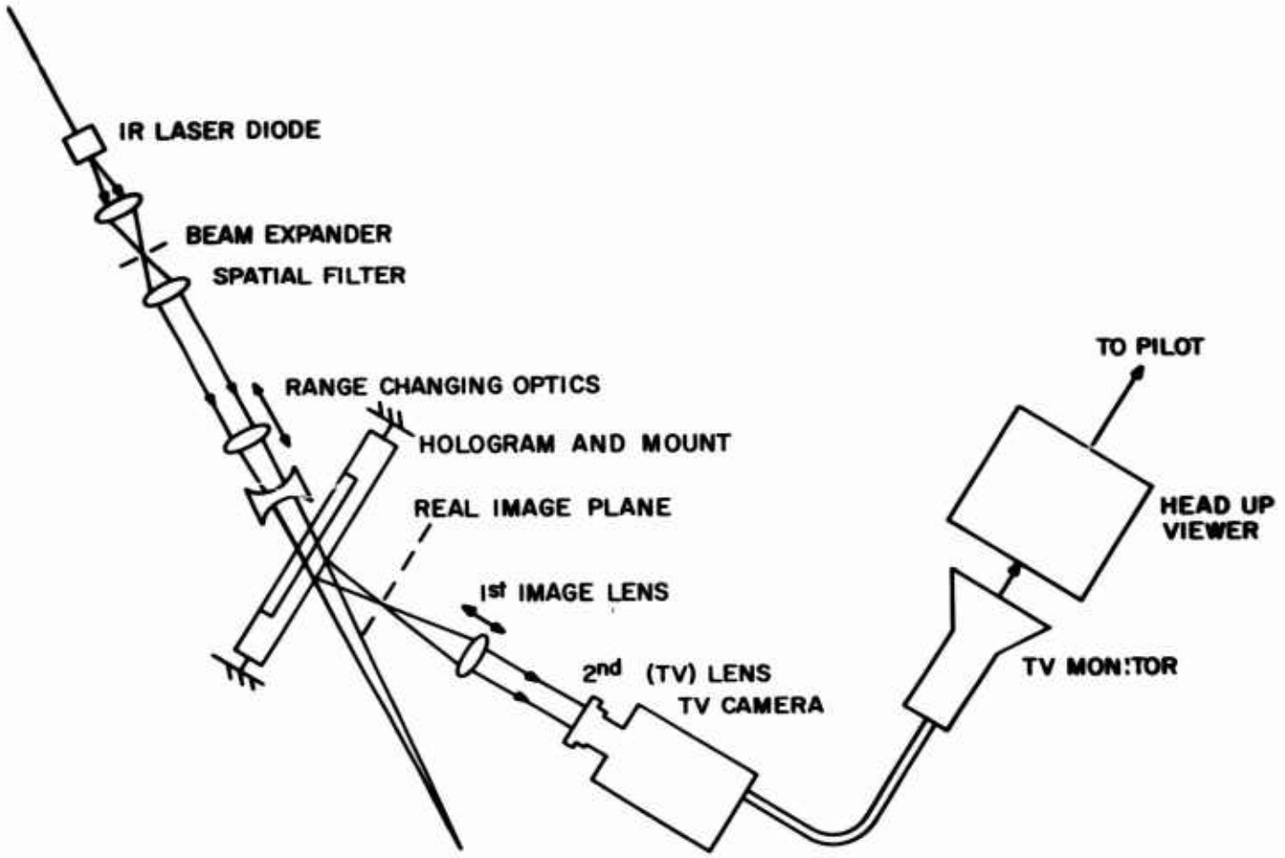

Figure 19. System Optics.

In the demonstration model a small (1 mW) HeNe laser is used in place of the IR laser diode. The beam expander consists of a negative lens followed by a positive lens to shorten the longitudinal size. No spatial filtering is done. The expander increases the beam diameter approximately 5 times to about 1/2 inch before entering the range changing optics. There will be no head-up viewer to project the image to infinity. The output will simply be the TV monitor viewed at a normal distance.

As a summary, Table II lists the view parameters and the areas within the model that control them.

Table II. View Parameters.

PARAMETER	CONTROL
RANGE	HOLOGRAM AND OPTICS TV SYSTEM (SHRINKING RASTER)
GLIDE PATH (PERSPECTIVE)	HOLOGRAM TRANSLATION & ROTATION
PITCH YAW	DEFLECTION COILS OF TV MONITORS
ROLL	TV CAMERA ROLL

5.2 OPTICAL DESIGN

5.2.1 Range Change Optics

In order to simulate range change, the reconstructed image must be continually altered in size. As was indicated, a magnification or demagnification of a holographic image can be provided by altering the curvature of the readout wavefront. Implementation of this effect is subject to certain constraints. Of primary concern is the interfacing of the optical system with the telemetered range data. That is, it is desirable that the magnification be controlled by a simple motion of some optical elements. In view of this, the primary empha-

sis was placed on designing a magnification system that requires only the translation of a single lens. As a further design goal both the lens translation and resulting magnification were required to be linear functions.

Several optical systems that satisfy these requirements were subsequently designed. While they all provided the desired effect, some were judged either to have too long an overall length or to require an excessive length of travel. The lens system that was finally adopted and implemented is shown schematically in Figure 20. Since the requirements on linear motion prevent a random selection of the optical parameters, their interrelationship will now be derived.

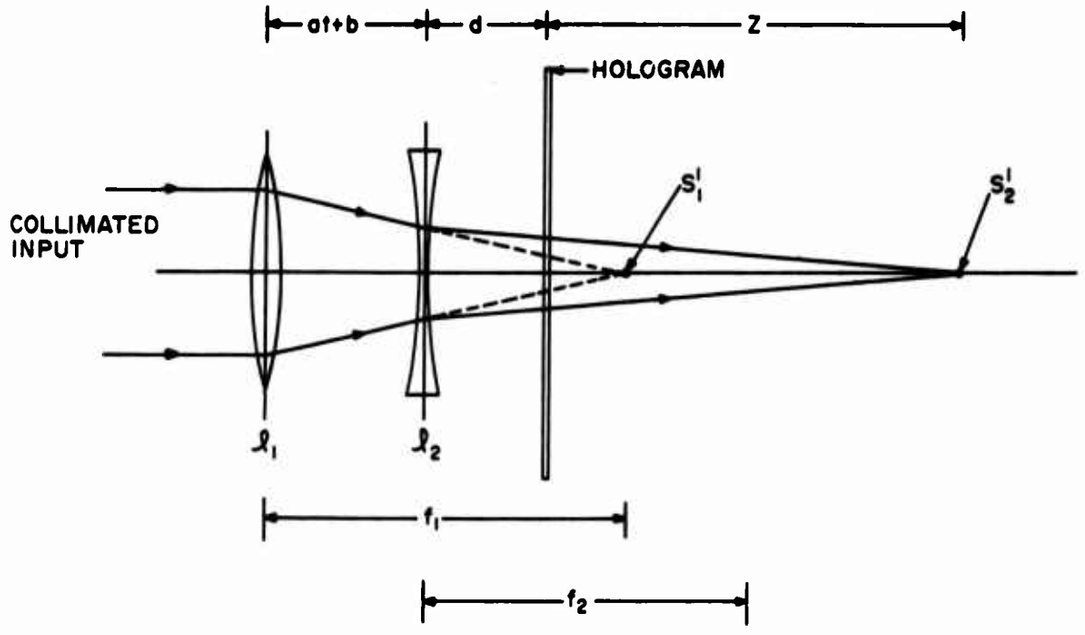

Figure 20. Lens System to Change Curvature of Illuminating Wavefront.

As shown in the figure, a collimated input to lens ℓ_1 will be converged towards the focal point of this lens. That is, $s'_1 = f_1$ and this point becomes a virtual object for lens ℓ_2. With respect to ℓ_2 the position of this object is

$$s_2 = f_1 - (at + b) \qquad (35)$$

where $at + b$ is the instantaneous separation between the two lenses. The function $at + b$ represents a linear motion of lens ℓ_1 with respect to lens ℓ_2. According to the lens equation, the image formed by lens ℓ_2 will be located at a point s'_2 given by

$$s'_2 = \frac{s_2 f_2}{s_2 - f_2} \tag{36}$$

If we substitute the expression for s_2 given in equation (35) we get

$$s'_2 = \frac{[-at + f_1 - b] f_2}{at - f_1 + f_2 + b} \tag{37}$$

This is now the point of convergency of the readout illumination.

According to the treatment given in Section 2, the magnification of a real image is given by (34).

$$M = \left(1 + \frac{z_o}{z} - \frac{z_o}{z_r}\right)^{-1} \tag{38}$$

Since we have used a collimated reference beam in the generation of the hologram, we can set $z_r = \infty$ and the magnification expression becomes

$$M = \frac{z}{z + z_o} \tag{39}$$

The parameter z is the distance between the hologram and the point of convergency of the readout illumination. For this lens system

$$z = s'_2 - d \tag{40}$$

Combining (37), (39), and (40), and collecting terms, the magnification as a function of time becomes

$$M(t) = \frac{-(f_2 + d)at + (f_2 + d)(f_1 - b) - f_2 d}{(z_o - d - f_2)at + (z_o - d - f_2)(b - f_1) + f_2 (z_o - d)} \tag{41}$$

In order that this magnification variation be a linear function of time, the coefficient of time in the denominator must vanish. Hence, our first constraint becomes

$$z_o - d - f_2 = 0 \tag{42}$$

Equation (41) now reduces to

$$M(t) = \frac{-z_o at + z_o (f_1 - b) - f_2 d}{f_2^2} \tag{43}$$

For this preliminary design we would like the image magnification to vary from 0.2 to 1.0. Hence, (43) gives

$$M(t=0) = 0.20 = \frac{z_o (f_1 - b) - f_2 d}{f_2^2} \tag{44}$$

Using this, we find that

$$M(t=T) = 1 = \frac{-z_o aT}{f_2^2} + 0.2 \tag{45}$$

or

$$\frac{-z_o aT}{f_2^2} = 0.8 \tag{46}$$

Using a hologram-to-object separation (z_o) of 10", the magnification limits indicate that the image moves over a distance of 8". To facilitate driving both the range change lens and the relay lens in synchronization, their distances of travel should be integrally related. For that purpose, the distance of travel of lens ℓ_1 was selected to be 2". We can now set aT = -2" in (46) and solve for f_2.

$$f_2^2 = 2.5\, z_o \tag{47}$$

Since z_o = 10", we have now determined that f_2 = 5". At the same time we find from the constraint, (42), that d = 5". Thus, the hologram is to be positioned in the focal plane of lens ℓ_2. The only restriction on the focal length of lens ℓ_1

is that its focal point should coincide with the focal point of lens ℓ_2 when t = T. (This is to provide a collimated illuminating beam and hence unit magnification.) Consequently, $f_1 = f_2 + \delta$ where δ is the distance of closest approach of the lenses ($\delta = aT + b$). The minimum distance is governed by the thickness of the lenses. Since lenses are not conveniently available at all desired focal lengths, a stock item was selected that would allow a reasonably close approach (to minimize overall systems length). The selected focal length of lens ℓ_1 is 5-5/8" (143 mm). Lens ℓ_1, therefore, translates to within 5/8" of lens ℓ_2. (I.e., aT + b = 5/8", but aT = -2"; hence, b = 2-5/8".) To summarize, the various parameters are repeated below. The parameter D is the maximum range change systems length.

f_1 = 4.625" (143 mm)
f_2 = -5.000" (-127 mm)
d = 5.000" (127 mm)
b = 2.625" (67 mm)
δ = 0.625" (16 mm)
aT = -2.000" (51 mm)
z_o = 10.000" (254 mm)
D = 7.625" (194 mm)

If we substitute these values back into (43), we find that

$$M(t) = 0.8 \left(\frac{t}{T}\right) + 0.2 \qquad (48)$$

This shows that the magnification is linear with time and varies between 0.2 and 1.0. The equation of motion of the separation between lenses ℓ_1 and ℓ_2 (at + b) is now lens ℓ_1

$$-2 \left(\frac{t}{T}\right) + 2.625 \qquad (49)$$

Figure 21 shows a typical relationship between lens position and resulting image magnification and position. Lens ℓ_1 is shown in two different positions.

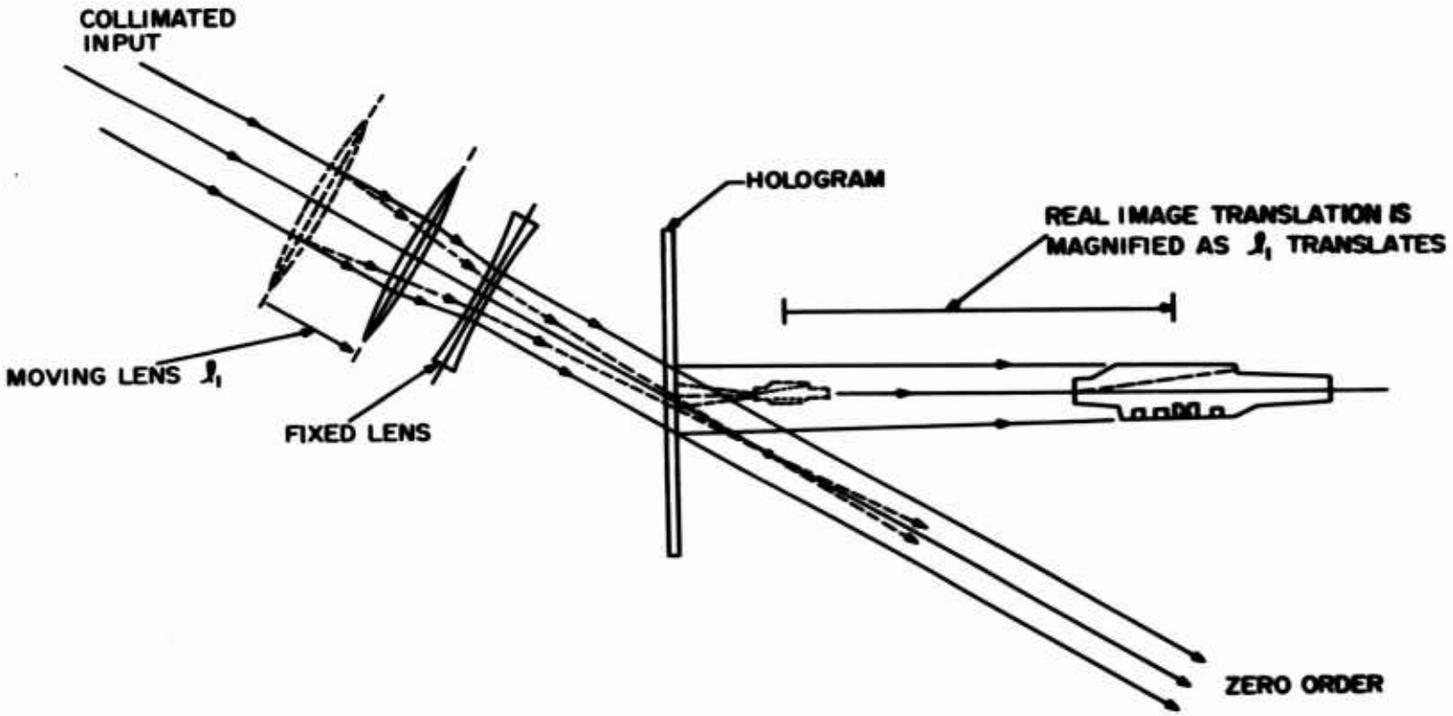

Figure 21. Range Change System Showing Lens and Real Image in Two Different Positions.

5.2.2 Imaging Optics

The imaging optics consist of an achromatic lens approximately 5 to 6 inches in focal length and large enough in diameter to collect sufficient light from the reconstructed image. Typical sizes of images (carrier models) used are 1 to 2 inches wide. This lens is mounted on a linear stage that is motor driven (along with the range change optics). The drive positions the lens such that its focal plane always coincides with the reconstruction image plane. This means the lens must traverse a distance of about 8" for the total designed optical change (5X). Rays from points in the object plane are collimated by the lens. The TV camera (2" fl.) lens intercepts these rays and focuses them at the camera tube face. If the tracking between the reconstructed image and moving imaging lens is held to within the depth of field of the imaging lens combination (approximately 0.050"), the final image will remain in acceptable focus. Another problem inherent in this method is the collection of off-axis rays due to the finite extent of the reconstructed image. This collection becomes more critical as the separation between the first imaging lens and camera lens increases. For example, points at the extreme edge of the image will pass through the first lens at an angle proportional to the ratio of edge distance, y, to lens focal length, f_1. These rays will miss the TV camera lens unless it has a value equal to or greater than

$$d = \frac{Ly}{f_1} \tag{50}$$

where L is the separation of the lenses. Fortunately, when L is large, the reconstructed image y is small, so that these two factors tend to cancel each other. Hence, readily available lenses under 2" in diameter are adequate for small ship models.

The TV camera tube face has a useful diameter of about 0.6". The size of the projected image must, naturally, fall within this value. Hence, if we start out with an image whose largest size is about 1.5", the demagnification necessary is 3X. Thus a 6" lens followed by a 2" TV lens is appropriate.

5.2.3 Laser Optics

Selection of a light source is one of the primary factors that must be considered during the design of an optical simulator. In particular, the realization of an airborne system imposes even more stringent requirements. Not only must the source satisfy the optical requirements of the simulator, it must also meet certain systems constraints. These include the effect of the source on the overall systems size and weight, the stability of the source and its ability to withstand forces that may be encountered during airborne operations, and the complexity of the source as to its maintenance and/or replacement.

While a gas laser certainly satisfies the optical needs of the system, its packaging is not consistent with size and weight considerations. In addition, the long narrow discharge tube is under high external pressure. Distortion of the tube in many cases will prohibit laser action. Insertion of a new tube and alignment of the mirrors can be a time-consuming task.

These problems can be circumvented by structuring a system utilizing a solid-state injection laser as the source. Within the capabilities of the present state of the art, the gallium arsenide (GaAs) laser diode is the most suitable. While this device provides a solution to the systems requirements of size, weight, etc., it does so at the price of some optical trade-offs. In order to operate present injection lasers in a continuous mode they must be cooled to liquid nitrogen temperature ($77^{\circ}K$). This is primarily to reduce driving currents and to provide for heat dissipation. As a result, a low-temperature cooling system would have to be designed for airborne operation. This would, of course, add to the systems weight. It is possible, however, to operate an injection laser at room temperature if it is done on a pulsed basis. To do this, high-current drivers must be designed that will provide sufficient peak output power. The system, however, will respond to the average output, which is the product of the peak power and the pulse rate (duty cycle). In most cases the duty cycle is limited by heat dissipation in the laser rather than in the driving circuits.

A driving circuit for room temperature operation has been designed and is shown schematically in Figure 22.

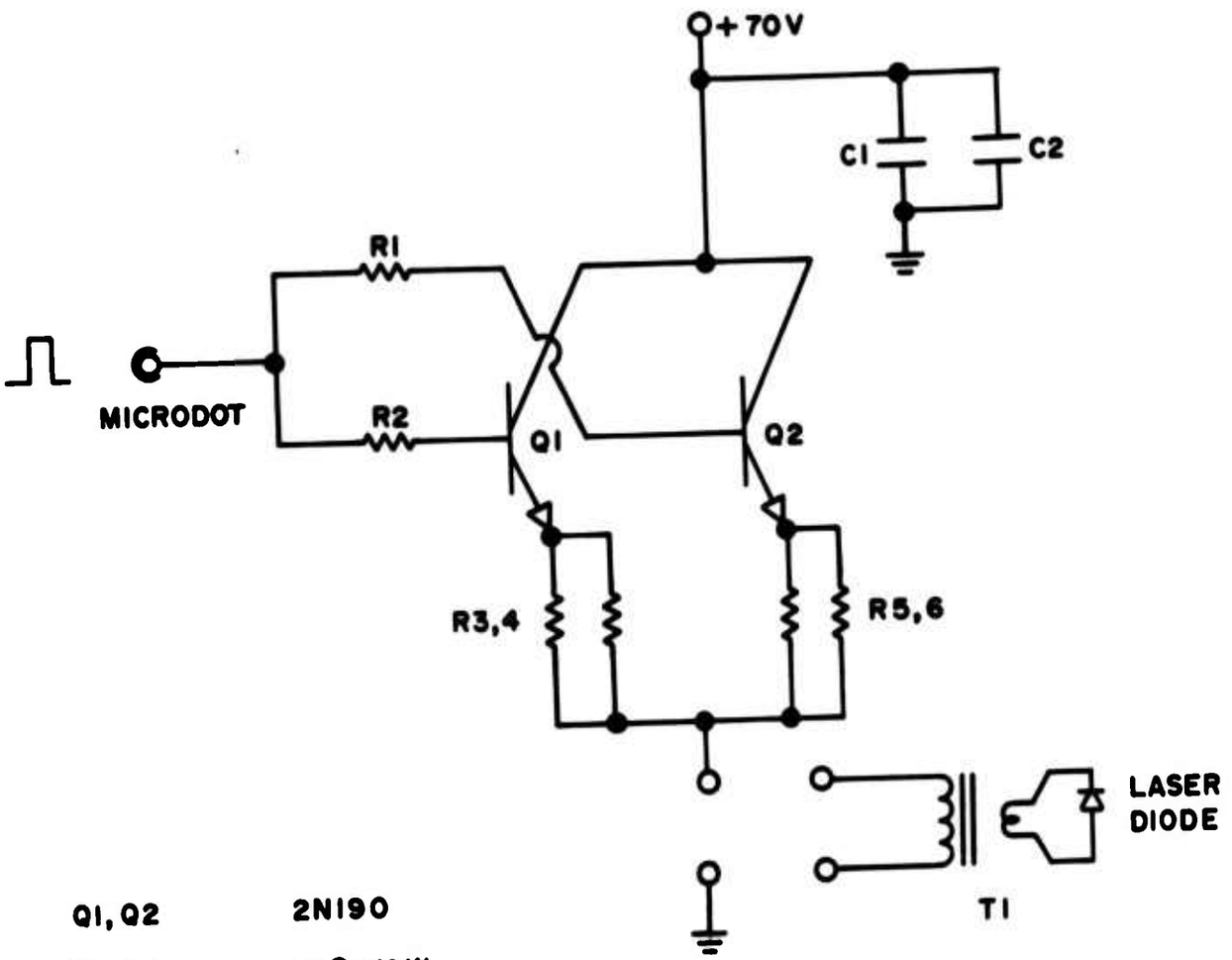

Q1, Q2	2N190
R1, R2	10Ω 1/4 W
R3, R4, R5, R6	1Ω 1/4 W
C1	1MF 200V DMP2W1 CDE
C2	0.1MF 200V M16A
T1	3d3 FERRITE TORROID

Figure 22. Driver Circuit for Operation of an Injection Laser at Room Temperature.

The transistor laser driver uses two TRW 2N1900 power transistors. Drive is supplied as a 100 nsec positive pulse through a 10 ohm resistor to the base. Two 1 ohm carbon resistors in parallel make up the emitter resistor for each transistor. The emitter resistor serves as a sampling resistor, and primarily as a means of balancing the currents through each transistor. Both 2N 1900's are chosen to have gains that match as closely as possible. If one draws more current than the other, a different drop across each emitter resistor will compensate the circuit, and cause the other transistor to pick up the current difference. The 2N 1900's can supply 10 amps peak current, and by making use of a core transformer with a 4 to 1 ratio currents of 80 amps can be established through the diode. Heat dissipation is provided for the transistors by using two IBM 483117 standard heat sinks. These were milled down to appropriate size, and a copper bus was used to connect them together.

The driver is operated at a duty cycle of 0.1% by using a pulse width of 100 nsec and a repetition rate of 10^4 cps. Current through the transistors and all the resistors will average far below their wattage ratings if this duty cycle is adhered to.

The transformer is a ferrite toroid 3d3 material wound with a 5/64" x 5 mil copper strip with Teflon tape as the insulator. Noninductive carbon resistors and noninductive capacitors were used. In order to realize fast rise times, all leads were kept to an absolute minimum length.

Typical operation of an injection laser with this driver provided an output pulse with peak power on the order of 4 watts. This represents an average power of 4 milliwatts to the system. Pulse rise times are in the order of 35 nsec.

The packaged driver with mounted laser is shown in Figure 23, and the laser device is shown in Figure 24. The laser material is sandwiched between the two heat sink bars and is not visible in the photograph. Laser action is restricted to a 0.010" region of the junction.

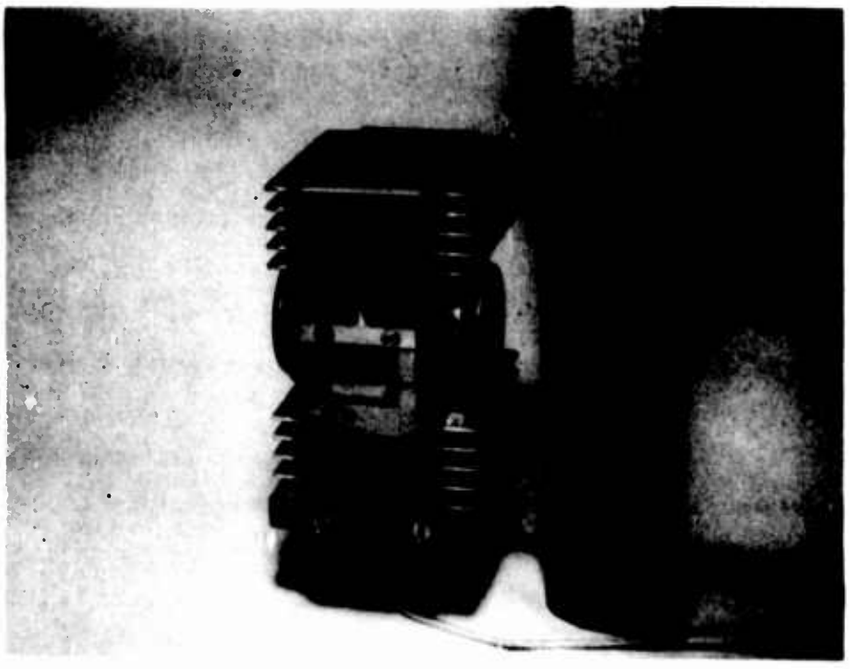

Figure 23. Injection Laser Driver. a. Transistors, b. Transformer, c. Injection Laser.

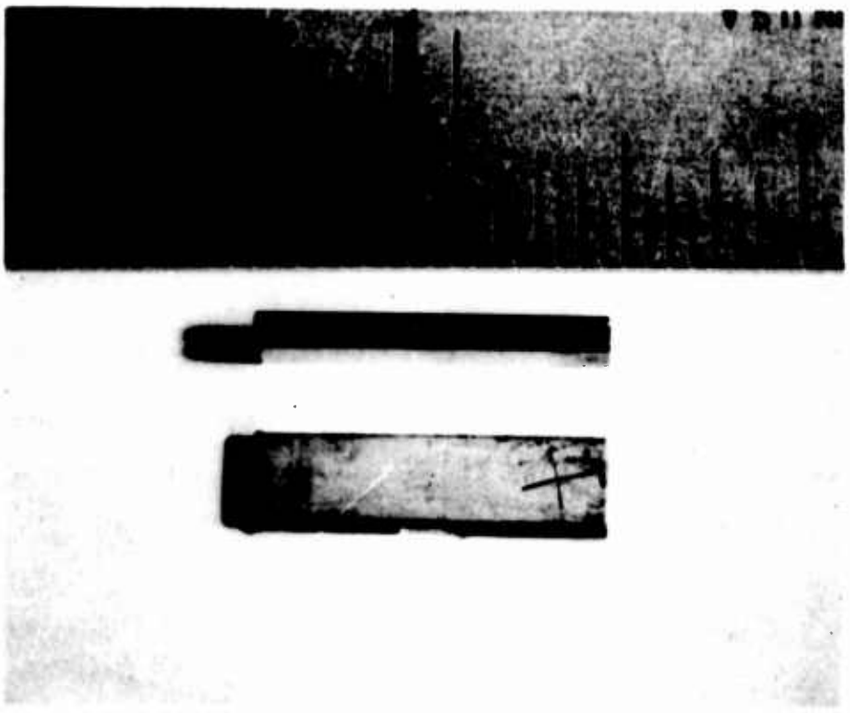

Figure 24. GaAs Injection Laser in its Mount (Two Views).

Due to the band gap of the gallium arsenide material, its output radiation occurs in the infrared region of the optical spectrum. The exact wavelength depends on the temperature of operation. At room temperature this is typically in the 9400 Å range. Since this is beyond the range of the human eye, some form of image conversion must be performed. This is one of the reasons for structuring the feasibility model around a closed circuit television system. By using an infrared sensitive vidicon (such as the RCA C74125) the reconstructed image can be displayed on the monitor. The TV approach also provides some gain and thus renders the displayed image more visible.

The implementation of an injection laser into the display system is shown in the overall systems drawing of Figure 19. The output of the laser is spatially filtered and formed into a collimated beam. This serves as the input to the range change optics.

5.3 HOLOGRAM MANIPULATOR MECHANISM

5.3.1 Description

The hologram manipulator mechanism provides a means for mechanically positioning a hologram in such a way that the three-dimensional real image produced by the hologram may be rotated in two axes to display continuously variable perspective views of the holographic scene without displacing the image from its nominal position in space.

The kinematic constraints of the mechanism are that a 4 inch by 5 inch photographic plate (the hologram) supported by the mechanism must translate and rotate in two axes in such a way that a perpendicular to the plate's center point always passes through a fixed point in space (A) 10 inches removed from the photographic plate along a fixed optical axis. A cylindrical volume around the optical axis must remain unobstructed by linkages or structural supports, so as not to obscure the optical path. This constraint precludes placing a fixed pivot at the virtual center of rotation (A) and running a radial link back to the hologram carriage, which would have been the easiest way to generate the required motion.

Basically, the mechanism consists of an X-Y carriage that is supported on the inner frame of a two-axis gimbal system. The X-Y carriage permits interrogation of any point of the 4 inch by 5 inch hologram to within 1/4 inch of its edges; the gimbals permit rotation of about $\pm 14^{\circ}$ about that point of interest. Translational motion is coupled to the rotational motion, in either of the orthogonal planes, by a novel system of spring tensioned flexible cables. This configuration eliminates cross-coupling between axes. The hologram, mounted to the X-Y carriage, must move in precisely coordinated translation and rotation in order to generate continuously variable perspective views of the holographic image. The geometry of the motion that the hologram must describe is shown, in one of the two orthogonal planes containing the optical axis, in Figure 25. The X-Y carriage and the two-axis gimbal permit the necessary freedom of motion for the hologram; the tension cable coupling provides the necessary kinematic constraint to that motion.

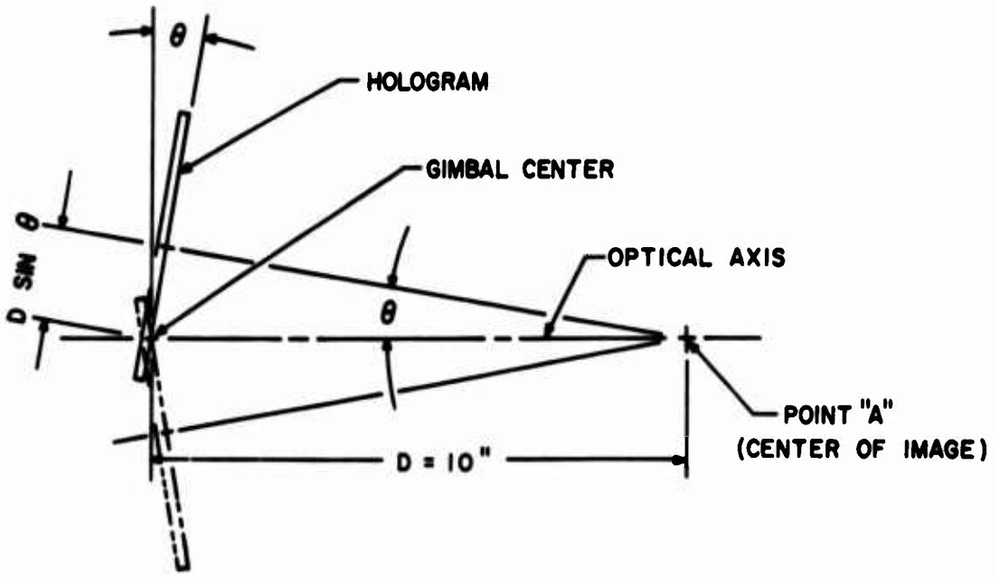

Figure 25. Geometry of Hologram Manipulator (in one plane).

The arrangement of the tension cable coupling is shown conceptually in Figure 26. The driving end of each cable is attached to the periphery of a circular sector beyond the cable's point of tangency with that sector. The driven end of the cables are attached as shown.

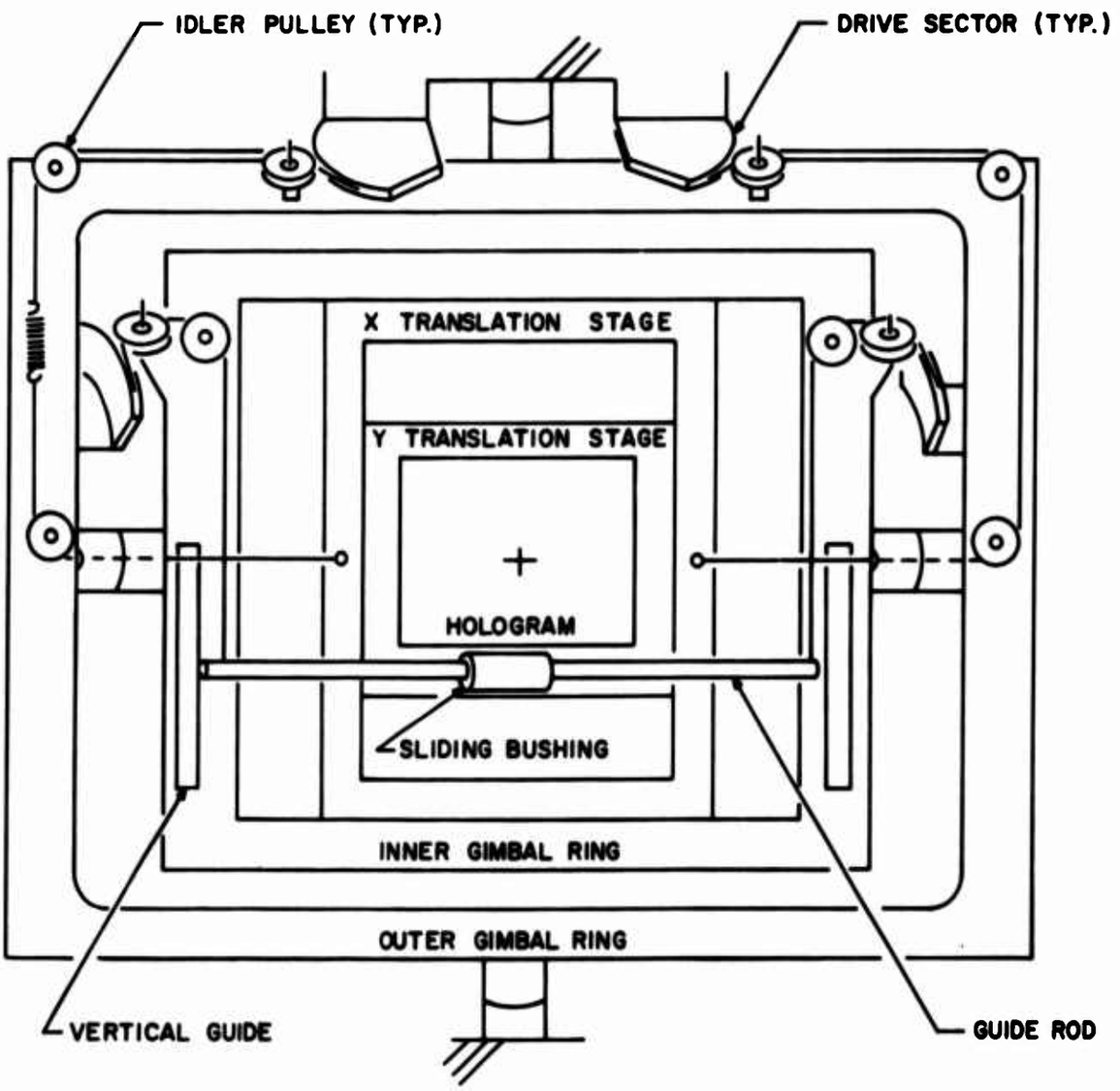

Figure 26. Conceptualized Mechanical Schematic of Hologram Manipulator.

Motion in the vertical plane is coupled as follows. Relative angular motion between a set of pulleys on the inner gimbal frame and a circular sector attached to the outer gimbal frame (and having its center at the horizontal gimbal axis) takes up or lets out a length of cable proportional to the angular displacement of the inner gimbal ring. This linear displacement is transferred through the cables to a guide bar, which is constrained to up and down motion. A bushing attached to the Y-translation stage rides on the guide bar, coupling the vertical motion of the stage to the bar while permitting horizontal motion relative to it.

In the horizontal plane, relative angular motion between a set of pulleys on the outer gimbal frame and a circular sector attached to the support frame (and having its center at the vertical gimbal axis) takes up or lets out a length of cable proportional to angular displacement of the outer gimbal frame. This linear displacement is transferred by the cables to the X-translation stage. In passing from the outer gimbal frame to the X-translation stage the cables pass through the center of the horizontal gimbal bearings, exactly coincident with the horizontal axis of rotation. This ensures that the angular motion between the inner and outer gimbal frames does not affect the positioning of the X-translation stage. In other words, cross-coupling between the two orthogonal planes is completely eliminated.

5.3.2 System Errors

To generate the exact motion described by the geometry depicted in Figure 25 the linear displacement of the hologram carriage ideally should be a sine function of the angular displacement of the gimbal, rather than being a linear function of the angle, as is the case with the model that was built. The difference between the linear function and the sine function (the displacement error) is so slight for angles up to $\pm 14^{\circ}$ (the limit of angular travel) that the error could be neglected in this application. Also, by proper selection of the proportionality constant between translation and rotation (controlled by the radius of the sector) it was possible to divide this error equally on both sides of the nominal displacement function, effectively halving the absolute error. The resulting positional error in the holographic image resolves into a maximum focus error of less than

0.002 inch (which is inperceptible due to the great depth of focus of the image) and a maximum lateral error of only 0.006 inch.

It would have been possible to generate the sine function exactly, of course, by making the drive sectors with a radius that varied as a function of the angle from the center point of tangency. However, it was much cheaper to make the sectors circular, and the slight error incurred is tolerable.

5.3.3 Displacement Doubling

In order to generate the motion described in Figure 25, with point A removed 10.00 inches from the gimbal center, the effective radius of the sectors must be 9.93 inches. This dimension is out of line with the size of the rest of the mechanism, so it was decided to make the drive sectors with an effective radius exactly half of the 9.93 dimension and use an additional stage of pulleys to double the displacement generated by the sectors. The principle of this displacement doubling is illustrated in Figure 27.

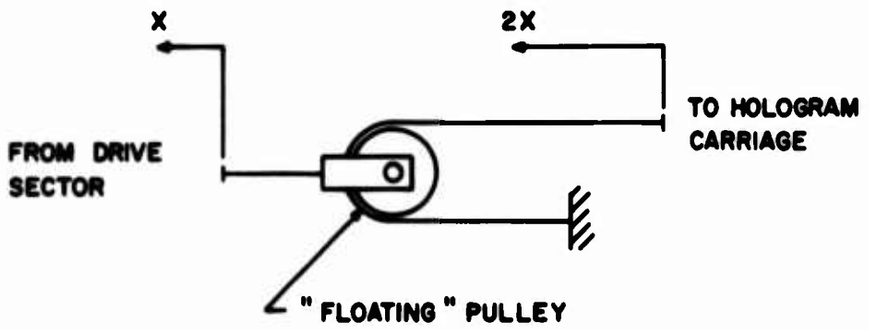

Figure 27. Method of Doubling Displacement.

5.3.4 Engineering Model

The actual engineering model, as it was built, is illustrated in the isometric view of Figure 28. This illustration shows the cable routing, the location of the tensioning springs, and the "floating" pulleys, which double the displacement generated by the sectors. The structure attached to the inner gimbal frame supports two adjustable mirror mounts, a fixed negative lens mount, and a traveling positive lens mount, which together comprise the variable divergence angle

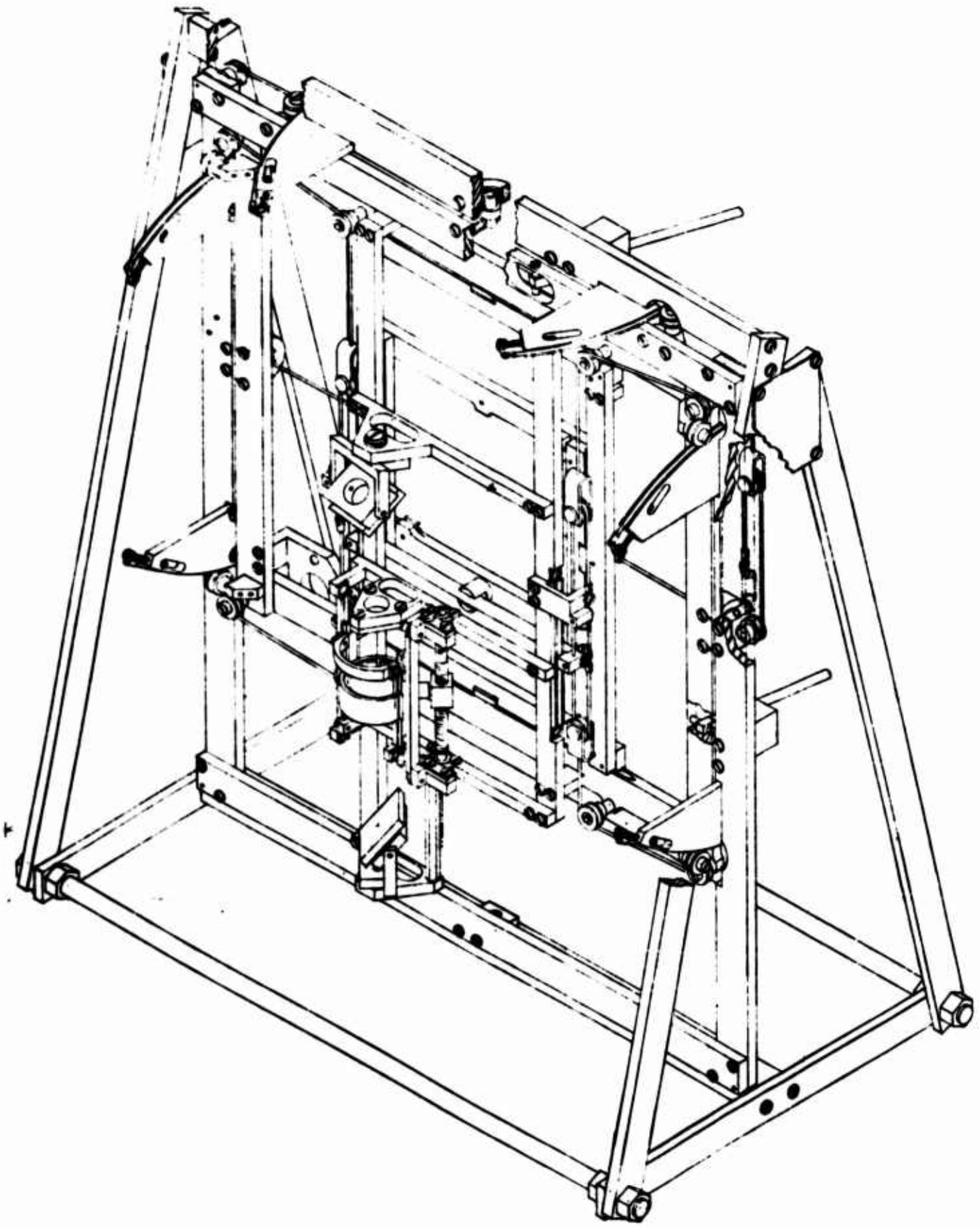

Figure 28. Engineering Model of Hologram Manipulator.

optics, and the lead screw drive for the traveling positive range change lens. This lead screw is coupled by a flexible shaft to a lead screw driving the first imaging lens in the image relaying optics, so that the two lenses move in synchronism. Not shown is the small HeNe one-mW laser, which mounts to the lower left-hand corner of the inner gimbal frame.

The X-translation stage travels in the horizontal direction within the inner gimbal frame on a linear ball track at the top and bottom of the stage. The balls roll in a 90° vee groove, are held captive, and are spaced at the proper interval by a sheet-metal ball retainer. The ball retainer is limited in its travel by tabs that ride in recesses in either side of the ball track. The Y-translation stage travels in the vertical direction within the X-translation stage on linear ball tracks similar to those previously described.

The horizontal and vertical gimbal axes are supported on double-shielded, single-race, ABEC-7 ball bearings. End play in the horizontal axis is taken up by a small amount of axial preload. End play in the vertical axis is taken up by the weight of the gimballed assembly, gravity providing the axial preload. All of the vertical thrust load is carried by the lower of the two vertical gimbal bearings; the upper bearing "floats" on its stub shaft and sustains only radial loading. The axial position of each of the four bearings within its housing is adjustable by means of laminated shims, which permit adjustment in 0.002 inch increments.

The majority of the parts used in the hologram manipulator mechanism were fabricated from either 6061-T6 aluminum or type 302 stainless steel. Type 302 stainless steel was used in all members having linear ball races because of the material's hardness and resistance to permanent deformation caused by the high-contract stress induced by the small-diameter balls at their points of contact. This material was also used for all fabricated shafts. Aluminum 6061-T6 was selected, of course, for its lightness and also for its availability in a variety of mill sizes Other materials used in the hologram manipulator included sintered bronze used in bushings and the floating pulleys, and aluminum 5052-H32 for all formed-sheet parts. The completed assembly is shown in Figure 29.

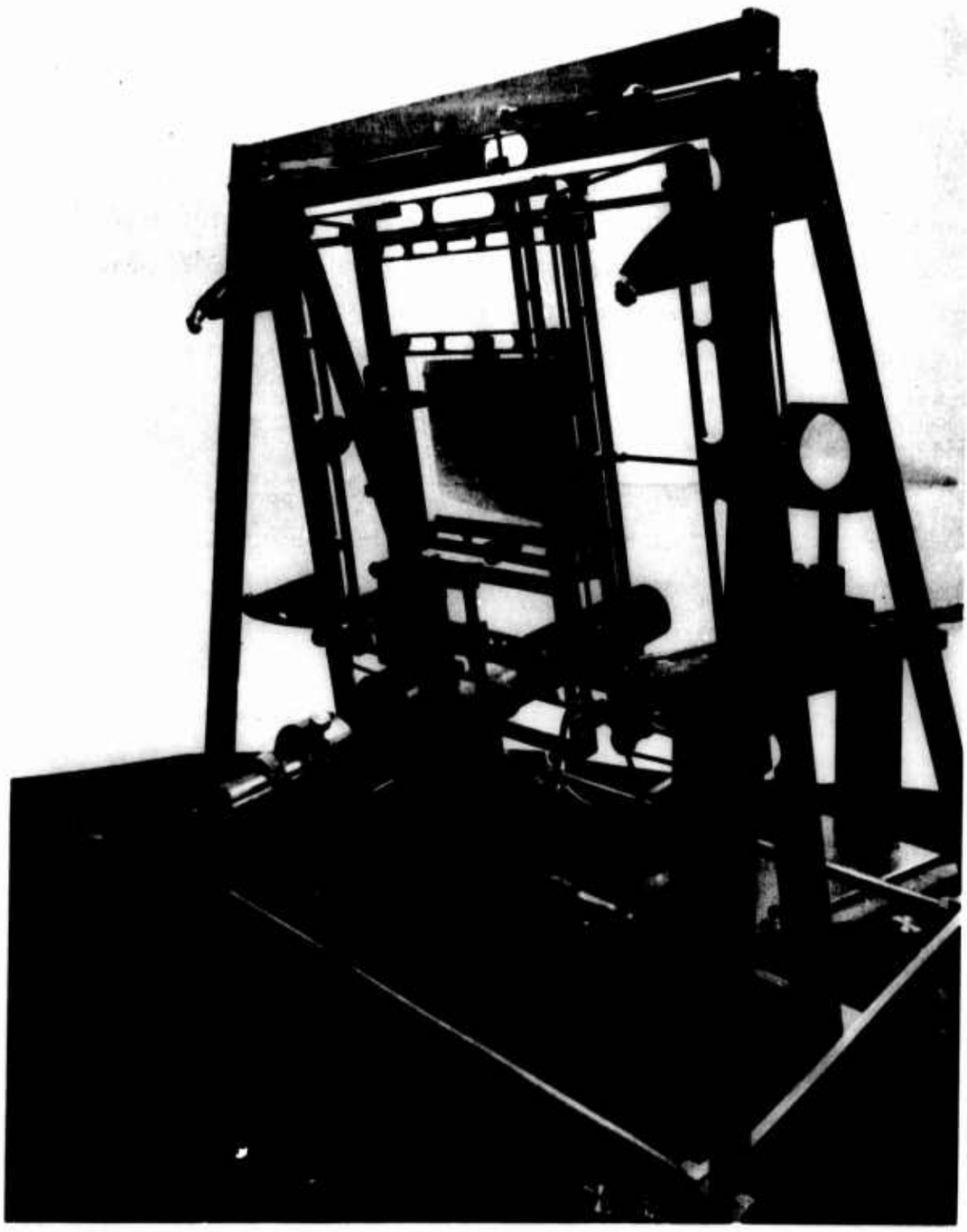

Figure 29. Assembled Hologram Manipulator.

5.4 ELECTRONICS

A CRT television display system was chosen for the holographic head-up display system. The choice of this system was based on size and complexity versus optical coupling. Several advantages were gained by the TV approach.

1. The size of the image could be made variable by varying the video sweep size.
2. Pitch and yaw could be simulated by varying the sweep positioning.
3. Roll could be accomplished by physically rotating the camera.
4. The camera could be sensitive to infrared emission, thus permitting the use of a GaAs laser without image converters.

The camera design is based upon standard vidicon practices with several modifications.

1. An infrared sensitive vidicon is used, which permits the use of an IR laser.
2. Ramp drive sweep is used rather than reactive or flyback sweep, which permits variable sweep size.
3. Beam positioning, which is externally controllable for use in pitch and yaw simulation, is provided.
4. A cylindrical camera housing, which permits easy camera rotation for roll simulation, is used.
5. The output is standard 525-line interlaced television for simple connection to TV monitors. Separate video and synchronization outputs are provided so that the system will operate into standard video monitors without modification.

The vidicon can be replaced in future systems by solid-state devices.[10]

The camera housing and IR vidicon are shown in Figure 30. Within this housing is the deflection yoke, the video preamplifier, and RFI filters. An outline drawing of the camera housing is shown in Figure 31. This unit is connected to the camera control unit (CCU), shown in Figures 32 and 33, which contains power supplies, deflection amplifiers, synchronization and sweep generators, video processing, and controls. Provision is included for rotation of the camera

assembly within its housing for roll simulation. This is shown in Figure 34. Maximum roll angle is $\pm 10^{\circ}$. The interconnection is made via (24) conductor cable and 2 coaxial cables. Remote from the CCU are the sweep size controls, which are driven by the traveling lens in the relay optics as shown in Figure 35.

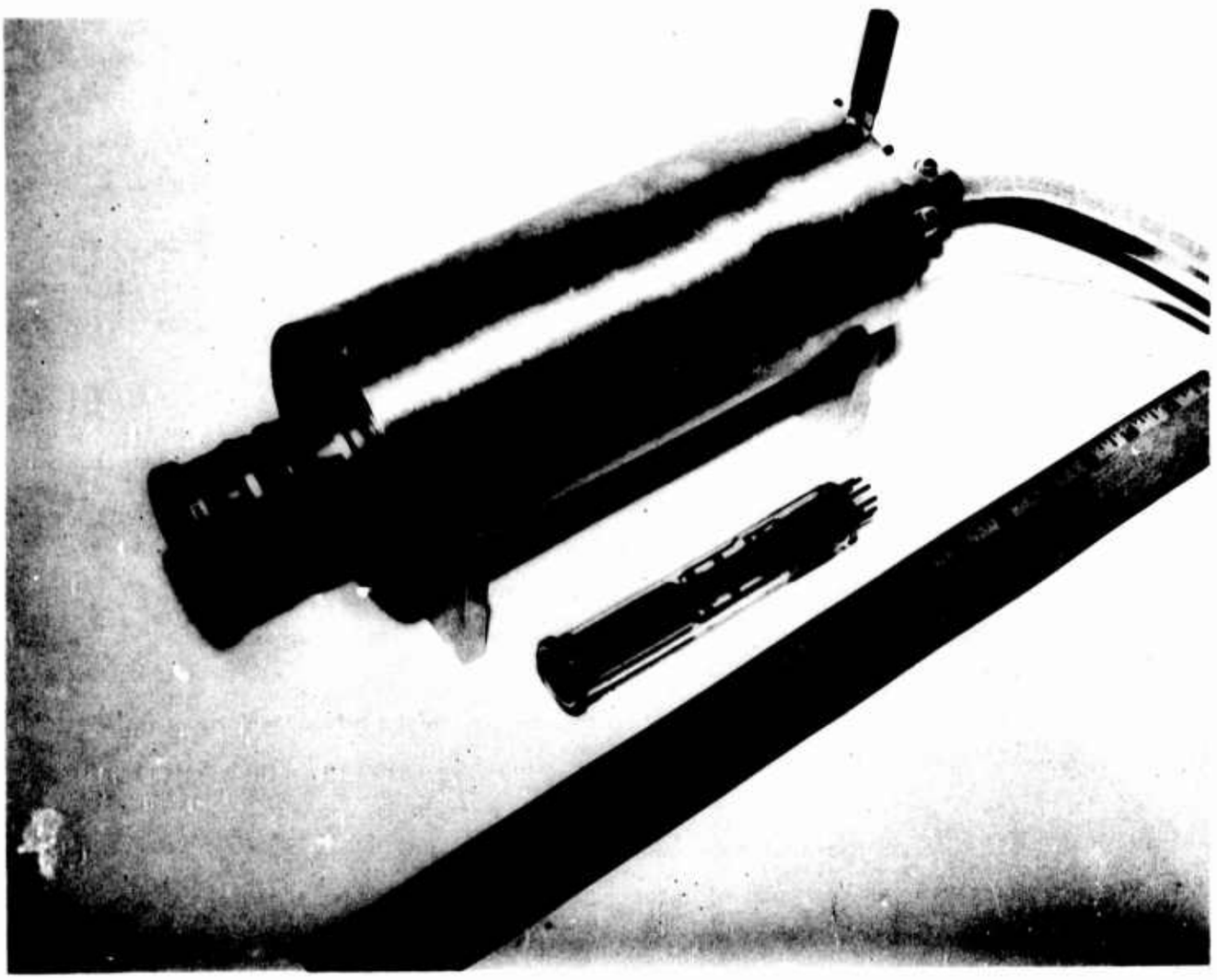

Figure 30. Camera Housing and IR Vidicon.

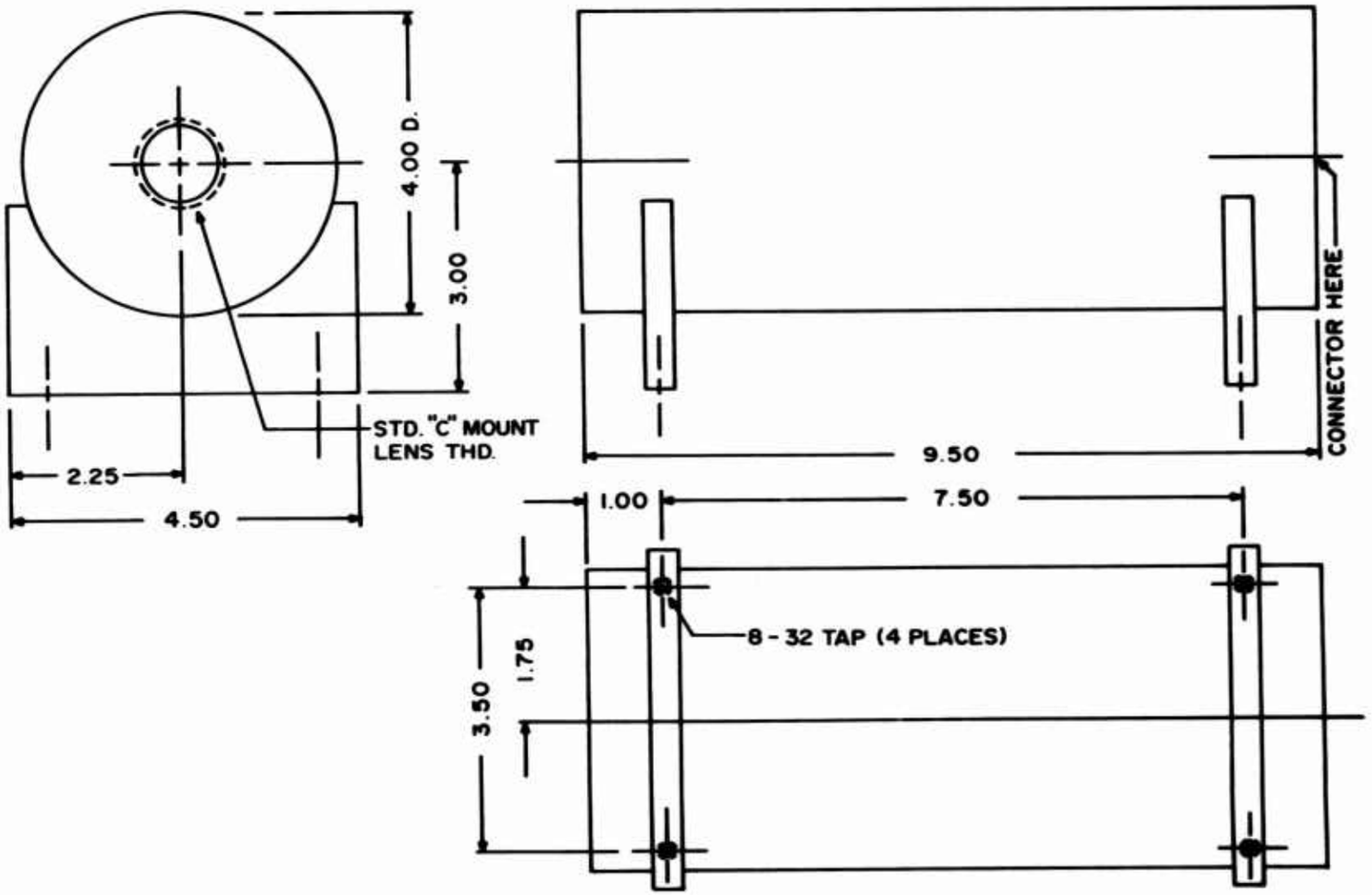

Figure 31. Outline Drawing of IR Vidicon Camera.

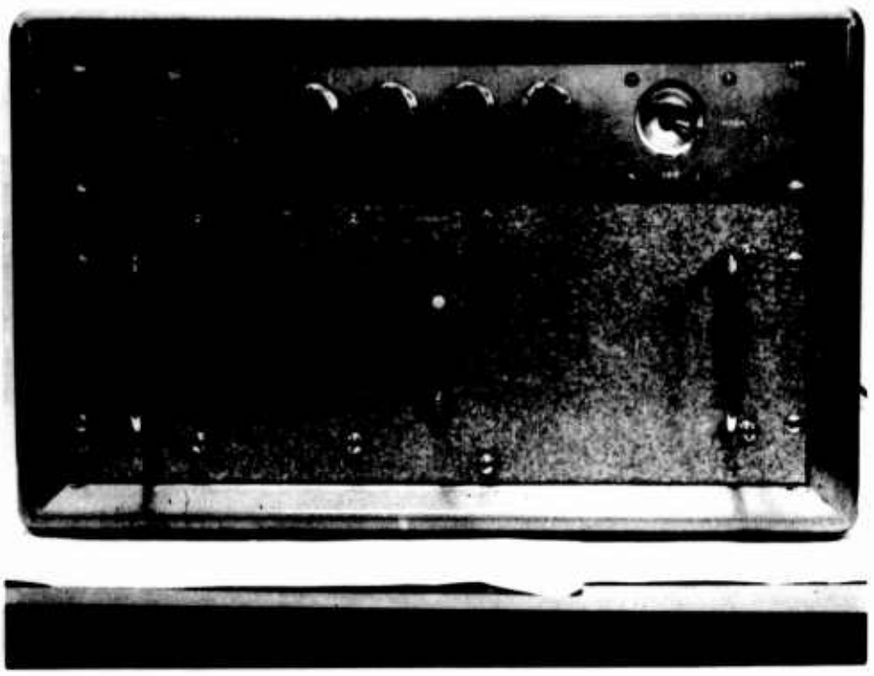

Figure 32. Camera Control Unit, Exterior.

Figure 33. Camera Control Unit, Interior.

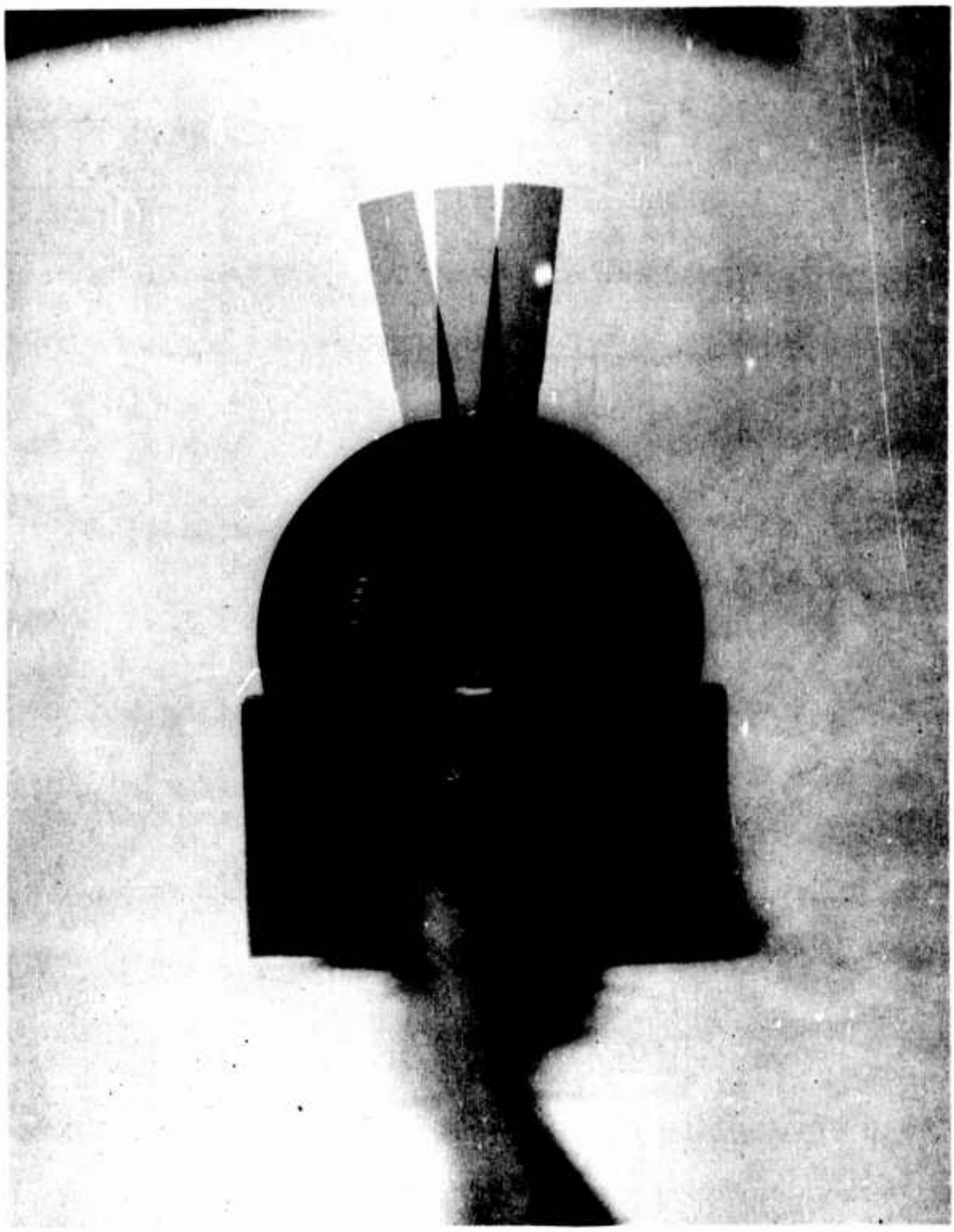

Figure 34. Rotation of Camera Assembly Within its Housing Provides Roll Simulation.

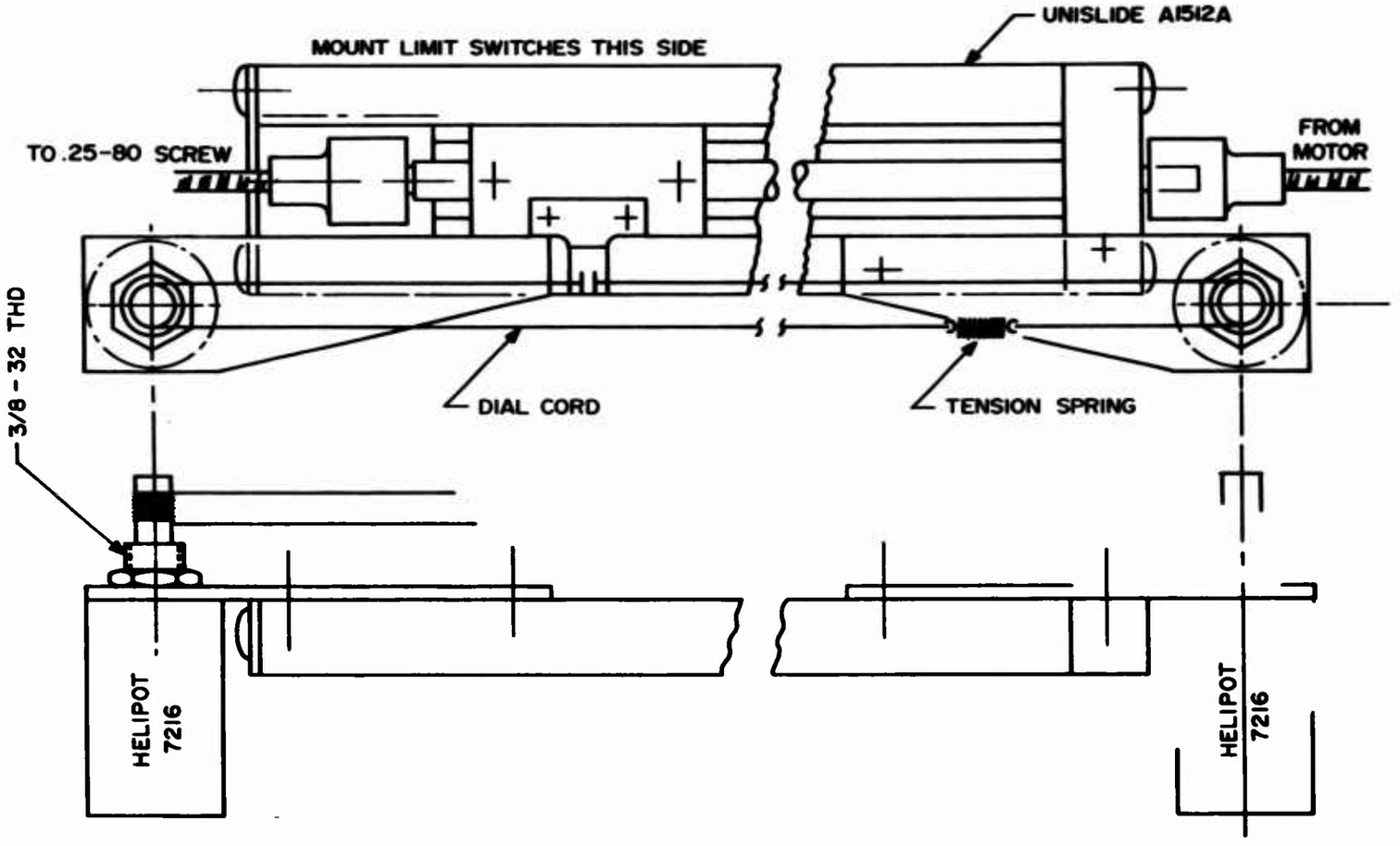

Figure 35. First Imaging Stage and Sweep Control Potentiometers.

6. RESULTS

6.1 INTRODUCTION

The assembled laboratory model is shown in Figures 36 - 43. All of the components described in the previous section are included except for the infrared-sensitive vidicon. The small HeNe laser can be seen mounted on the lower left-hand side of the inner gimbal frame. Attached to the end of the laser are the beam expanding optics and a mirror. (See Figure 29 for a closeup.) The range change optics system is visible just below the mounted hologram. The first imaging lens (in a black frame) can be seen mounted on its translation stage between the hologram and TV camera. The stage is connected to a motor by means of a flexible shaft. The motor control unit is at the extreme left of the photograph. The TV camera shown was mounted into the system for testing purposes. It will be replaced by the infrared camera when its fabrication is complete. The second imaging lens is mounted on the front of the camera. The resulting image is displayed on a TV monitor shown in the background. In all cases as was pointed out previously, the image on the CRT monitor is the mirror image of the actual scene stored in the hologram. No provisions were made in the laboratory model to correct this image reversal. The photographs in Figures 36 - 43. however, have been flopped over to present the image on the monitor as it will be viewed in a system that incorporates a means for correcting the holographic real image reversal. Various tests were conducted on this unit, the results of which are presented in the following sections.

6.2 AXIAL INVARIANCE

The mechanical device for projecting the real image along a fixed optical axis has been assembled and tested. The synchronization of translational and rotational motions in two dimensions operates as intended. The present frame, however, is too light to support the mechanism rigidly, particularly when the small HeNe laser is mounted. This results in some distortion of the gimbal frames. There is also some tendency of the frame to distort when the initial force is applied to operate the mechanism. This causes a slight angular shift in the optic axis that reduces to zero as soon as the inertia of the system is overcome. Both of these problems can be easily alleviated by more rigid construction techniques. The system can also be improved by driving the translational

motion and letting the rotational motion follow. This would allow most of the driving force to be applied in the plane of the system rather than perpendicular to it.

The operation of this mechanism to provide the perspective views corresponding to different glide paths is shown in Figures 37 - 40. In each photograph a different glide path is addressed and the resulting image presented on the monitor. The spot on each hologram is caused by scattering of the laser beam as it passes through the emulsion. It can be seen in a different location for each image. As designed, the system provides a continuous change in perspective view over a horizontal range of $\pm 13^{\circ}$ and a vertical range of $\pm 10^{\circ}$. The axial invariance of this system is not affected by the range change optics and the resulting image magnification.

6.3 OPTICAL TRACKING

Range change simulation is accomplished through image size changes. This is effected by changing the curvature of the beam illuminating the hologram. Figure 41 shows the feasibility model with the image at its smallest size. The reconstructed image is at the closest distance to the hologram. Note the position of the first-imaging lens. It is relaying the holographic image to the TV camera from a position about 8" from the hologram. As the range changing optics move and converge the rays farther from the hologram, the image becomes larger and moves away from the hologram plane. This is shown in Figure 42. The first imaging lens has moved toward the camera about half way on the stage. The moving portion of the beam-forming optics is visible just under the hologram. The image on the monitor has increased by a factor of about 4X. As the optics are driven further, the image enlarges to its maximum size (Figure 43). The total size change shown here is about 7X, and it was made entirely optically; that is, no shrinking raster technique was employed.

During the range change simulation, a slight defocusing of the final image takes place. This is due to the fact that the tracking between the optics producing the holographic image and the imaging lens is not perfectly correct. Rather than tracking linearly with the imaging lens, the holographic image moves more slowly as the image enlarges, continuously falling more behind. This could be due to several reasons, for example, by inaccurate lens focal lengths or spacings or by a discrepancy between design and actual hologram parameters. Nevertheless, it is a solvable engineering design problem.

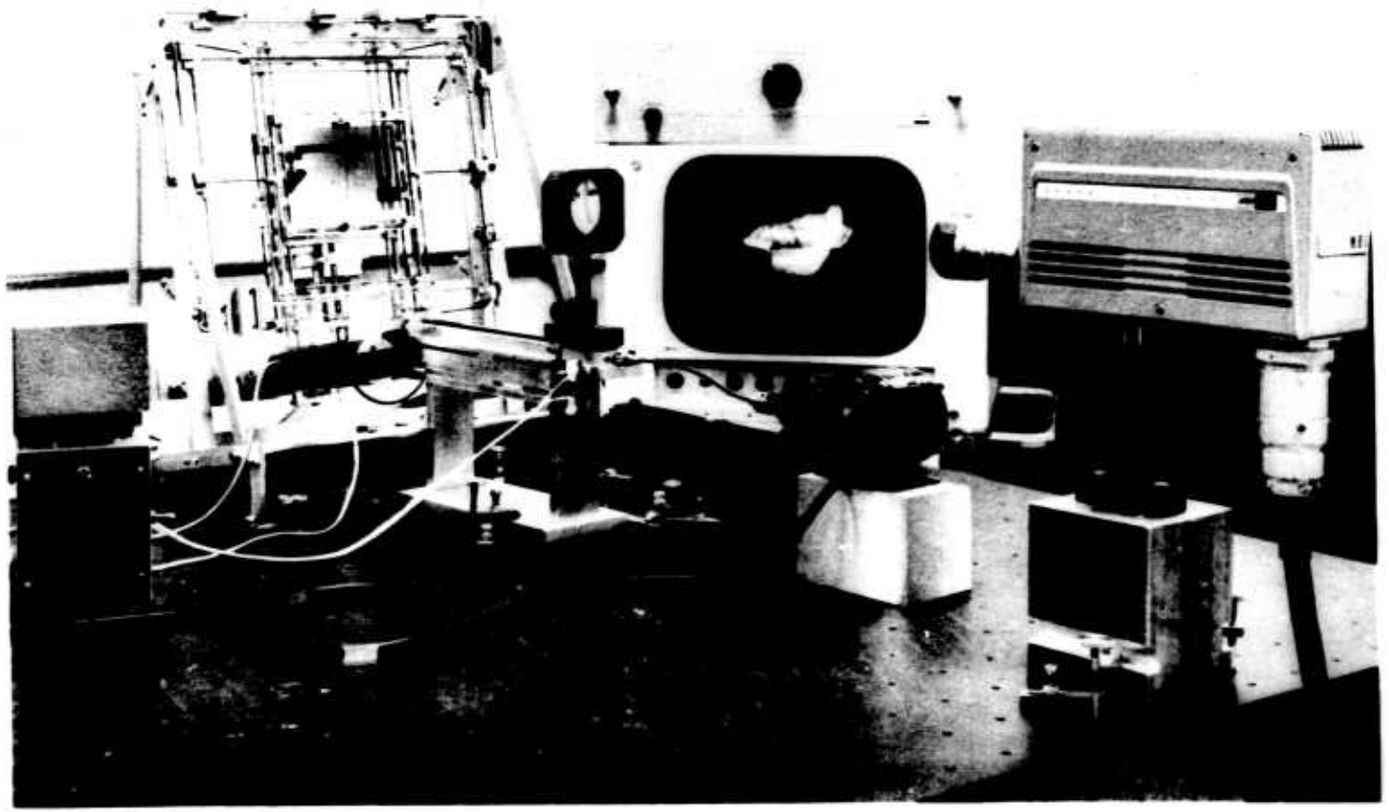

Figure 36. Image Corresponding to Glide Path Selection Near Center of Plate.

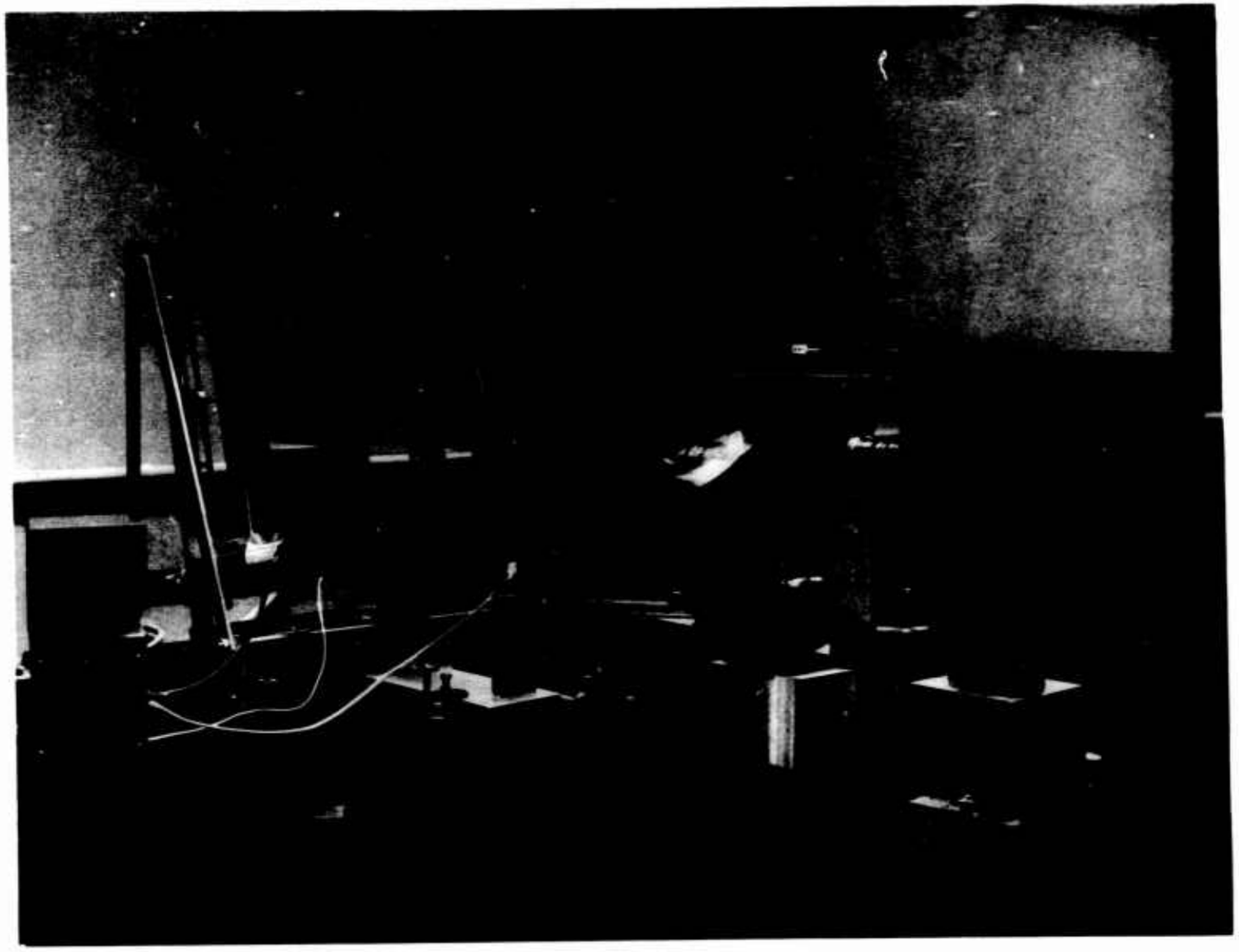

Figure 37. Image Corresponding to Glide Path Selection Near Right Side of Plate.

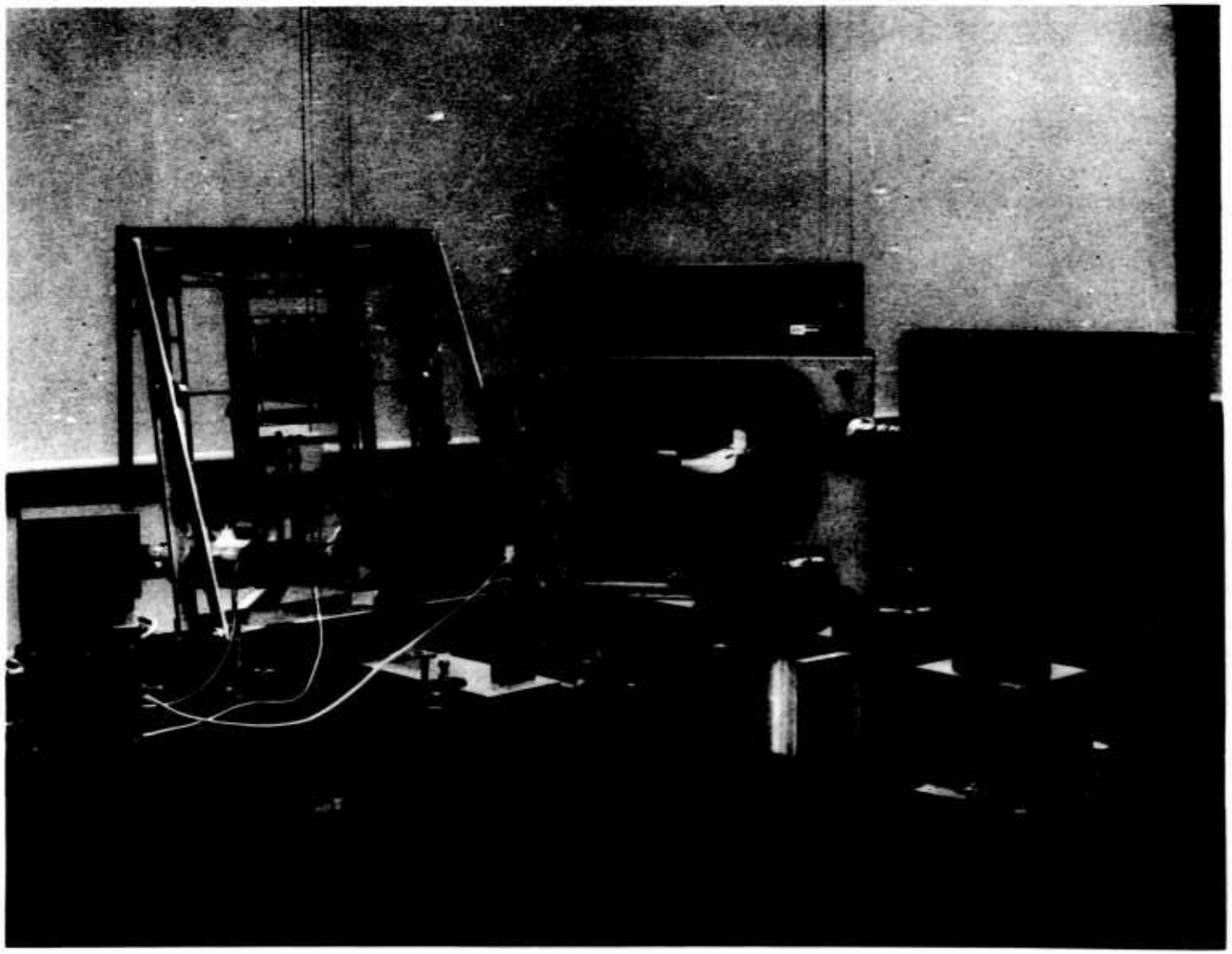

Figure 38. Image Corresponding to Glide Path Selection Near Bottom of Plate.

Figure 39. Image Corresponding to Glide Path Selection Near Left Side of Plate.

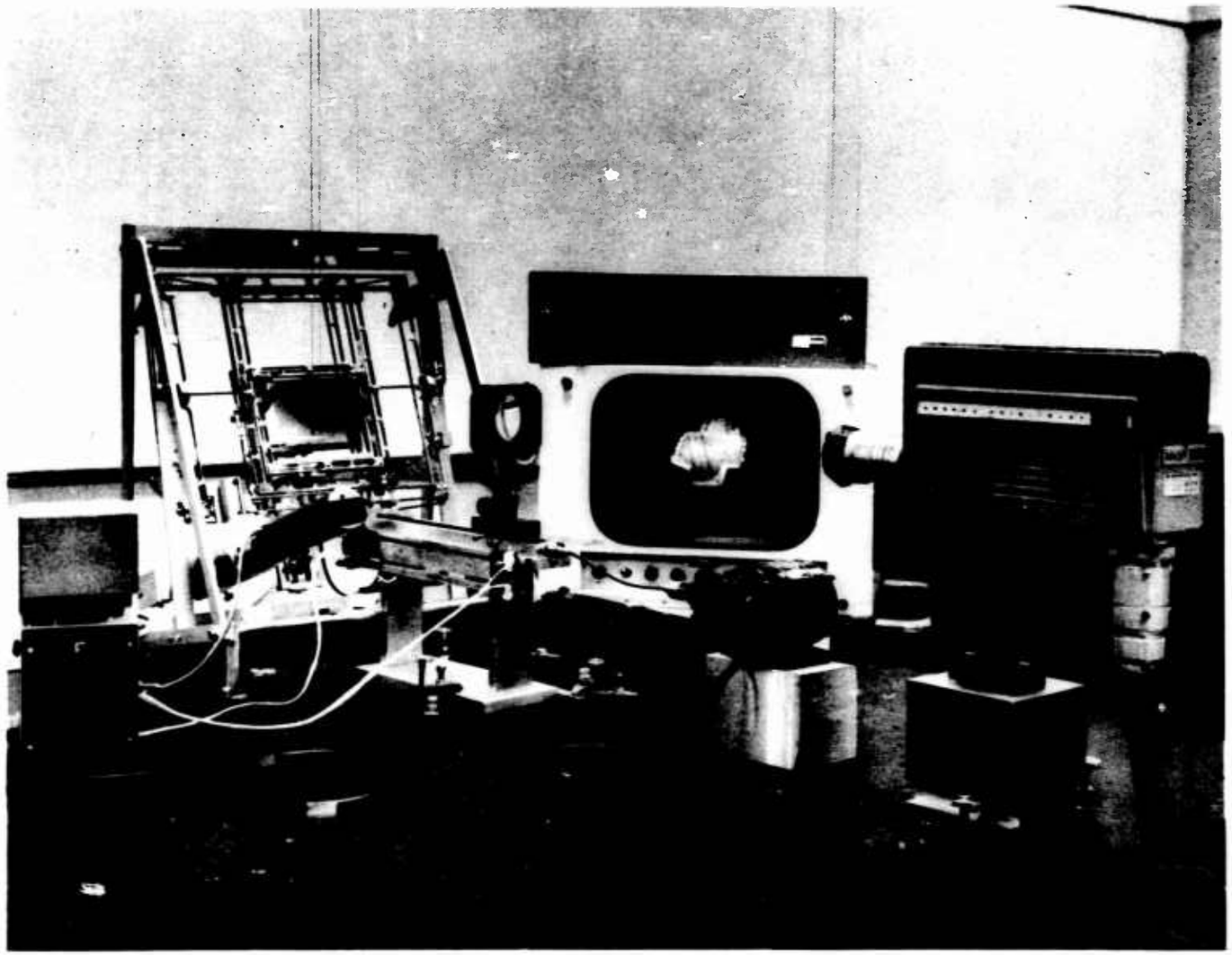

Figure 40. Image Corresponding to Glide Path Selection Near Top of Plate.

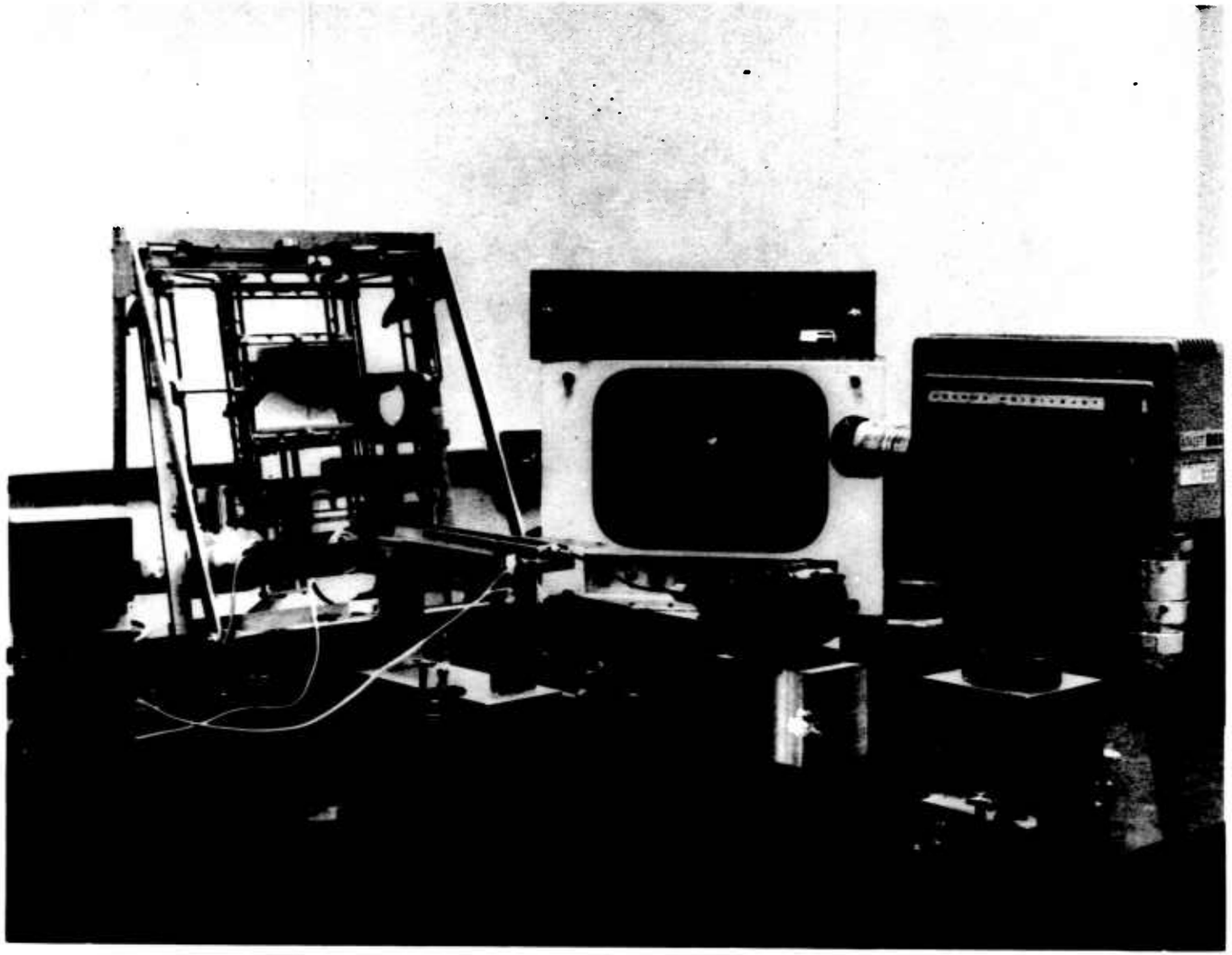

Figure 41. Minimum Image Size within Demagnification Range.

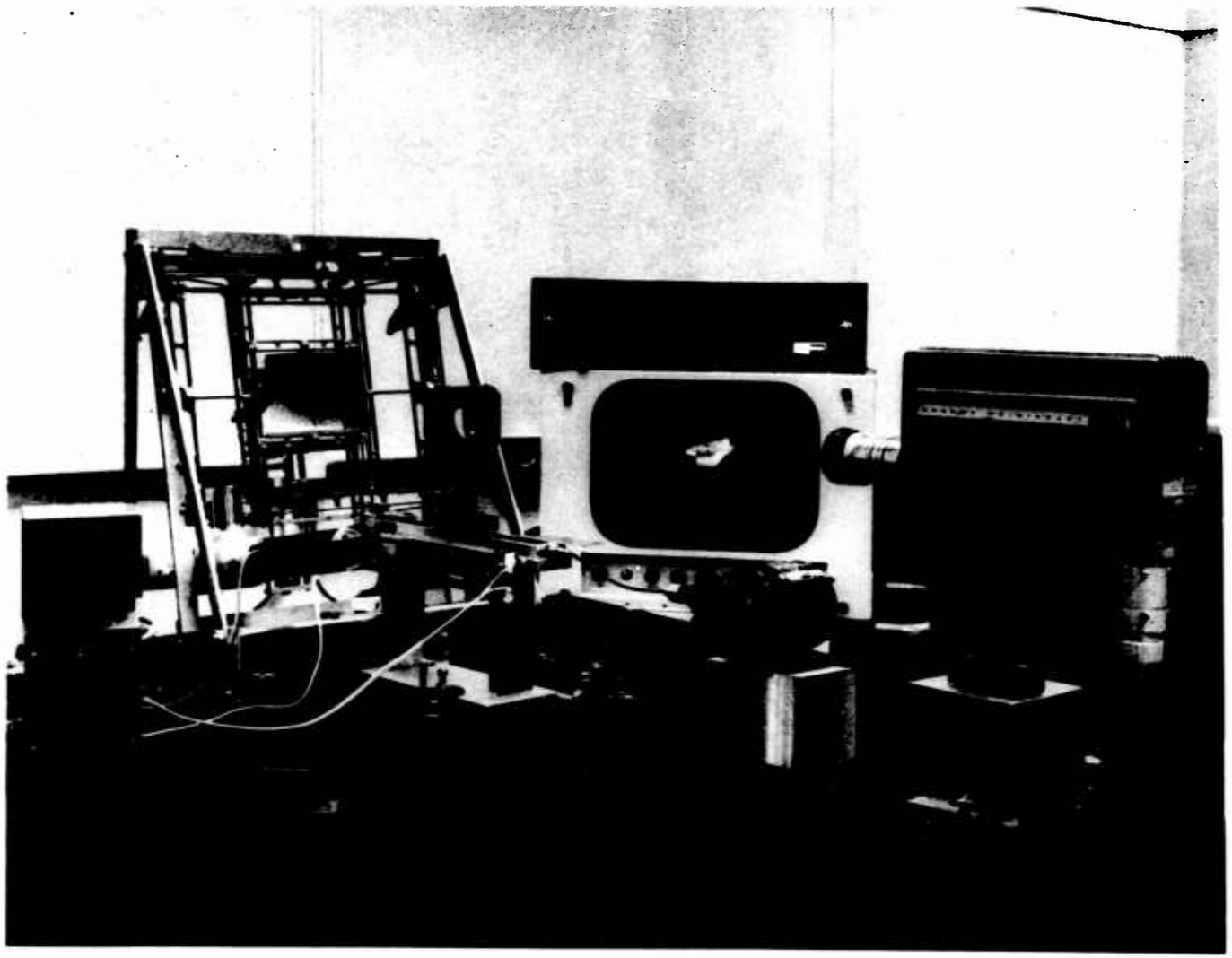

Figure 42. Intermediate Position in Demagnification Range.

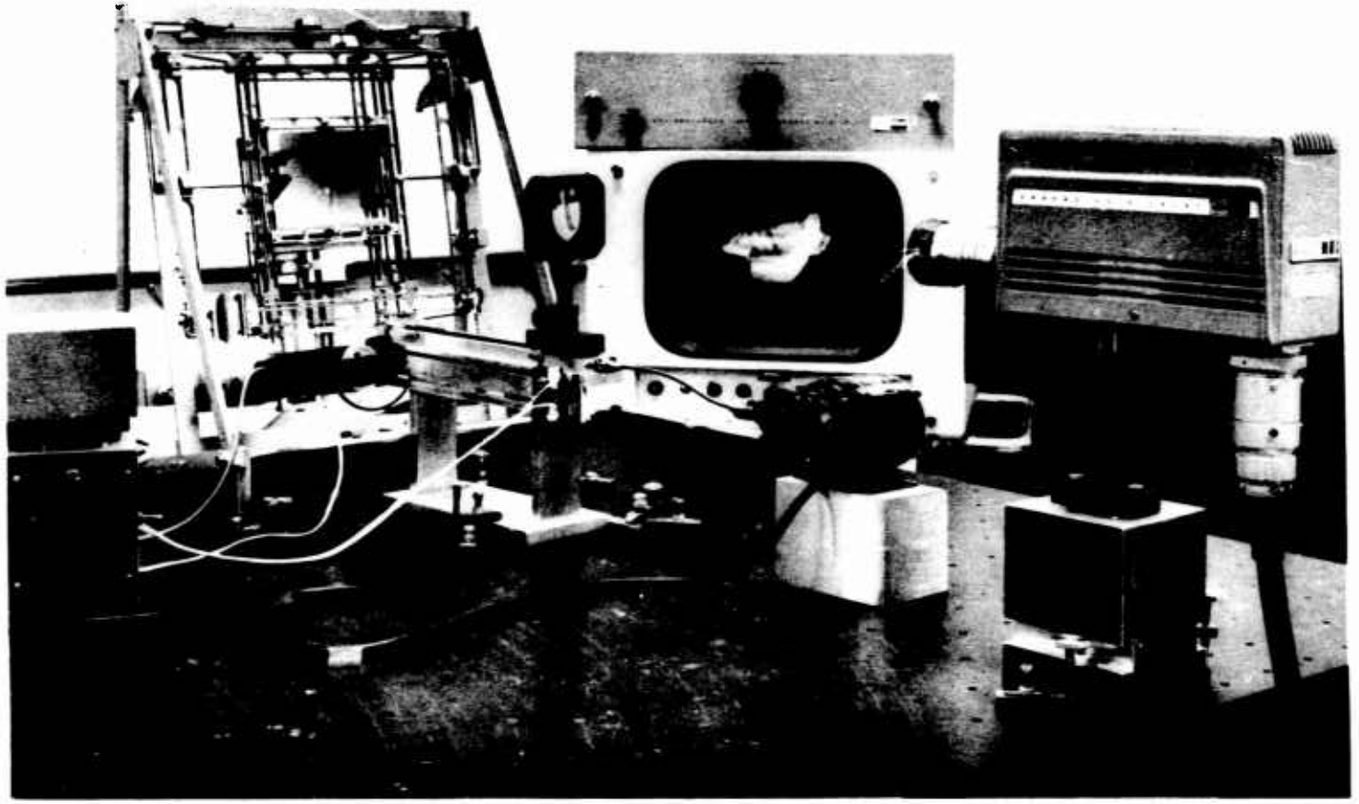

Figure 43. Maximum Image Size Within Demagnification Range.

As the image enlarges, its brightness falls off since the power output of the laser is constant. The image brightness from the TV monitor decreases as the simulated range reduces. In order to correct for this, it will be necessary to provide an automatic brightness control circuit within the TV system.

6.4 IMAGE QUALITY

The ability of a hologram to record depth information about a three-dimensional object is not necessarily a desirable feature for every application. This is because it is inherent in the process that the reconstructed images also be three-dimensional. This presents a problem, as the real image cannot be viewed directly due to its pseudoscopic nature. Consequently, the real image must be focused onto a viewing screen or, in our case, the photocathode of a vidicon. The requirement of imaging a three-dimensional object onto a two-dimensional plane is not, in itself, unique. It is encountered in photography, motion pictures, and television. For these applications, the solution is to reduce the aperture of the imaging lens and thereby increase its depth of focus. This can be done in holography also by reducing the diameter of the illuminated area of the hologram. The difference arises, however, in the type of radiation used to illuminate the object(s). In conventional applications incoherent light is used, which causes each object point to act as an independent source. In holography, coherent light is used, which results in a constant phase relationship between each object point. As a result, neighboring object points can, and do, interfere with one another. This causes the information about these points to be nonuniformly distributed in the recording plane. The hologram retains this nonuniformity. If, during reconstruction the illuminated area is small, there is a finite probability that there may be little or no information about some object points within that area. The resulting image will have a granular or speckled appearance when viewed. Consequently, as the illuminated area is reduced to improve depth of focus, the image begins to lose continuity. A trade-off therefore exists between image quality and depth of focus. (See Figure 36 of the Phase I report, p. 93.) Such a trade-off can be seen in Figures 44 and 45. Figure 44 is a photograph of a 2-1/2" scale model illuminated with incoherent white light. This model

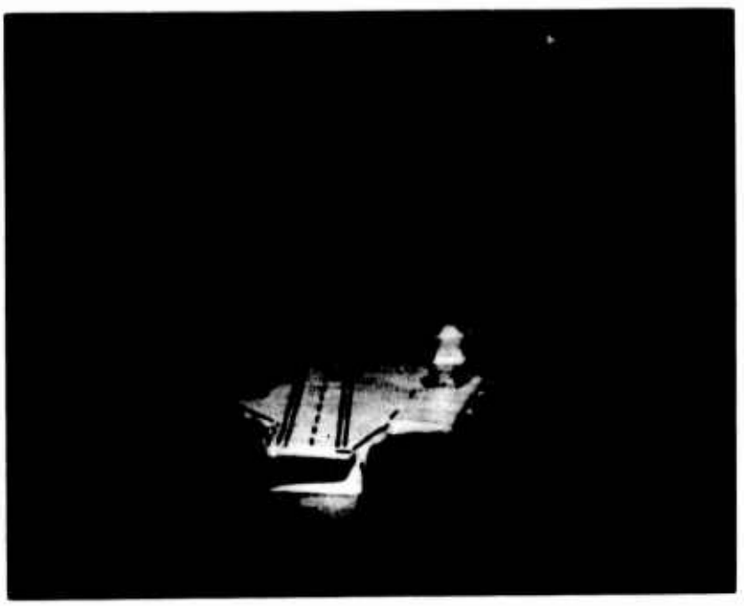

Figure 44. Model Illuminated with White Light.

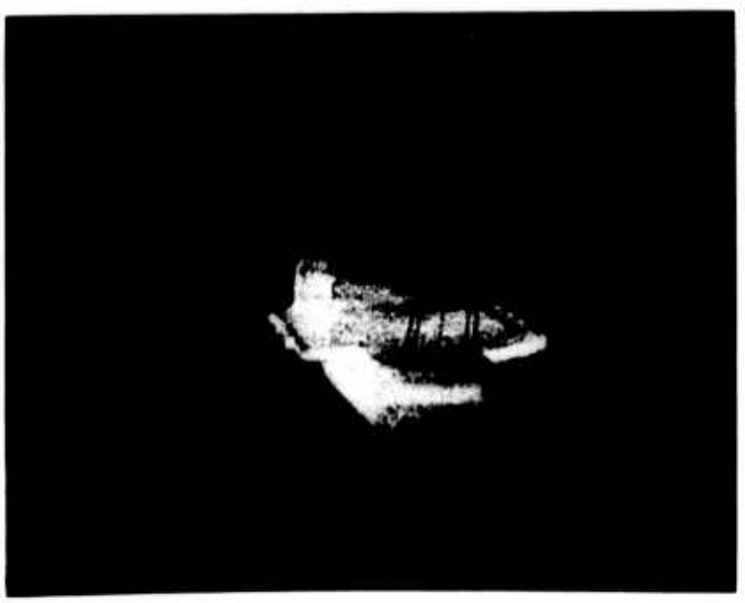

Figure 45. Reconstructed Real Image as Displayed on Monitor Screen.

was fabricated in the laboratory and coated with magnesium oxide in a PVA binder to provide a diffusing surface. The image can be seen to be reasonably acceptable although the coating is not particularly uniform. A hologram of this model produced the real image shown in Figure 45. For approximately the same depth of focus, there is obviously a degradation of image quality.

Several techniques to reduce this effect were proposed and subsequently tested. These included multiple exposure of the hologram with the introduction of a different phase shift between each exposure, use of rotating diffusers or vibrating optical elements during both recording and reconstructing steps, reduction of the coherence length of the readout light, and variations of the recording parameters such as reference to signal-beam ratios. No significant improvement in image quality could be obtained with any of these techniques. Other techniques have recently been proposed, but they are as yet untested. One method is to obtain as small a carrier model as possible while still maintaining the desired degree of detail. This should reduce the depth of field over which the system must operate. In addition, the type of diffusing surface used on the model(s) should be investigated to see if relative roughness has an effect on image quality. Another technique is to perform a high-speed optical scan of the interrogated area rather than illuminate the entire area simultaneously. This should prevent interference effects during readout since the individual reconstructions are independent. Finally, the multiple-exposure technique may be expanded to the generation of independently accessible holograms.

Additional problems may be introduced when the injection laser is used to reconstruct the image. These are expected to arise due to the difference between recording and reconstructing wavelengths. Although we have viewed the reconstructed image in the infrared through an image converter, the quality of the device prohibits a good assessment of image quality. The infrared-sensitive vidicon should be used for testing when its fabrication is complete.

6.5 OTHER RESULTS

The infrared-sensitive vidicon has not yet been tested in the system. Its fabrication was delayed due to unavailability of components. In conjunction with this, the associated techniques of shrinking raster, image displacement, and image roll are untested. Our present monitor has horizontal and vertical position controls that do demonstrate pitch and yaw motions. The design however, includes these features in the camera electronics shown in Figure 33.

7. FUTURE TASKS AND RECOMMENDATIONS

The results of this investigation indicate that a device using holography in an aircraft head-up display is feasible. Alternate nonholographic approaches such as viewing a scale model with a TV system were considered. The advantage of the holographic technique over the model approach is that of storing a large number of airfields and carriers in a library within the landing system for selection as needed.

The following tasks should be considered for future work.

1. Improvement in holographic image quality. Through the use of specially prepared, smaller, and more accurate models and through the use of more refined holographic techniques, image quality can be further improved. Additional improvement should be possible during and throughout view parameter changes, particularly range. More precise control on the illuminating beam and image track should help. It should be pointed out, however, that holographic images (when relatively small areas of the hologram are illuminated) are inherently inferior to images generated with white light.
2. Simplification of the mechanical system and making it more rugged.
3. Increasing the variation in view parameters, particularly magnification (range), pitch, and yaw.
4. Optimizing size and packaging of the system.
5. Developing interfacing and control system concepts and circuitry.
6. Testing psychological effects of the optical system and generated image with a head-up viewer.
7. The implications of the airborne environment, such as vehicle vibrations.

8. The implications and possible difficulties of introducing the production of holograms to field and fleet type personnel and equipment.
9. Investigating the possibilities of a nonmechanical glide-path select technique, using, for example, digital or analog laser beam deflectors.
10. Building and testing a display system using an articulated scale model viewed in white light with the TV system.
11. Comparing both the holographic and model approaches for the best overall usefulness and practicality.
12. Investigating solid-state vidicons for more reliable systems.

An appropriate next step appears to be the development of a general-purpose holographic image generator. The holographic image generator would be able to generate an almost endless variety of imagery by the substitution of appropriate holograms. It would have as its output a standard 525-line video signal that could be adapted to noncommercial displays by image conversion. It could feed a variety of displays such as head-up displays, video projectors, and ordinary TV displays. The holographic image generator could provide inputs for simulation and training equipment or could serve as part of a flyable breadboard of advanced display systems. It could generate images of airfields or aircraft carriers for simulators or prototypes of actual landing aids. It could generate images of aerial or ground targets for weapons delivery, and it could even generate symbolic perspective imagery for contact analog displays.

The holographic image generator could use the holographic reconstruction techniques and basic optical system developed during Phase II of the holographic head-up study, but it would depart from the laboratory breadboard built during this program in significant areas.

First, the holographic image generator would use as a radiant energy source a small pulsed GaAs injection laser rather than the cumbersome gas laser used in the laboratory model. A GaAs laser would operate near the sensitivity peak of the IR vidicon camera developed during the Phase II program and at the same time would permit a significant reduction in size.

Second, provisions could be made for driving each of the six degrees of image freedom by means of an electrical signal input rather than the manual drives used on the laboratory demonstration breadboard. Closed-loop servo-mechanical drives would provide the degrees of freedom that require mechanical articulation (the two perspective changes and range change). All six signal inputs would be analog to permit interfacing with the greatest variety of simulation equipment or flight instrumentation.

Second, provisions could be made for driving each of the six degrees of image freedom by means of an electrical signal input rather than the manual drives used on the laboratory demonstration breadboard. Closed-loop servo-mechanical drives would provide the degrees of freedom that require mechanical articulation (the two perspective changes and range change). All six signal inputs would be analog to permit interfacing with the greatest variety of simulation equipment or flight instrumentation.

8. APPENDIX

In the treatment of magnification theory in Section 2.3, an expression was used to represent the equation of a spherical wavefront with respect to the recording plane. This expression will now be derived.

In Figure 46, the location of the point of origin of a spherical wave can be described by the vector $\vec{r}_o$. The point of interest in the hologram plane (x, y, 0) can be described by the vector $\vec{r}$. Since the phase is only a function of the scalar distance between the point of origin and P, we can write the equation of a spherical wave as

$$U(r) = Be^{ik|\vec{r} - \vec{r}_o|}$$

We can write the optical path vector as

$$\vec{r} - \vec{r}_o = (x-x_r)\hat{i} + (y-y_r)\hat{j} + z_r\hat{k}$$

when $\hat{i}$, $\hat{j}$, and $\hat{k}$ are unit vectors along the x, y, and z axes respectively.

Hence, $$|\vec{r} - \vec{r}_o| = [(x-x_r)^2 + (y-y_r)^2 + z_r^2]^{1/2}$$

If we use the paraxial approximation that both $(x-x_r)$ and $(y-y_r)$ are much smaller than z_r,

$$|\vec{r} - \vec{r}_o| \approx z_r + \frac{1}{2z_r}[(x - x_r)^2 + (y - y_r)^2]$$

Expanding this and collecting terms we obtain

$$|\vec{r} - \vec{r}_o| = z_r + \frac{1}{2z_r}(x_r^2 + y_r^2) + \frac{1}{2z_r}(x^2 + y^2) - \frac{1}{z_r}(xx_r + yy_r)$$

If we wish to measure all phases with respect to the origin of the coordinate system rather than with respect to the origin of the reference beam, then we can subtract the distance $|\vec{r}_o|$ from the above.

$$|\vec{r}_o| = (x_r^2 + y_r^2 + z_r^2)^{1/2} \simeq z_r + \frac{1}{2z_r}(x_r^2 + y_r^2)$$

Hence, the optical path difference Δp becomes

$$\Delta p = \frac{1}{2z_r}(x^2 + y^2) - \frac{1}{z_r}(xx_r + yy_r)$$

The cross product in the last term is simply the dot product of $\vec{r}$ and $\vec{r}_o$. That is,

$$\vec{r}_o \cdot \vec{r} = xx_r + yy_r$$

In addition, the magnitude of $|\vec{r}_o|$ is approximately equal to z_r. Hence $\vec{r}_o/z_r$ is a unit vector in the direction of $\vec{r}_o$. We now have

$$\Delta p = \frac{1}{2z_r}(x^2 + y^2) - \frac{1}{z_r}(\vec{r}_o - \vec{r})$$

Inserting this back into the expression for the spherical wave, we obtain the expression used in equation (2) of the text.

$$U(x, y) = e^{\frac{ik}{2z_r}(x^2 + y^2)} e^{-i\vec{k} \cdot \vec{r}}$$

where $\vec{k}$ is a vector in the direction of $\vec{r}_o$ and has a magnitude $|\vec{k}| = \frac{2\pi}{\lambda}$.

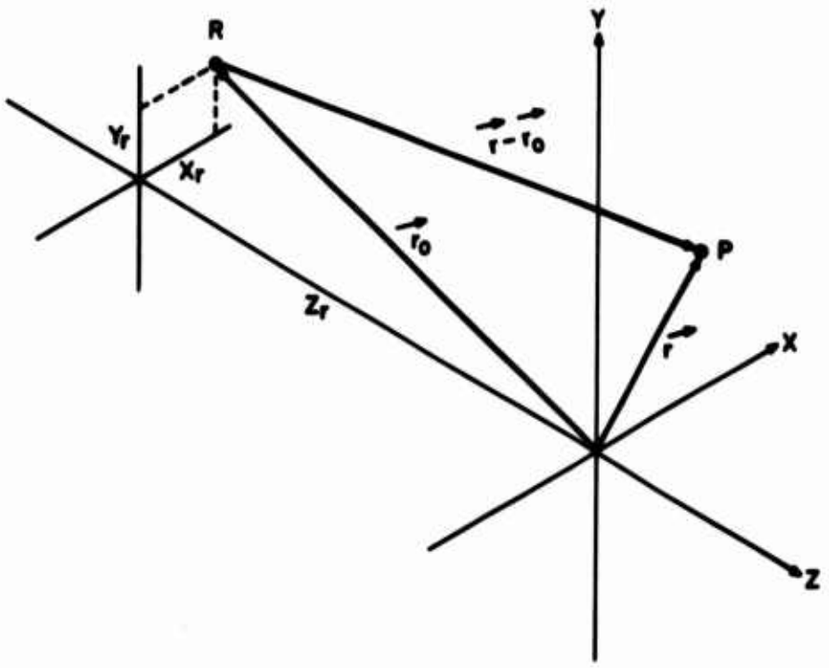

Figure 46. Vector Relationship for Determining Equation of a Spherical Wave.

9. REFERENCES

1. T. J. Harris, et al., "Holographic Head-Up Display - Phase I," AD 825633L, December 15, 1967.
2. J. H. Hammond, Jr., Navigational Guidance System. U. S. Pat. 2,027,530, January 14, 1936.
3. W. H. Miller, et al., Pictorial Display Air Navigational System. U. S. Pat. 2,959,779, November 8, 1960.
4. W. B. Klemperer, Visual Simulator for Flight Training Device. U. S. Pat. 2,979,832, April 18, 1961.
5. L. N. Wells, Visual Flight Simulation Systems. U. S. Pat. 3,362,089, January 9, 1968.
6. R. P. Baird, Jr., Visual Landing Simulator for Instrument Flying. U. S. Pat. 3,383,679, May 14, 1968.
7. M. C. Ellison, Simulated Landing Signal Apparatus. U. S. Pat. 3,127,685, April 7, 1964.
8. A. F. Giordano, Three-Dimensional, Two-Planar Projection Display. U. S. Pat. 3,281,519, October 25, 1966.
9. K. J. Stein, "Head-Up Unit Displays Low-Light Level TV," Aviation Week and Space Technology, February 19, 1968, pp. 66-72.
10. P. K. Weimer, et al., "A Self-Scanned Solid-State Image Sensor," Proceedings of the IEEE, 55, p. 1591.

Unclassified

Security Classification

DOCUMENT CONTROL DATA - R & D

(Security classification of title, body of abstract and indexing annotation must be entered when the overall report is classified)

1. ORIGINATING ACTIVITY (Corporate author)	2a. REPORT SECURITY CLASSIFICATION
International Business Machines Corporation Systems Development Division Poughkeepsie, N. Y.	Unclassified 2b. GROUP not applicable

3. REPORT TITLE

Holographic Head-Up Display -- Phase II, Final Report

4. DESCRIPTIVE NOTES (Type of report and inclusive dates)

Technical Report (TR 00.1996 (June 4, 1968 - March 27, 1970)

5. AUTHOR(S) (First name, middle initial, last name)

Harris, Thomas J. Hanna, David W.
Schools, Rodman S. Delay, Dennis G.
Sincerbox, Glenn T.

6. REPORT DATE	7a. TOTAL NO. OF PAGES	7b. NO. OF REFS
March 27, 1970	107	10

8a. CONTRACT OR GRANT NO.	9a. ORIGINATOR'S REPORT NUMBER(S)
N 00014-67-C-0453 b. PROJECT NO.	JANAIR Report 680709
c. d.	9b. OTHER REPORT NO(S) (Any other numbers that may be assigned this report) None

10. DISTRIBUTION STATEMENT

This document has been approved for public release and sale; its distribution is unlimited.

11. SUPPLEMENTARY NOTES	12. SPONSORING MILITARY ACTIVITY
Joint Army Navy Aircraft Instrumentation Research Program (JANAIR)	Office of Naval Research, Naval Air Systems Command, Army Electronics Command (Code 461), Washington, D.C. 20360

13. ABSTRACT

Numerous applications of display systems require the presentation of visual information that can be continuously altered with time. In particular, a head-up display system as used by an aircraft commander must provide a simulation of the real-world exterior to his vehicle, and, at the same time, represent any change in his attitude with respect to a predetermined segment of this real world. In the particular case of an aircraft landing approach, one can characterize the pilot's view of the aircraft carrier and its subsequent variations into six degrees of freedom. The display must provide the view corresponding to the instantaneous values of these parameters and change as any one or more of the parameters change. This report describes the results of a continuation of the development work initiated in Phase I of the contract on displays of this type using sideband or carrier-frequency Fresnel holographic recorded images. The goals of Phase II were to study the various modes and techniques derived in Phase I and other possibilities, to select the approach that offered the best potential for use in Navy carrier-based aircraft and to build a laboratory model of this selected system. The selected approach uses a GaAs injection laser diode light source to interrogate a hologram of an aircraft carrier model. The real image from the hologram is optically relayed to a special IR vidicon, and the image is then transmitted electrically to a CRT monitor. This approach was selected for several reasons, but chiefly because it is compatible with some of the existing aircraft equipment. A laboratory model of this system was constructed. This work was performed by the IBM Systems Development Division, Product Development Laboratory, at Poughkeepsie, N.Y. with assistance from IBM's Federal Systems Division, Electronics Systems Center, at Owego, N.Y.

DD FORM 1 NOV 65 1473 REPLACES DD FORM 1473, 1 JAN 64, WHICH IS OBSOLETE FOR ARMY USE.

Unclassified

Security Classification

Unclassified

Security Classification

14. KEY WORDS	LINK A		LINK B		LINK C	
	ROLE	WT	ROLE	WT	ROLE	WT
Displays Head-Up Di. ıay Holographŋ						

Unclassified

Security Classification